UC Berkeley
UC Berkeley Electronic Theses and Dissertations

Title

Surfactant Properties of Per- and Polyfluoroalkyl Substances (PFAS): Implications for Detection, Fate, and Transport in Environmental and Treatment Matrices

Permalink

https://escholarship.org/uc/item/03j872m2

Author

Steffens, Sophia D

Publication Date

2022

Peer reviewed|Thesis/dissertation

eScholarship.org Powered by the California Digital Library
University of California

Surfactant Properties of Per- and Polyfluoroalkyl Substances (PFAS): Implications for Detection, Fate, and Transport in Environmental and Treatment Matrices

by

Sophia D. Steffens

A dissertation submitted in partial satisfaction of the

requirements for the degree of

Doctor of Philosophy

in

Chemistry

in the

Graduate Division

of the

University of California, Berkeley

Committee in charge:

Professor Lisa Alvarez-Cohen, Co-chair
Professor Christopher Chang, Co-chair
Professor Felix Fischer
Professor Baoxia Mi

Fall 2022

Surfactant Properties of Per- and Polyfluoroalkyl Substances (PFAS): Implications for Detection, Fate, and Transport in Environmental and Treatment Matrices

Copyright 2022
by
Sophia D. Steffens

Abstract

Surfactant Properties of Per- and Polyfluoroalkyl Substances (PFAS): Implications for Detection, Fate, and Transport in Environmental and Treatment Matrices

by

Sophia D. Steffens

Doctor of Philosophy in Chemistry

University of California, Berkeley

Professor Lisa Alvarez-Cohen, Chair

'Forever chemicals' is on its way to becoming a household name. Yet as researchers, we are still identifying the numerous data gaps in our understanding of bio- and chemical transformation, toxicity, transport processes, and physicochemical behavior of the poly- and perfluorinated alkyl substances (PFAS) that have earned this colloquial title. This dissertation addresses how the unusual surfactant properties of PFAS derived from fluorine chemistry impact their behavior in the context of environmental management and treatment technologies.

The physicochemical properties investigated in this work are aggregation, surface activity, and sorptive behavior, all of which have the potential to cause artifacts of removal in treatment systems, as well as unexpected behavior in the environment. The aggregation of PFOS with specific groundwater relevant salts is investigated in order to understand an artifact of PFOS removal in high ionic strength treatment-like matrix. Additionally, the surface activity and interfacial accumulation activity of PFOS is evaluated using the Langmuir-Szyszkowski adsorption model (Chapter 2). This work is expanded upon by investigation of the aggregation and surface accumulation properties of an industrial AFFF, which is more representative of the complex PFAS contamination matrices that may be subject to high salinity conditions in the environment (Chapter 3). Lastly, sorption processes related to PFAS removal in a bio-based treatment system are uncovered through a mechanistic investigation of a multi-step oxidative treatment mechanism (Chapter 4).

Overall, this works serves to provide researchers with a more complete picture of the complexities associated with PFAS treatment in relation to their unique surfactant properties.

To my East Bay community–

my Fulton Home, the Clog House, my Nabolom gals and fancy night pals, and trail friends

–who helped me build a life, here.

Contents

List of Figures

List of Tables

Acknowledgments

In my 5+ years as a Berkeley graduate student, I have found community in a lot of places both on and off campus. In catching up with old friends, and especially when meeting new people, the question of "so how did you decide to do a PhD?" or, more often, a statement like "Woah... a Chem PhD...?" comes out. Then, I try to explain how I got here in the next thirty or so seconds of the conversation. That, coming to Berkeley wasn't something I conceived of and decided on one day in college PChem, nor had I set my sights on a PhD during our 5th grade field trip to the Lawrence Hall of Science. That, like most things in life probably are, the path doesn't take the shape of a path until you're at the end of it. Or, at least at a rest stop along the way. Thirty seconds isn't really enough time to explain that path, or more importantly, the people that helped build it, but this page might be.

I want to first thank my grandparents, Diane and Douglas Scalapino (Baba and Pa, to me) for showing me over many years of summer visits, and throughout my time as an undergrad at UC Santa Barbara, that a university was a community. My grandparents built a lot of their life around Pa's research at UC Santa Barbara. In 7th grade, they took me on my first trip to Europe where Pa was giving talks at summer conferences, and where I fell asleep next to Baba during his seminar on superconductivity in Dresden, Germany. We also hiked the fjords, and stayed up until midnight in the long twilight of Norwegian summer– the physicists never running out of something that needed theorizing. Baba and Pa were instrumental in my decision to go to UC Santa Barbara, because it had always felt like a second home to me. They also were the first to tell me about the College of Creative Studies, which is how I found my way to research.

I took freshman General Chemistry not because I wanted to become a chemist, but because it was a requirement for the Bio Psychology degree I'd decided on. During my senior year of high school, I was reading a lot of WIRED magazine articles on topics in neuroscience, and was fascinated by how little we knew about the brain, and how much was still left to figure out. The Bio Psych major seemed like the path to learn more. But in Gen Chem, I felt like I was learning the language I'd always wanted to know. This is how I can explain things, this is how I can understand the world around me. During a break from studying for Winter quarter finals, I remember taking a beach walk mulling over enthalpy and entropy and everything I was supposed to know about thermodynamics. I remember realizing that even the sand I was walking on could be explained by entropic forces. I think at that same moment, I realized I had to major in Chemistry. I wanted to learn this language as fully as I could.

Thank you to the UCSB College of Creative studies, for welcoming me into the Chemistry Major. Thank you to Professor Javier Read de Alaniz, who spent extra office hours helping me learn OChem my sophomore year, and served as a mentor through the rest of my undergrad and when I was struggling during my first year of grad school. Thank you to Dr. Dan Little and CCS for supporting my first research pursuit in electrochemistry and to the CCS SURF Fellowship for the summer research support. I have immense gratitude for the Zakarian Group, who without, I truly would not have found myself pursuing a PhD.

Thank you to Dr. Armen Zakarian and Dr. Jeff Jackson, who taught me the art of total synthesis. Organic chemistry was not my strong suit in the classroom, but in the lab, I learned to love the processes it entailed. Thank you Jeff, for your patience and support as a mentor. For teaching me how to use Reaxys, run a proper column, set up a distillation, take an NMR, safely use n-BuLi, clean glassware, and maximize a yield. Your teaching gave me the foundation I needed to succeed in research. Thank you for also being supportive, when I decided to try out industry, with my first job at Apeel Sciences. Thank you to my colleagues and mentors at Apeel, especially Alex Thomas, Grant Rickon, Jenny Du, and Chuck Frazier. Thank you for challenging me to think creatively and for teaching me how to communicate my science as a story.

When I started my PhD at Berkeley, I was completely overwhelmed by what was being required of me– teaching an undergrad lab, trying to keep up with Phys Org, applying to fellowships, starting research– and I wasn't sure if I could actually do it. Thank you to my mentors in the Yaghi group that supported me in applying for a National Science Foundation (NSF) GRFP Fellowship. Thank you to the NSF, for supporting my individual research and scholarship– the support from the NSF Fellowship allowed me to pursue original research as a chemistry student in an environmental engineering lab. I'm thankful that I found my way to the Berkeley Center for Green Chemistry (BCGC) Fellowship program during my time in Dr. Yaghi's lab, which helped me pivot into water research.

My connections through BCGC led me to Dr. Lisa Alvarez-Cohen's lab in the Civil & Environmental Engineering Department. Thank you, Lisa, for introducing me to AFFF and all of the PFAS acronyms during the first group meeting that I joined in Summer 2018. Thank you to Dr. Emily Cook and Dr. Chris Olivares, for letting me shadow you in the first couple of months in the Alvarez-Cohen lab as I navigated research in an entirely new setting. And, for all of the project discussions and feedback in the years that followed. Thank you to my whole lab group– Emily Cook, Chris Olivares, Ned Antell, Katerina Tsou, Christian White, Eric Troyer, Emily Gonthier and Shan Yi.

Thank you to my family– Mom, Dad, Helena, Isabel, and Caroline– who emotionally, I would not have made it through grad school without. Thank you for supporting me whether everything was going well, or whether I was considering leaving and becoming a cheese maker. Thank you especially, in these past few months as I finish my degree and look to the next phase of my career, for encouraging me to take the path less known. For spending hours on the phone as I weighed decisions, both listening to me and giving your perspectives. I can just barely see the trail marker at the path of this new chapter, but I cannot wait for it to unfold.

Chapter 1

Introduction

1.1 What are PFAS?

Per- and polyfluoroalkyl substances (PFAS) are pervasive, recalcitrant, and ubiquitous environmental contaminants, yet have proved to be a nearly irreplaceable chemistry in countless formulations whose function we now take for granted. PFAS are referred to as 'fluorocarbons', 'PFCs', 'perfluorochemicals', and, more colloquially, as 'forever chemicals', due to their environmental persistence. PFAS are recognizable by their multiple carbon-fluorine (C–F) bonds, the strongest covalent bond in organic chemistry. Their structure is also revealing of their synthetic quality; fluorinated compounds are very rarely found in nature, which has been attributed to the low concentration of fluoride in seawater and subsequent low utilization in metabolic evolution [1]. The combination of these two factors– high bond strength and low natural occurrence– is the root cause of high persistence of PFAS in the environment. Very few biological defluorination pathways have been identified [2] [3].

While the strong C–F bond lends resistance to biological degradation, it likewise resists thermal and chemical degradation, making it an extremely useful chemistry for the production of long lasting, inert materials. PFAS are surfactants, and are dually hydro- and oleophobic due to their low polarizability [4]. Their surfactant structure lends to high surface activity and wettability, making them highly valued in technical applications. Incorporation of PFAS into industrial processes, and consumer and industrial products, has led to their widespread distribution in the environment [5]. PFAS are now inextricably linked to the water cycle, and can be found in rainwater and polar regions [6]. Unfortunately, we now know that PFAS are toxic and bio-accumulative; they have been linked to multiple human health endpoints, including endocrine disorders, hepatotoxicity, reproductive effects, decreased immune response, increased cholesterol, and increased risk of prostate, kidney, and testicular cancers [7–13].

The challenge of PFAS is two-fold: one, can we identify safer replacement chemistries? And two, how do we deal with the massive scale of environmental contamination we are now confronted with? Addressing both of these challenges will require further innovation and

unrelenting attention.

1.2 Discovery

Organofluorine compounds contain the strongest single bond in organic chemistry– the carbon-fluorine bond. The utility of this bond was not lost on chemists, who began synthesizing organofluorines even before elemental fluorine had been isolated [14]. In the 1940s, as organofluorines were being researched in the context of the Manhattan project and wartime materials, chemists recognized that the small spatial requirements of fluorine could allow for hydrogen atom substitution in any hydrocarbon or derivative. The 'patterning' of organofluorine compounds over the known organic compounds at the time suggest a trillion new fluorinated compound structures [15]. The fact that we now know of the existence of over 9000 PFAS in the environment [16], is, by comparison, almost minuscule.

One of the first commercialization of PFAS was carried out by 3M (Minnesota Mining and Manufacturing Company) in the 1940s [15]. Initially derived from perfluorocarbon acyl and sulfonyl fluorides, PFAS were synthesized by electrochemical fluorination (ECF) reactions which substituted all of the H-atoms with F-atoms. Due to the free radical nature of the ECF process, a suite of PFAS containing linear and branched structures, a range of fluorocarbon chain lengths, and various functional groups including perfluoroethers, perfluoroacyl fluorides, perfluoroalkane sulfonyl fluorides, and perfluorinated amines result from the synthesis [14].

Quick to realize the utility of fluorocarbon chemistry, 3M developed one of their most well-known products, Scotchguard, which could be used as an oil- and water-repellent treatment for textiles such as carpet [14]. Around the same time, scientists at DuPont discovered that the polymerization of tetrafluoroethylene (TFE) produced the substance polytetrafluoroethylene (PTFE). PTFE proved to have high thermal and chemical stability and resisted adherence to other substances, making it a high performance coating. In 1948, Teflon became the first commercial PTFE product sold by DuPont [14], and has now become nearly synonymous with non-stick cookware.

In the 1970s, a new synthetic route to fluorocarbons, termed telomerization, was developed. Telomerization utilizes a taxogen and a telogen, namely, perfluoroethylene and perfluoroethyl iodide, to produce even numbered, straight chain perfluorinated iodides. From perfluorinated iodides, perfluorinated carboxylic acids, fluorotelomer alcohols, and fluorotelomer olefins can be produced [17]. Unlike the ECF-production method, telomerization does not yield branched or cyclic compounds, and is a more controlled synthetic route. Now, more than 80 years after their initial discovery and synthesis, PFAS have found their way into countless consumer and industrial applications.

1.3 Applications

PFAS applications are numerous. As consumers, we benefit from the material properties imbued by their chemistry in water- and oil-repellent textiles, such as durable water repellent (DWR) outdoor gear, stain-resistant upholstery and carpet, non-stick cookware and grease-resistant food packaging. In industrial processes, PFAS are utilized in metal plating and etching, wire and semiconductor manufacturing, and as mold-releasers in plastics manufacturing [18]– essentially, PFAS aid in keeping surfaces clean, and preventing sticking in materials extraction and extrusion processes. PFAS have become valued for fighting hydrocarbon-fuel based (Class B) fires; they are a critical component in aqueous film forming foam (AFFF), a blend of fluorocarbon and hydrocarbon surfactants formulated to have high spreadability over hydrocarbon fuel, imparting fire-quenching properties [19]. While the technical performance requirements in these applications vary, the material properties are leveraged in these many applications. However, upon finding their way into the environment, the surfactant properties of PFAS present an entirely new set of challenges.

1.4 Physicochemical properties

The role of PFAS surfactant physicochemical properties in their environmental behavior and remediation has gained substantial interest in recent years. Namely, the tendency for interfacial accumulation (e.g., water–air, soil–water) and aggregation (e.g., micelle, hemimicelle formation) has the potential to significantly impact PFAS fate and transport, as well as influence considerations for PFAS detection and treatment [20–22]. Evaluating the impact of PFAS physicochemical properties in the environment is complicated due to the fact that compound structure (e.g., perfluorinated chain length, head group, branched or linear isomer) and compound concentration must be taken into consideration [23, 24]. Additionally, interactions between different PFAS and co-contaminating chlorinated solvents (i.e., BTEX, TCE), as well as site specific characteristics (i.e., temperature, pH, salinity, total organic carbon), can impact surfactant behavior [21, 25–28].

Numerous early studies on PFAS behavior in heterogeneous systems reported sorption effects that are related to PFAS interfacial activity, without necessarily describing them as such [29–31]. Some studies described formation of PFAS hemi-micelles, particularly in porous materials that promoted the concentration of monomers within small pore volumes compared to the bulk solution [32–35]. ‘Salting-out’, a characteristic related to surfactant solubility and aggregation in saline conditions, has also been used frequently in the literature to describe PFAS behavior [36–39].

Currently, there are intensified research efforts related to PFAS partitioning in saline environments [36–44] and related to measuring and modeling PFAS interfacial behavior [20, 24, 28, 45–50]. While challenging, it is critical to address the physicochemical properties that can contribute to enhanced accumulation and potential for decreased detection in order to effectively manage contamination.

1.5 Health & Environmental Consequences

Perfluorooctanesulfonic acid (PFOS), one of the dominant PFAS to emerge from early ECF production processes, was also the first to be identified globally in biota and humans [51] [22], propelling PFAS research into the spotlight. For humans, ingestion of PFAS is a major exposure route, either through drinking water or diet [52–57], but dermal contact through personal care products and the built environment [58–61] and inhalation of dust and airborne particles [62–64] are other common exposure routes. PFAS accumulation in bodily tissues varies, but unlike other persistent organic pollutants, PFAS tend not accumulate in fatty tissues due to their lipophobicity [65, 66]. Rather, PFAS have been shown to concentrate in blood and in brain, liver, and lung tissues [65, 67].

PFAS exposure has been linked to low birth weight, high cholesterol, decreased immune response, liver, testicular, and kidney cancer, and kidney disease [7–13]. The sheer number of PFAS makes it challenging to evaluate potential health endpoints of individual compounds, and there is increasing pressure to address exposure risks by addressing PFAS as a chemical class [68–70]. Further, stricter regulations to mitigate PFAS exposure are finally being implemented by governing agencies in the U.S.; in June 2022, the U.S. Environmental Protection Agency (EPA) released updated health advisory limits (to non-detectable limits) for PFOA and PFOS and added two additional PFAS, perfluorobutanesulfonic acid (PFBS) and perfluoroalkyl ether acids (GenX) to the advisory list [71]. Given these new regulations, there is mounting pressure to discover and implement robust treatment technologies across contamination matrices.

1.6 Treatment & Environmental Remediation

PFAS treatment faces a unique set of challenges. Perhaps most notably, the vast scale of PFAS contamination is daunting; a new presumptive contamination model determined nearly 60,000 sites in the United States that were identified as AFFF discharge sites, certain industrial facilities, or sites related to PFAS containing waste [72]. As evidenced by the number of contaminated drinking water sources– over 200 million U.S. residents receive PFAS-contaminated drinking water [73]– PFAS are not confined to point sources, but rather, are widely distributed across environmental matrices. Because of their recalcitrance, PFAS are essentially 'recycled' as they move through discharge and disposal routes, being transported through air, soil, and water [74].

PFAS treatment technologies fall under two main categories: sequestration or destruction. Sequestration can include coagulation and separation [34, 75–77], ultra filtration with advanced membranes [78–80], granular activated carbon (GAC) filtration [35, 81, 82], and removal with anion exchange resins [81–85]. While useful in preventing direct exposure, sequestration technologies ultimately require secondary treatment in the form of a destructive technology, in order to fully remove PFAS from environmental cycles. PFAS destructive technologies are typically chemically and/or energetically intensive, including thermal treatment

(e.g., incineration, pyrolysis, smoldering) [74, 86–89] advanced reduction processes (e.g., hydrated electrons) [90–92], advanced oxidation processes (e.g., heat activated persulfate oxidation) [78, 93, 94], and supercritical water oxidation [95–98].

The high chemical and energy requirements of destruction technologies will remain a challenge in PFAS treatment going forward, and synergistic treatment strategies will be required to optimize PFAS remediation. In a recent review, the authors write,

> "An appropriate treatment strategy for PFAS-impacted waste [includes] multiple treatment technologies in series to concentrate PFAS into the smallest volume possible for energy-intensive destruction." (McDonough et al. 2022) [95].

While practical to utilize energy intensive processes most efficiently, the immense scale of contamination makes bioremediation a more desirable strategy. However, biological treatment of PFAS has proved extremely challenging. Transformation of polyfluorinated compounds in the environment and in isolated microcosms has been studied and has indicated pathways by which perfluoroalkyl acids are produced from precursor (i.e., polyfluorinated) compounds, yet the mechanisms have not been fully elucidated [99–104]. Transformation of perfluorinated compounds has rarely been observed; recently, an *Acidimicrobium* species was reported to defluorinate PFOA and PFOS, but results from preliminary studies have yet to be reproduced [3]. Similarly, PFOA and PFOS transformation have been reported in a fungal-based treatment system [105, 106], but defluorination was not substantiated and no further evidence has been reported in the literature.

Recently, the case has been made for consideration of enhanced attenuation (EA) processes for PFAS groundwater remediation [41]. While originally established as a framework in the early 2000s for chlorinated groundwater contaminants, identification of mass flux and travel time of PFAS from a contamination plume would help to identify sites that could benefit from EA strategies. Given that PFAS do not fully degrade in the environment, EA strategies would merely serve to sequester (i.e., permanent trapping of PFAS) and retain (i.e., storage for a limited amount of time) PFAS [41, 107–109]. However, this approach would still be useful in prioritizing treatment sites and evaluating exposure risk at sites with different characteristics.

1.7 Scope of Work

This work was initiated from the investigation of two PFAS treatment technologies; the first, a thermally-activated chemical process, and the second, a bio-activated chemical process. While seemingly quite different methods, the concept of both is the same: in the first, heat activates persulfate into sulfate radicals which are strong oxidizing agents capable of degrading persistent organic pollutants (POPs) [110]. This reaction is termed heat activated persulfate oxidation (HAPO) and is a widely applied method of in situ chemical oxidation (ISCO) [111–114]. In the second, a fungal multi-copper oxidase (MCO) enzyme

activates a small-molecule chemical mediator into nitroxyl radicals, also capable of degrading POPs [115–118]. This reaction is termed the laccase-mediator system (LMS).

In evaluating HAPO treatment for groundwater from sites contaminated with legacy AFFFs, we observed an artifact of PFOS removal that was not well understood or previously reported in the literature. It became evident that the high concentration of salts used in HAPO were causing PFOS losses in the treatment matrices that were not due to PFOS transformation or degradation. Following this observation, we investigated the mechanism of the salt effect and its origin in the surfactant physicochemical properties of fluorocarbon compounds (Chapter 2 & Chapter 3). In evaluating LMS treatment for PFAAs, which has recently been reported as a potential bio-based strategy for PFAA degradation [105, 106], we were unable to reproduce results supportive of PFAA transformation. This led to a systematic investigation of the LMS mechanism in an attempt to achieve successful treatment of PFAAs. While ultimately we were not able to prove that a LMS is capable of PFAA oxidation, we instead uncovered an important artifact of PFOA and PFOS removal in the treatment system which was attributed to sorption by the enzyme (Chapter 4).

PFAS are notoriously challenging to treat, and researchers are continually looking to new technologies as a boon for PFAS treatment– particularly, for the most recalcitrant perfluorinated carboxylic and sulfonic acids. The surfactant chemistry of PFAS, and the unique physicochemical properties associated with it requires that special attention be paid to the evaluation of PFAS treatment methods in order to prevent 'removal' from being equated with 'degradation'. Overall, this work provides insights into the complexities associated with PFAS chemistry and environmental remediation, and recommendations for how to leverage PFAS surfactant chemistry in designing and optimizing treatment systems.

Chapter 2

Aggregation and interfacial activity of perfluorooctanesulfonic acid (PFOS) in high ionic strength solutions

Parts of this chapter are included in the publication, "Under-reporting Potential of Perfluorooctanesulfonic acid (PFOS) under High Ionic Strength Conditions" (Steffens et al. 2021)

2.1 Synopsis

The surfactant properties of PFOS, namely, its critical micelle concentration and air-water interfacial activity, are influenced by the presence of salts in aqueous solution. This chapter describes how mono- and divalent salts affect PFOS solution behavior and the potential consequences to PFOS detection, accumulation, and transport in treatment and environmental matrices.

2.2 The salting-out phenomenon

The 'salting-out' phenomenon is commonly used to describe the decrease in aqueous solubility of non-electrolytes upon salt addition [119–123] and is frequently used in the context of protein and surfactant phase partitioning behavior [124–127]. Although numerous investigators of the common fluorinated surfactants per- and polyfluoroalkyl substances (PFAS) have used the term 'salting-out' to account for PFASs behavior in the environment [37, 44, 84], none have provided a thorough investigation of the salting-out phenomenon as it relates to PFAS detection in bulk solution. Some investigators have reported the effect of low concentration electrolytes on increasing interfacial activity of PFAS [24, 45–47], yet there has been no investigation of specific cation effects on interfacial activity and bulk solution behavior of PFOS.

PFAS surfactant properties pose unique challenges to both their environmental and experimental detection and monitoring. The interfacial behavior and critical micelle concentration (CMC) of fluorinated surfactants are influenced by counterions [128–131] and are critical properties for monitoring and modeling environmental fate [20, 21, 24, 49, 120]. Understanding the relationship between ionic strength and PFAS solution behavior can inform prediction of partition coefficients associated with air-water, soil-water, and, particularly important to PFAS contamination, non-aqueous phase liquid (NAPL)-water interfaces [28, 132].

We chose to focus on perfluorooctanesulfonic acid (PFOS) because it was one of the first detected, most environmentally persistent, and challenging to treat of the PFAS class [133–135] and has known toxicity effects in humans [63, 136, 137]. Despite its halt in production in the early 2000s, PFOS continually enters the environment via biological breakdown of precursor substances, compounding legacy contamination [134] and necessitating continued monitoring and treatment efforts. PFOS is sometimes present in high ionic strength conditions when accurate detection and monitoring are important. For example, in situ chemical oxidation (ISCO) often employs potassium or sodium persulfate concentrations as high as 0.7 M for remediation of chlorinated volatile organic compounds (cVOCs), which often co-occur with PFOS contamination [27, 112, 138]. Salt and PFOS are also present in brines from reverse osmosis (RO) and ion exchange (IX) treatments [139–141] and landfill leachate often contains high PFOS levels in high ionic strength conditions [142]. Further, PFOS may be present in saltwater impacted sites with high ionic strength [143] The detection and quantification of PFOS in high salinity matrices necessitates a better understanding of the relevance of the salting-out effect and warrants investigation of the associated mechanisms to improve transport models and detection accuracy.

The objective of this study was to assess the role of high ionic strength, with a focus on specific cation effects, in the salting-out and surface behavior of PFOS in aqueous solutions. We quantified PFOS in bulk solution under conditions typical of persulfate ISCO and in seawater and evaluated the effect of common mono- and divalent cations (K^+ Na^+, Mg^{2+}, Ca^{2+}) on PFOS behavior. To further evaluate the mechanism of the salting-out phenomenon, we measured surface tension isotherms of salt-containing PFOS solutions via pendant drop tensiometry. Surface activity and CMCs were calculated from the surface tension isotherms.

2.3 Materials & Methods

Chemicals

PFOS stock solutions were prepared from reagent grade perfluorooctanesulfonic acid (40% in H_2O (T)) from Sigma-Aldrich. All salts were purchased at the highest purity available from Sigma-Aldrich or Fisher Scientific. A PFAS analytical standard mixture containing PFOS (PFAC-MXA, 5 μg/mL in MeOH) and mass-labeled analogs containing sodium perfluoro-1-[1,2,3,4-$^{13}C_4$]octanesulfonate (MPFAC-MXA, 2 μg/ml in MeOH) was

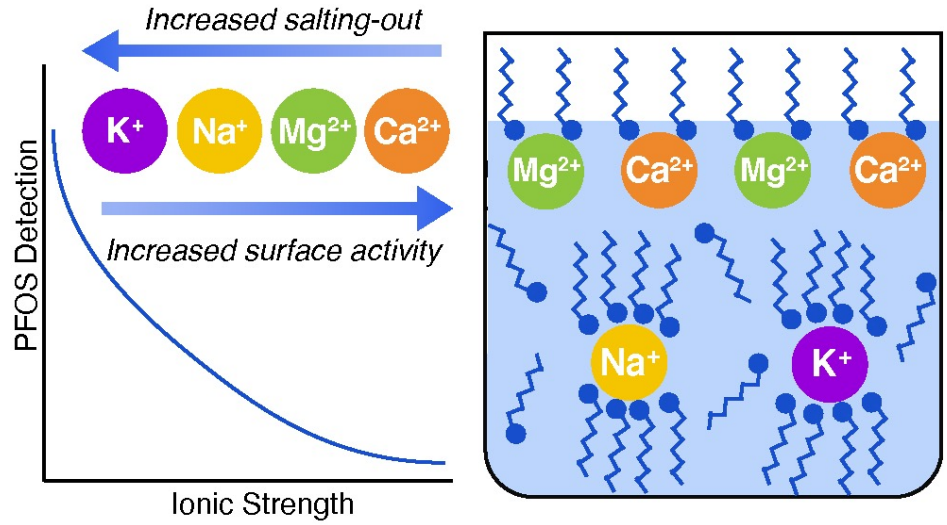

Figure 2.1: The presence of mono- and divalent cations in aqueous solution affects sorption of PFOS at the air-water interface and aggregation and detection of PFOS in the bulk solution.

obtained from Wellington Laboratories Inc. Ottawa sand (50-70 mesh particle size) was purchased from Millipore Sigma.

Sample Analysis

PFOS was quantified by LC-MS/MS equipped with electrospray ionization in negative mode (Triple Quad 6460A, Agilent Technologies) multiple reaction monitoring (MRM). Gas and Sheath Gas Heater temperatures were 325 and 350°C respectively. Gas and sheath gas flows were 9 L/min. The nebulizer was kept at 25 psi and the capillary voltage was 3.5 kV. Samples were prepared for analysis by dilution in MeOH to a target concentration of 10 μg/L to ensure quantification within the calibration range (0.2-10 μg/L). The isotope dilution method was used to account for any potential matrix effects. Mass labeled [^{13}C]-PFOS (2 μg/L) was added to LC-MS/MS sample vials for each sample in the final stage of sample preparation. Analytes were separated using a Zinc-Diol guard column coupled to Zorbax C18 XDB guard and analytical columns (Agilent Technologies). The mobile phase (0.4 mL/min) was 10-mM ammonium acetate in water (A) and 10-mM ammonium acetate in MeOH (B) with a solvent gradient: hold 0-2 min 90% A, ramp to 5% A by 8 min, hold 8-12 min 5% A, ramp to 90% A by 14 min, hold 14-18.5 min 90% A. During the first seven minutes, the flow from the column was diverted to waste to prevent accumulation of non-volatile salts at the ionization source and capillary. The LC-MS/MS setup includes delay C18 columns at the outlet of each of the pump heads to decrease contamination from PTFE components in the instrument. PFOS was quantified by the transition 499.0 $\rightarrow$ 80.0 (Collision Energy

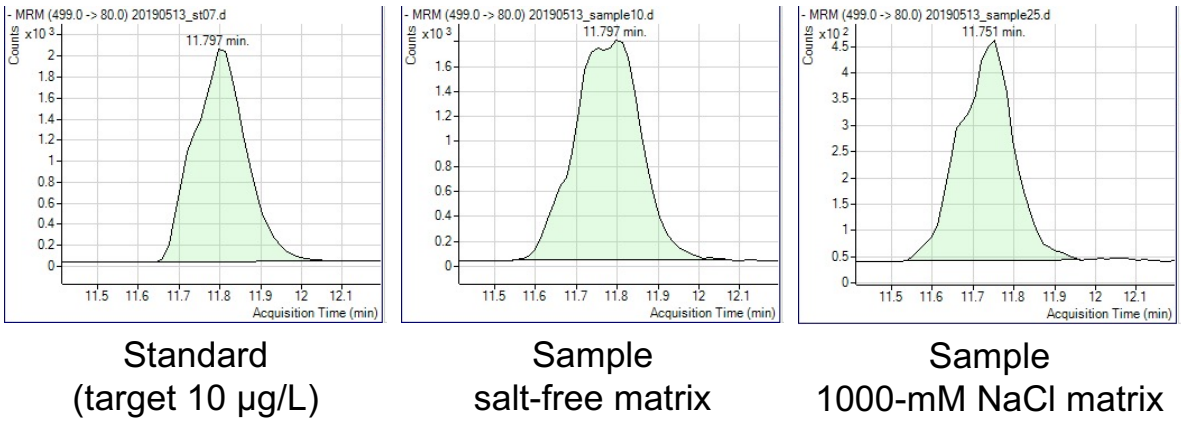

Figure 2.2: Observed PFOS retention time in a calibration curve standard, a salt-free sample, and a sample diluted from a high ionic strength solution.

(CE) 50 V), and the mass labeled PFOS (MPFOS) by the transition 503.0 → 80.0 (CE 60 V). Qualifier transition for PFOS was 499.0 → 90 (CE 80 V). The relative response of PFOS/MPFOS was used to build a calibration curve (0.2-10 μg/L, $R^2 \geq 0.99$). PFOS and MPFOS had a retention time close to 12 min. Mobile phase blanks were run every 10 samples and select calibration samples were re-run every 20 samples to prevent contamination or carryover in the analysis. The retention time for PFOS in standards, salt-free samples, and high ionic strength samples were compared to ensure accurate quantification. No major shifts in retention time were observed, as shown in Figure 2.2.

ISCO Experimental Set-up

PFAS-contaminated aquifer water and dried, homogenized, sieved aquifer solids (NAS Jacksonville, FL, 5-35' below ground surface) from Naval Air Station Jacksonville, FL were used and dosed with concentrated persulfate solution. Groundwater and solids were added to polypropylene 200 mL bottles in a one-to-one ratio (v/w). This slurry was subjected to a short peroxide pretreatment step to simulate a potential in situ strategy for persulfate heat-activation. Four total doses of sodium persulfate were each targeting 200-mM. Slurry samples were taken weekly, centrifuged at 10,000 g for 10 minutes, and supernatant was stored in a -20°C freezer in a one-to-one ratio of methanol for LC-MS/MS analyses. Bottles were kept in an incubator set to 37±3°C for continuous heat-activation of the persulfate and periodically mixed. Initial slurry pH was 5-6 and dropped to approximately 2 within three days from persulfate degradation.

Solids extraction assay to confirm recovery in high persulfate dosing experiment

To ensure PFOS was not merely adsorbing to solids in the ISCO experiments, we used a similar soil extraction method to the methods described in Houtz et al. [144]. Approximately 500 mg of soil samples from the final time point of high persulfate HAPO experiment were homogenized and placed in a 15 mL centrifuge tube. Then, 2.5 mL of 0.1% ammonium hydroxide in methanol was added to the soil samples. The centrifuged tubes were vortexed for 20 seconds, sonicated for 30 minutes, shaken on a rotating table (130 rpm) for two hours, and centrifuged at 5000 rpm for five minutes. Supernatant was pipetted to a new tube. This process was repeated two more times and the combined volume was dried and reconstituted with methanol. The tubes were vortexed for at least 10 minutes before further preparation for LC-MS/MS analysis. There is a total difference of approximately 0.9 µM (450 μg/L) PFOS between the first and final time point of the experiment; less than 0.02 μM (9 μg/L) PFOS was recovered from the soil extraction assay, suggesting that adsorption did not cause the PFOS decrease. The PFOS extracted from the soil extraction assay could be attributed to residual groundwater saturating the solids.

Bulk Solution Experiments

Bulk solution PFOS was quantified by LC-MS/MS. PFOS solutions were prepared in Milli-Q water in polypropylene centrifuge tubes, to which solid salts were added; solutions were left to equilibrate in a 37±3°C incubator for at least 3-hours after salt addition. Aqueous samples taken before and after salt addition were diluted in methanol to ensure that PFOS concentrations would be in the linear range of the LC-MS/MS calibration curve; therefore, the ionic strength of prepared samples was significantly lower than in the experimental conditions. The isotope dilution method was used to account for any potential matrix effects. Mass labeled [^{13}C]-PFOS (2 μg/L) was added to LC-MS/MS sample vials for each sample in the final stage of sample preparation. To evaluate salt effects, batch experiments were performed in 15- or 50-mL polypropylene centrifuge tubes or 150 mL polypropylene bottles. Milli-Q water was used to prepare all solutions, except for the solutions prepared in sea water. Seawater was collected (37º51'44.9"N 122º18'48.7"W) and filtered with a Corning 0.22 µM PES filter prior to preparing PFOS solutions. Seawater was characterized by ion chromatography (465-mM Na^+, 9.3-mM K^+, 59.1-mM Ca^{2+}). In bulk solution experiments, PFOS was added from a 5-mM stock solution. PFOS solutions were left to equilibrate in a 37±3°C incubator for at least 12 hours prior to salt addition. After salt-addition, PFOS solutions were left to equilibrate in a 37±3°C incubator for at least 3 hours. Aliquots from experiment bottles were centrifuged (10,000 *g*, 10 minutes, 25°C), then a portion (≤50% volume) of the aqueous sample was diluted in MeOH (50/50 v/v). For all prepared salt solutions (Na_2SO_4, NaCl, KCl, $MgCl_2$, $CaCl_2$) concentration loss was calculated by sampling and measuring PFOS concentration in prepared Milli-Q water solutions before and after salt addition. For quantifying concentration loss in the seawater solutions, one set of PFOS

solutions was prepared in Milli-Q water and one set was prepared in seawater; equal volumes of PFOS stock solution were added to equal volumes of seawater to obtain the range of target concentrations. Besides the persulfate treated solutions in the ISCO experiments, the pH of all high ionic strength solutions was between pH 7-8 due to the use of chloride salts (K^+ Na^+, Mg^{2+}, Ca^{2+}).

Surface Tension Experiments

Surface tension isotherms were measured using the pendant drop method on a KRÜSS tensiometer. Solutions used for surface tension measurements were prepared at least 24 hours prior to measurement. The CMC of PFOS was determined from the intersection a linear fit in the pre-CMC region of the vs. ln C plot and the surface tension minima [145–147]. The Szyszkowski equation (2.1) was fitted to the measured data to determine surface activity [45]:

$$\gamma = \gamma_0[1 - a \times ln(\frac{C}{b} + 1)] \tag{2.1}$$

γ_0 represents the surface tension of ultrapure water, C represents the bulk solution concentration, and a and b are fitted parameters related to the maximum surface excess and surface activity, respectively.

The fitted parameters a and b were determined using a non-linear regression using NumPy, SciPy, and Pandas packages in Python 3.8.5.

Langmuir-Szyszkowski equation fitting

The fitted parameters were determined using a non-linear regression using NumPy, SciPy, and Pandas packages in Python 3.8.5; workflow is summarized in Figure 2.3. Surface tension data was imported and the SciPy curve_fit function was used to calculate the parameters a and b in the Szyszkowski equation. The R^2 values for the fitted data were calculated using the r2_score function from the sklearn.metrics package. The data was fit in a limited range up to the apparent CMC in each of the conditions, to obtain the best fit. By determining the a and b parameters for the specific cations tested, the maximum surface excess and surface activity of PFOS was calculated using the Langmuir-Szyszkowski equation [45],

$$\Gamma = \frac{\gamma_0 a}{RT} \frac{C}{C + b} \tag{2.2}$$

where the term Γ represents the maximum surface excess as a function of the parameter a, and the parameter b is the surface activity of the as it relates to the free energy required to transport a surfactant molecule from the bulk solution to the air-water interface.

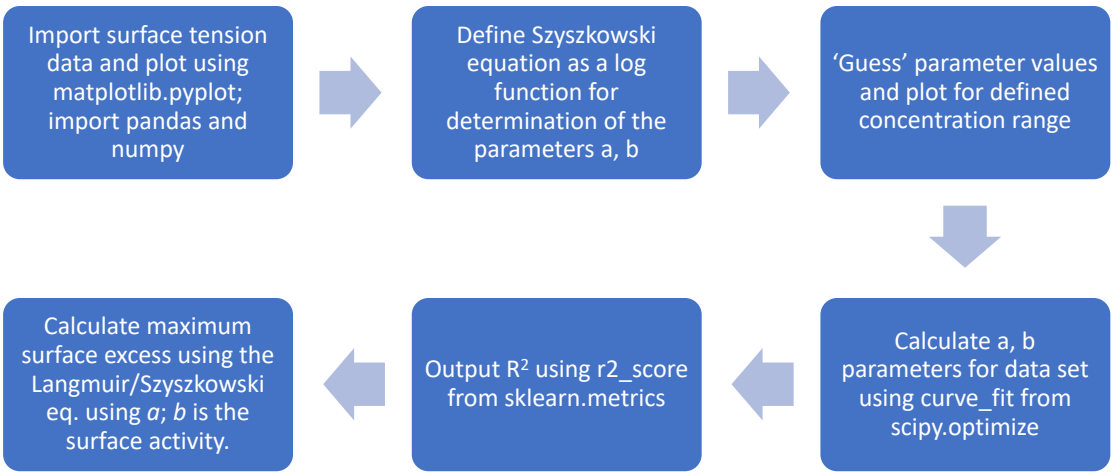

Figure 2.3: Workflow of fitting Szyszkowski equation parameters from surface tension isotherm data using Python.

Mass balance for bulk solution interfacial PFOS

To determine if the PFOS concentration decrease in bulk solution was due to settling out and interfacial adsorption of aggregates, we sampled a PFOS containing bulk solution before and after addition of 200-mM Na_2SO_4. Upon preparation, the solution was left to equilibrate for 24-hrs prior to taking a Pre-Salt sample. After Na_2SO_4 addition, we sampled the bulk solution 5-minutes post-salt addition and 24-hrs post-addition, allowing the centrifuge tubes housing the solutions to rest on the bench top between sampling. Centrifuge tubes were not agitated in any way prior to sampling. After 24-hrs, the bulk solution was decanted, and the tubes were freeze-dried. To extract PFOS adsorbed onto the walls of the centrifuge tubes (Interfacial PFOS), 20-mL of 50/50 MeOH/H2O was added to the tubes. The tubes were thoroughly shaken and an aliquot was taken for quantification via LC-MS/MS. The approximate mass in the Bulk PFOS versus Interfacial PFOS was calculated based on the solution volume at the time of sampling and concentration as determined via LC-MS/MS quantification.

Air-water interface film experiment

Following an experimental procedure described by Schaefer et al. [47], we assessed PFOS adsorbed at the air-water interface by quantifying PFOS in the air-water 'film' of a bulk PFOS solution. Solutions containing *ca.* 10 mg/L PFOS were prepared in 50-mL centrifuge tubes with a small hole drilled at the bottom which were temporarily closed with tape. Solutions were prepared in triplicate for ultrapure and 200-mM Na_2SO_4 matrices. Solutions were left to equilibrate on the bench top for 48-hours, after which the bulk solution was carefully drained into another centrifuge tube, and a portion of the film-containing volume was collected separately. We retained about 0.3 mL of the original volume and measured the exact film volume by weighing the collected solutions. The concentration of PFOS in the Bulk and Film portion were quantified after dilution in MeOH. The mass of PFOS sorbed at the air-water interface (Γ (mg m^{-2})) and the associated air-water partition coefficients (k_{aw} (m)) were calculated using the following equations,

$$\Gamma = \frac{M_f - CV}{A} \tag{2.3}$$

$$k_{aw} = \frac{\Gamma}{C} \tag{2.4}$$

where Γ is equal to the mass of PFOS sorbed at the air-water interface, M_f is equal to the mass of PFOS in the collected film (determined from the concentration of PFOS in the film sample and the volume of the film sample collected), C is the concentration of PFOS in the drained sample, V is the volume of the film sample, and A is the air-water interfacial area of the vessel (22.9 cm^2 for the 50 mL centrifuge tubes).

2.4 Results & Discussion

Decreased PFOS detection in ISCO experiments

PFAS in contaminated groundwater often exist in complex mixtures from years of AFFF use [148, 149]. Heat-activated persulfate oxidation, a type of persulfate ISCO, is capable of mineralizing perfluorocarboxylic acids (PFCAs), but it cannot transform PFOS [150, 151]. To test persulfate concentrations needed to transform PFCAs in aquifer conditions, ISCO experiments were conducted using a one-to-one mass ratio of aquifer solids to PFAS-contaminated groundwater. Sodium persulfate was added weekly for four weeks. At the end of the experiment, the ionic strength (I) had reached 3.43 M and the pH had fallen to approximately 2. Measured PFOS concentrations decreased by approximately 61% by the end of the experiment but an increase in shorter chain PFSAs from the initial time point was not observed (Figure 2.4).

After ruling out PFOS adsorption to the soil by extracting solids with basic methanol (see Materials & Methods), we conducted experiments to evaluate the effect of high ionic

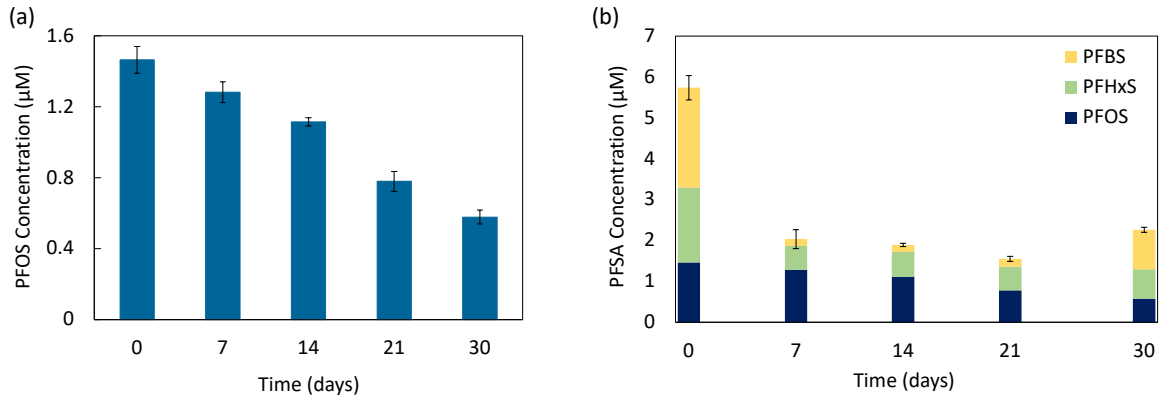

Figure 2.4: a) PFOS detection decreased weekly during a heat-activated persulfate ISCO test. Each week (Days 0, 7, 14, and 21), sodium persulfate was added to reach 200-mM persulfate. b) PFSA concentrations detected in reactors containing PFAS contaminated groundwater and solids from Naval Air Station Jacksonville, FL upon weekly dosing of 200-mM persulfate. Results from duplicate reactors are shown.

strength on PFOS measurements by using sodium sulfate as a control to sodium persulfate, without sulfate radical production.

Effects of pH and Ionic Strength on PFOS Detection

In order to mimic HAPO conditions and determine if $Na_2S_2O_8$ was responsible for the decrease in PFOS, we compared the effect of a 200-mM dose of $Na_2S_2O_8$ to a 200-mM dose of Na_2SO_4. Sulfuric acid was used to adjust the pH of the Na_2SO_4 amended solution to match the pH of the persulfate reaction. No chemical reaction was expected in the acidified Na_2SO_4 negative control. As shown in Figure 2.5 the PFOS concentration decreased immediately after dosing with $Na_2S_2O_8$ or Na_2SO_4, prior to any significant pH decrease in the solution. A similar PFOS concentration decrease was observed on Day 1 after salt addition in both conditions. After the initial decrease, the concentration remained relatively constant over the 5-day sampling period in both conditions.

The results of these experiments indicated that the PFOS concentration decrease was directly related to the salt addition and was not pH dependent. The insignificant effect of pH is likely related to the low pKa of PFOS. The calculated pKa of PFOS is -3.27, indicating that PFOS is a very strong acid [128, 152, 153]. Therefore, PFOS is expected to be fully ionized under the experimental conditions tested, and an increase in solution acidity to pH 1 would have a negligible effect on the ionization state of PFOS.

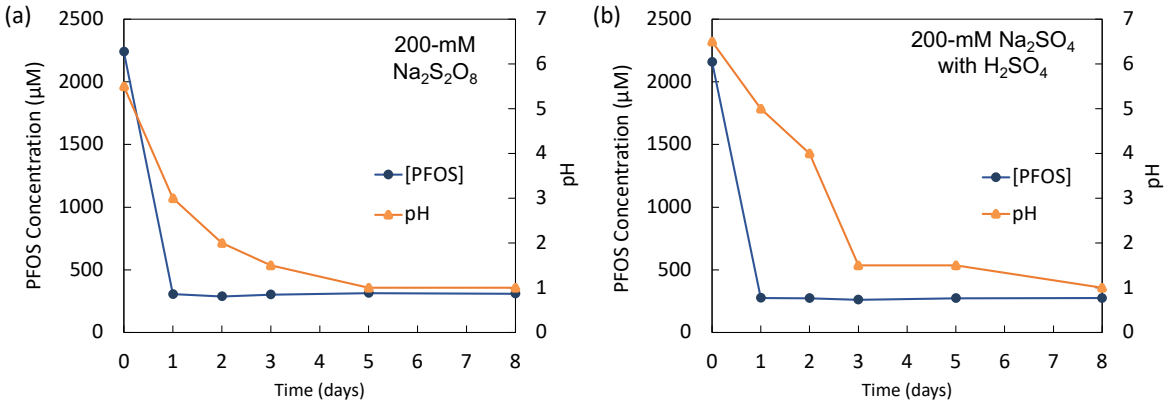

Figure 2.5: Change in PFOS concentration with pH decrease and an initial dose of (a) 200-mM $Na_2S_2O_8$ and (b) 200-mM Na_2SO_4. Bottles contained Milli-Q water, sand (50% w/v), and 2-mM PFOS. $Na_2S_2O_8$ and Na_2SO_4 were added after day 0 sampling; H_2SO_4 added after day 1 sampling to Na_2SO_4 condition only.

Effects of solids on PFOS detection

Control experiments with PFOS solutions containing a one-to-one ratio of sand to Milli-Q water and up to 1000-mM Na_2SO_4 ($I = 3$ M) indicated that detectable PFOS concentration in bulk solution decreased with and without sand, suggesting that sand was not simply adsorbing the PFOS (Figure 2.6). Among the three Na_2SO_4 concentrations studied, and compared to a salt-free control, no differences were observed between the bulk solution concentration of PFOS in the sand and sand-free reactors.

Sample preparation artifacts

To analyze the potential effect of subsampling from the experiment bottles, and to evaluate if sorption to the container could be driving observed decreases in PFOS concentration in the bulk solution, we performed full bottle extractions with MeOH in parallel with the routine sample preparation of solution aliquots. Results from the subsampling versus full bottle extraction experiment are shown in Figure 2.7. Surprisingly, almost no difference in PFOS concentration was observed after salt addition in the subsample or the full bottle extraction 3-hours after salt addition, despite that previous results indicated a sharp decrease in PFOS under equivalent conditions. We hypothesized that centrifugation of the aqueous solution, a step which was eliminated in this experiment due to the lack of solids, might be impacting the PFOS concentration in bulk solution.

To evaluate if the PFOS concentration decrease in bulk solution occurred in the aqueous sample centrifugation step, we analyzed the concentration detected in aqueous samples upon salt addition, with and without a centrifugation step. When a 25 mg/L PFOS solution was

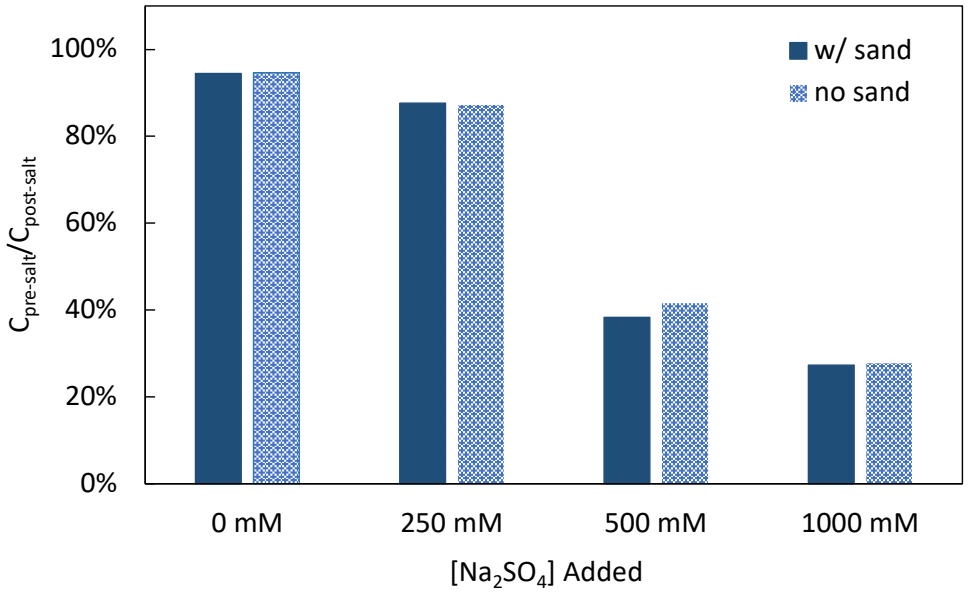

Figure 2.6: Detected PFOS concentration in bulk solution before and 1-hour after Na_2SO_4 addition, in reactors with and without sand. Initial PFOS concentration was ca. 10 mg/L; 250 to 1000-mM Na_2SO_4 was added as a solid. Values are averages of samples from duplicate reactors.

prepared in 500-mM Na_2SO_4 solution, only 40% of the added PFOS was detected after centrifugation at 10,000 *g*, whereas a 101% recovery was obtained in the non-centrifuged solution (Figure 2.8). Storing the salt-containing PFOS solution on a bench top for 24 hours prior to sampling the bulk solution yielded losses similar to those observed for the centrifuged solutions (Figure 2.8), which suggested that phase separation of PFOS in the bulk solution could also occur over time, in the saline conditions.

We found that the PFOS mass 'loss' upon centrifugation could be recovered by extracting the reaction tubes with methanol at the 24-hour time, confirming that the salt addition was causing phase separation of PFOS from the bulk solution. Other researchers have identified PFOS 'salting-out' processes in and resulting decreases in measured PFOS concentrations in brackish water- clay systems [38] and marine estuaries [39], as well as identified micelle formation or hemi-micelle formation as physical processes occurring in certain PFAS containing matrices [84, 154–156]. However, these studies lacked a mechanistic investigation of salting-out effects and quantitative analysis of aggregation and interfacial sorption. The following experiments describe our attempt to address those data gaps and present a more thorough evaluation of the salting-out phenomena and specific salt effects on aggregation and interfacial activity of PFOS in aqueous solutions.

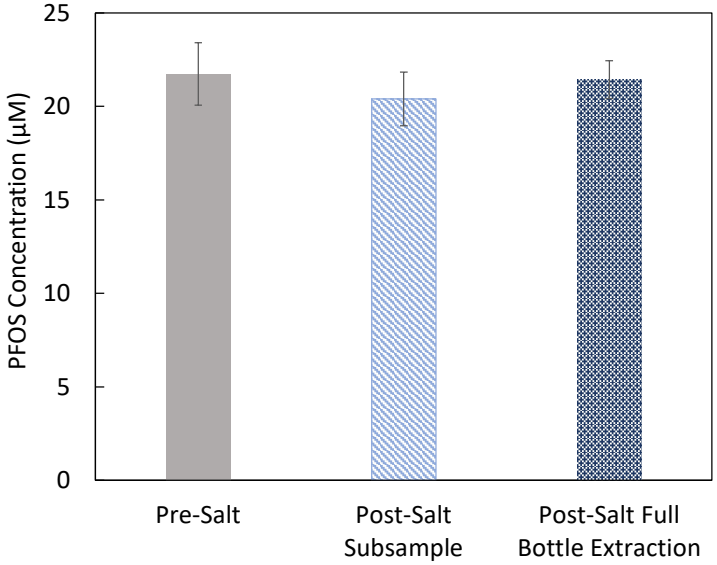

Figure 2.7: PFOS concentration detected pre-salt addition and post-salt addition, detected in an aliquot (subsample) and from a full bottle extraction. Reaction bottles were prepared in duplicate; samples were taken three hours after salt addition (1000-mM Na_2SO_4) in triplicate. Aqueous aliquots were removed and diluted in MeOH (2x dilution), then MeOH was added to the reaction bottle (2x dilution). Samples were centrifuged after dilution in MeOH. Values and error bars represent averages and standard deviations of six samples.

Validating detection loss of PFOS in high salinity environmental waters

While effects of high ionic strength are relevant to ISCO treated water matrices, we were interested in evaluating salting-out effects in a high salinity, natural water matrix. To this end, we measured and compared a range of PFOS concentrations in two high salinity matrices: a 200-mM Na_2SO_4 solution and seawater collected from the San Francisco Bay. We observed a significant loss of PFOS in both matrices at PFOS concentrations >5 mg/L, the loss ranging from 2-38 mg/L, that was dependent on the initial concentration of PFOS in Milli-Q water (Figure 2.9). At PFOS concentrations <5 mg/L, the concentration decrease was in the range of 0.2-0.6 mg/L, likely primarily due to container-water interfacial sorption. The concentration loss in seawater was generally higher than in the Na_2SO_4 solutions, which may be attributed to the presence of Ca^{2+} leading to enhanced surface activity and aggregation of PFOS.

The apparent loss of PFOS at relatively high concentrations tested (i.e., > 5 mg/L) is relevant to PFAS source zones such as AFFF-impacted firefighter training areas (PFOS levels reported up to 8.97 mg/L) [157]. A majority of ISCO projects (approximately 70%,

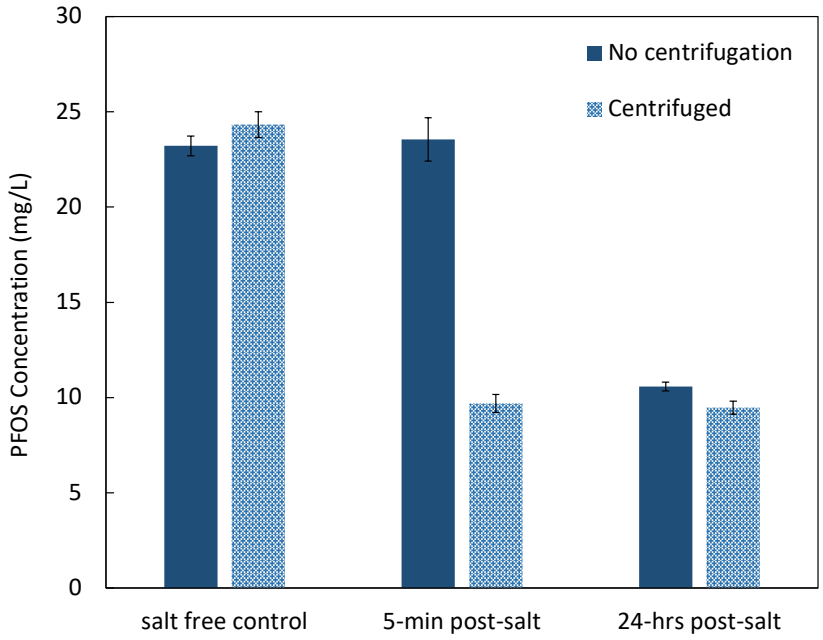

Figure 2.8: Effect of centrifugation of aqueous samples on PFOS detected in bulk solution. Initial PFOS concentration was ca. 25 mg/ L; 500-mM Na_2SO_4 was added. Error bars represent the standard deviation of triplicate samples.

n=215) have been conducted for treatment of chlorinated solvents, which are also commonly found in high concentrations at firefighter training sites, airports, and industrial sites [158]. Because PFAS and chlorinated solvents can coexist at these sites, it is possible that ISCO projects have inadvertently affected the behavior and detection of PFOS.

Mono- and divalent salts impact PFOS salting-out and interfacial accumulation

To assess the effect of specific cations on PFOS behavior, we tested chloride salts of sodium, potassium, magnesium, and calcium with an initial PFOS concentration of ca. 10 mg/L (Figure 2.10). Addition of monovalent salts caused decreases in measured PFOS concentration up to 68% and 83% for 1000-mM NaCl and KCl, respectively. For the divalent salts, the magnitude of PFOS decrease did not vary as significantly among the salt concentrations or cations tested; the maximum PFOS decreases were 25% and 26% for 1000-mM $MgCl_2$ and $CaCl_2$. This suggests that the monovalent salts cause a greater degree of 'salting-out' (i.e., decreased solubility) than the divalent salts due to the increased hydrophobic interactions between the bulk water molecules and the perfluorinated chain [159,

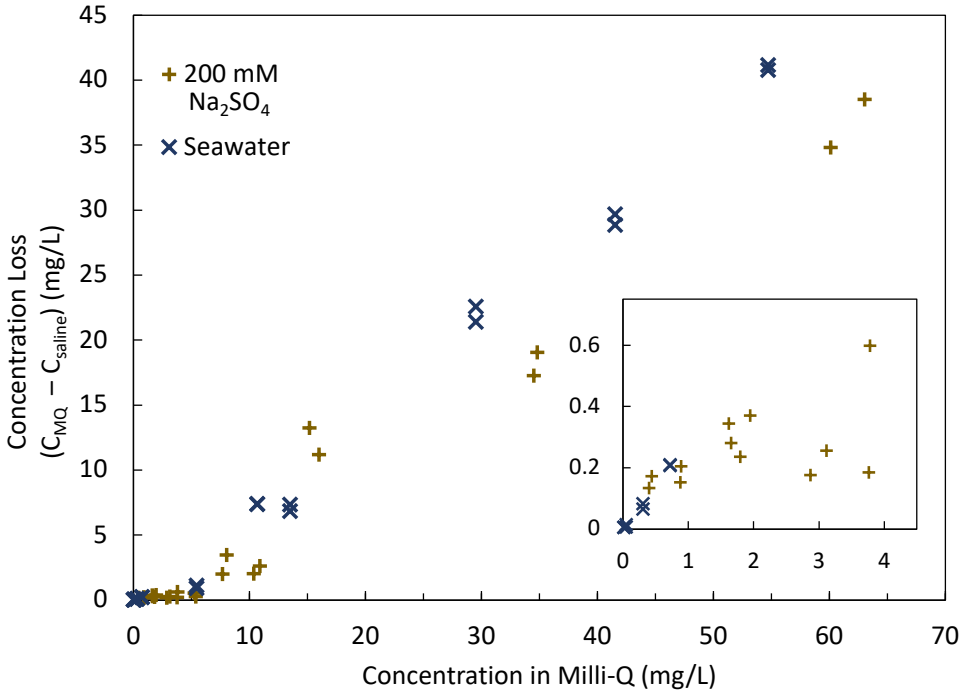

Figure 2.9: PFOS concentration loss in saline bulk solution compared to PFOS concentration detected in Milli-Q. For the Na_2SO_4 data, samples were taken from the same solution bottle before (C_{MQ}) and after (C_{saline}) salt addition. For the seawater data, PFOS was added to seawater (C_{saline}) and Milli-Q water solutions (C_{MQ}) in parallel and compared. Results from duplicate conditions are shown.

160].

To determine the extent to which PFOS reduction in bulk solution was due to accumulation of molecular or aggregated PFOS to the solution tubes, a mass balance experiment was conducted (described in Materials & Methods). We observed that 24-hours after salt addition, the reduced mass of PFOS in the bulk solution was accounted for by 'Interfacial' PFOS (i.e., PFOS sorbed to the polypropylene centrifuge tube) (Figure 2.11). This suggests that salt addition induces phase separation of aggregated PFOS from the bulk solution, driving uptake of PFOS to the water-container interface. In high salinity environmental matrices, increased solid-phase interfacial uptake may enhance PFOS retardation and lead to long term source zones [20, 21, 28, 49, 132].

Additionally, PFOS accumulation at the air-water interface was measured in an experiment similar to those described by Schaefer et al.14. Analysis of PFOS associated with the solution 'film' layer was quantified to determine the mass of PFOS sorbed at the air-water interface and calculate air-water partition coefficients (k_{aw}). The mass of PFOS sorbed at

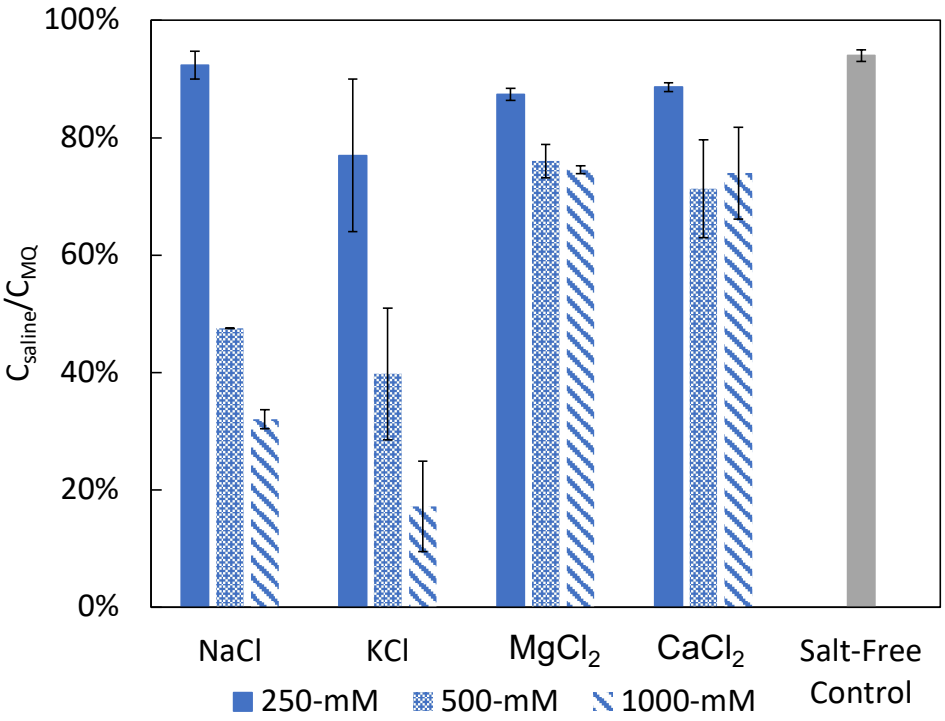

Figure 2.10: Effects of 250-1000-mM monovalent and divalent salts on PFOS detected in bulk solution. PFOS concentrations in Milli-Q water prior to salt addition were *ca.* 10 mg/L; PFOS concentration was measured before (C_{MQ}) and three hours after (C_{saline}) salt addition. No salt was added to the control. Error bars represent the standard deviation of triplicate samples.

the air-water interface, on the order of 0.252-0.536 mg m^{-2} for the Milli-Q water and 200-mM Na_2SO_4 solutions, respectively, was not appreciable compared to the mass decrease observed in bulk solution (Table 2.1). However, the corresponding k_{aw} values for the Milli-Q and 200-mM Na_2SO_4 solutions indicate that sorption at the air-water interface increases in the saline matrix, which agrees with findings reported by Costanza et al. [45]

Decreased critical micelle concentration and increased interfacial activity of PFOS

Although the PFOS concentration was well below its reported CMC (i.e., 2,750-4,250 mg/L PFOS) [128, 161], inorganic salts are known to decrease the CMC and increase aggregate size for ionic surfactants [119, 126, 162–166]. For example, the CMC of the ammonium salt of perfluorooctanoic acid (PFOA), the carboxylic analogue of PFOS, decreased by 22%

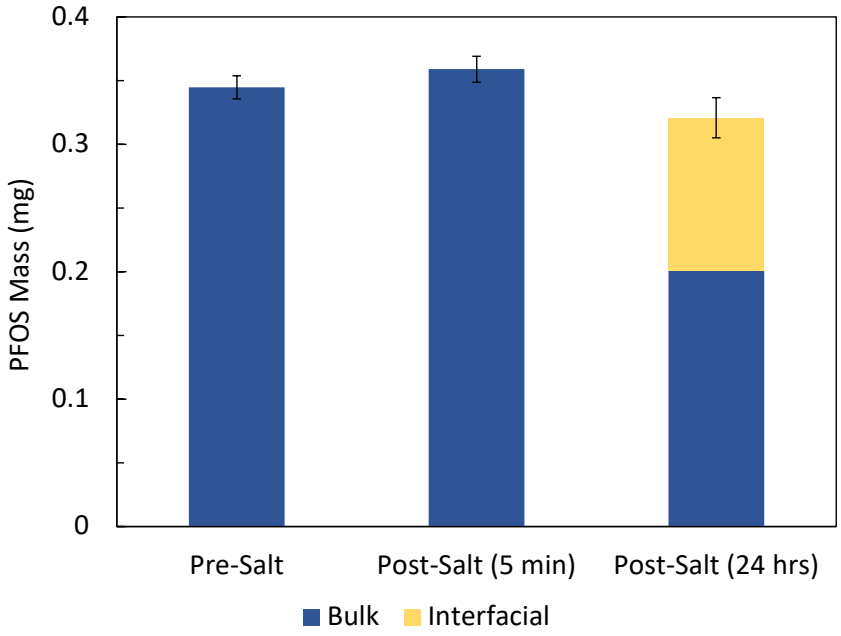

Figure 2.11: Mass balance for PFOS upon salt addition. PFOS concentration in the bulk solution was measured before, 5-minutes after, and 24-hrs after salt addition (200-mM Na_2SO_4). Adsorption of PFOS to centrifuge tubes was measured after 24-hrs to determine 'Interfacial' PFOS as described in the Supporting Information. Error bars are the standard deviation of triplicate samples.

	Γ (mg m^{-2})	**k_{aw} (m)**
Ultrapure	0.252 ± 0.051	2.24E-0.2 ± 5.1E-03
200 mM Na_2SO_4	0.536 ± 0.269	7.94E-02 ± 4.2E-02

Table 2.1: Air-water partitioning coefficients in saline and ultrapure matrices

in a 50-mM NaCl solution [160]. For the anionic surfactant sodium dodecyl sulfate (SDS), the CMC decreased by 42% in a 25-mM NaCl solution, and up to 85% and 87% with 20-mM KCl and 25-mM $Mg(ClO_4)_2$, respectively [167]. While specific salt effects in relation to the CMC and bulk solution behavior of PFOS have not been well documented, formation of PFOS aggregates in the presence of mineral surfaces [83] and Fe (II/III) oxides [168] has been observed, even at concentrations below the CMC. The high Na^+ concentration used in the ISCO and sodium sulfate experiments may have led to formation of aggregates in the aqueous phase that were separated from bulk solution via centrifugation, or even by gravity after sitting for 24 hours at room temperature, due to the high density of perfluorocarbons (1.25-1.6 g/cm^3) [169, 170].

Previously, Costanza et al. [45] reported increased surface excess of PFOS and decreased surface tension in PFOS solutions containing a mixture of major cations found in groundwater. Schaefer et al. [47] reported a minimal impact of 10-mM NaCl on PFOS air-water partitioning behavior at low PFOS concentrations. To add to the established effects of cations on PFOS interfacial behavior and to address the effect of specific cations, we measured surface tension isotherms of PFOS solutions containing 500-mM NaCl, KCl, $MgCl_2$ and $CaCl_2$. We observed significant reduction in surface tension in the presence of the divalent salts, with apparent reduction of CMCs to 172 mg/L and 98 mg/L for Mg^{2+} and Ca^{2+} respectively, compared to 1530 mg/L for PFOS in ultrapure water (Figure 2.12, Table 2.2). K^+ also significantly reduced apparent CMC to 1021 mg/L, while Na^+conditions indicated an apparent CMC of 1860 mg/L. We suspect that the actual CMC of the free acid is higher than the CMC of PFOS in the NaCl solution; however, reduced drop stability for highly concentrated PFOS solutions, particularly in ultrapure water, may have caused this apparent result. Previously reported data on the CMC of the free acid PFOS is sparse, although the CMC of the potassium and sodium salts of PFOS has been reported in the range of 2,750-4,250 mg/L, as mentioned earlier in the text.

The Szyszkowski equation [28, 45, 171] was used to fit the surface tension data and determine surface activity and surface excess parameters (see Materials & Methods). Results from this analysis indicate that Mg^{2+} and Ca^{2+} drive greater surface excess (Γ) of 1.92 and 2.29 mg/m^2, compared to Na^+ and K^+, for which surface excess was 1.29 and 1.35 mg/m^2, respectively (Table 2.3). This agrees with previous findings by Brusseau and Van Glubt [21] that a divalent cation ($CaCl_2$) increased surface activity of PFOA more so than monovalent cations (NaCl, KCl).

The significant decrease in PFOS detection in saline conditions, at concentrations below the CMC, suggests that aggregation is occurring in the pre-micellar region, a phenomenon that has been previously reported [172–174]. Furthermore, there may be some difference in aggregate geometry associated with specific cation-PFOS interactions that contributes to the concentration differences observed in bulk solution. For example, divalent cations can act as bridging cations between anionic PFOS head groups, affecting the curvature of the aggregate formed [165, 175] whereas monovalent aggregates interact through other mechanisms. Further research is needed to characterize structural differences of the aggregates in the presence of different cations.

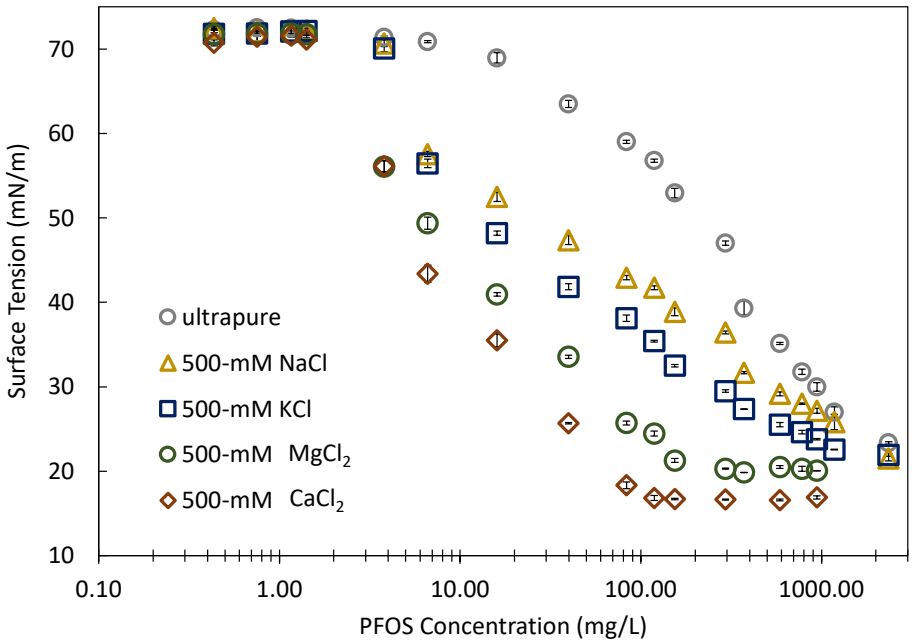

Figure 2.12: Surface tension isotherms for PFOS in 500-mM salt solutions at 22°C. Surface tension values are the average of three drop measurements, error bars indicate the standard deviation. The addition of monovalent (Na^+, K^+) and divalent cations (Mg^{2+}, Ca^{2+}) lowers the surface tension of the solutions below that of PFOS at equivalent concentrations in ultrapure water.

	$\partial\gamma/\partial \ln C$	y-intercept	IFT Minima (mN/m)	ln(CMC)	CMC (mg/L)	R^2
ultrapure	-12.592	115.7	23.36	7.333	1530	0.9941
500 mM NaCl	-6.753	72.842	22	7.5281	1860	0.9922
500 mM KCl	-6.0854	64.086	21.92	6.929	1021	0.9809
500 mM $MgCl_2$	-8.8324	65.811	20.31	5.151	172	0.9953
500 mM $CaCl_2$	-9.9881	62.621	16.84	4.583	98	0.9986

Table 2.2: Summary of apparent CMCs of PFOS in the experimental conditions. Linear fits for the $d\gamma/dC$ curves were obtained in the pre-CMC region after a significant drop in surface tension was observed (i.e., below 70 nM/m) to obtain the best fits.

	γ_0 (mN/m)	Fit Range (mg/L)	*a*	*b*	Γ_{max} (mg/m^2)	R^2
ultrapure	72.24	40-1200	0.2084	58.27	3.04	0.990
500 mM NaCl	72.29	6-1000	0.0887	0.827	1.295	0.991
500 mM KCl	71.9	6-800	0.0908	0.473	1.350	0.988
500 mM $MgCl_2$	72.01	4-160	0.132	0.719	1.919	0.994
500 mM $CaCl_2$	71.81	4-120	0.158	0.778	2.286	0.968

Table 2.3: Summary of fitted parameters from the Szyszkowski equation and the calculated maximum surface excess values (Γ_{max}). Modeling and calculations are detailed in the Materials & Methods section.

To further explain this effect, the interfacial tension and interfacial activity are related to cation interactions with the polar monomeric headgroup (e.g., the carboxylate or sulfonate moiety), while the 'salting-out' effect is primarily caused by hydrophobic interactions of bulk water molecules with the monomeric fluorinated chain [160]. The difference in these two effects may explain the seemingly contradictory observations that monovalent salts (e.g., NaCl, KCl) more substantially decrease PFOS in the bulk aqueous phase, while divalent salts (e.g., $MgCl_2$ and $CaCl_2$) more substantially increase PFOS adsorbed at the air-water interface and induce aggregation at lower concentrations, lowering the CMC.

2.5 Environmental implications of PFOS salting-out and interfacial behavior

The interfacial accumulation of PFAS has come under increased scrutiny as researchers aim for a comprehensive picture of PFAS transport and attenuation in the environment. Work by Costanza et al. [45, 46], has investigated interfacial accumulation of PFOA, PFOS, and AFFF at air-water and NAPL-water interfaces, and proposed the Langmuir-Szyszkowski model as a tool for mathematical modeling. Brusseau [21], Lyu et al. [49], and Brusseau and van Glubt [24] have evaluated partitioning behavior in the vadose zone, where the potential for interfacial accumulation, particularly air-water interfacial accumulation, is high especially in dilute contamination zones. Schaefer et al. [47] further investigated interfacial accumulation and air-water partitioning coefficients in dilute PFAS containing solutions,

and evaluated the validity of the Langmuir-Szyszkowski model in comparison with the Freundlich model. The complexities arising from the concentration dependent effects inherent to surfactants, magnify the challenges associated with accurate modeling and quantification of interfacial behavior. This is compounded by the fact that environmental factors, namely, ionic strength and specific salt concentrations, may greatly impact the aggregation and interfacial behavior.

In this study, we found that at sufficiently high PFOS concentrations (i.e., above 5 mg/L), the salting-out effect can lead to under-reporting of PFOS concentrations under high ionic strength conditions. The effect of decreasing PFOS in bulk solution was strongest for monovalent salts, namely Na^+ and K^+. The effect of salt on increasing PFOS surface activity– a factor critical to fate and transport– was stronger for divalent cations (i.e., Mg^{2+} and Ca^{2+}) relevant to monovalent cations. These results suggest that the presence of monovalent salts is more relevant for sampling artifacts in bulk solution. The presence of divalent salts are more important for modeling partition coefficients and informing transport studies, particularly of PFOS in unsaturated zones [20, 28, 49]. Further investigation is needed to determine how salts affect PFAS under the complex conditions encountered at contaminated sites. For example, AFFF also contains hydrocarbon-based surfactants and solvents, such as diethylene glycol butyl ether (DGBE). Salts may also affect the behavior of shorter and longer chain PFAS (e.g., perfluorohexanesulfonic acid and perfluorodecanesulfonic acid). Finally, it may be possible to exploit salt induced aggregation behavior as a means of enhancing the removal of PFOS and other PFAS from hazardous waste and other matrices that contain high concentrations of contaminants.

While not as obviously applicable to PFAS, compared to biodegradable TCE or BTEX which can be fully mineralized [176, 177], monitored natural attenuation (MNA) or enhanced attenuation (EA) is receiving interest in its applicability to managing PFAS contamination [41, 107, 108]. As research informs how physicochemical properties of PFAS and solution properties can influence PFAS retention in contaminated source zones, retention may in fact prove to be a valuable tool in sequestering PFAS and preventing downstream contamination. The complex nature of PFAS contamination will continue to challenge researchers in developing practical and applicable solutions to their management, and understanding their physicochemical properties and retention mechanisms will aid in addressing these challenges.

2.6 Supporting Information

Additional Specific Cation Effects

In addition to the bulk solution effects with specific salts presented in the main text, additional salting out studies were conducted to evaluate the cation-specific effect. Specifically, Li^+ and NH_4^+ salts were evaluated. Results from these studies are detailed in Figures 2.13, 2.14, 2.15.

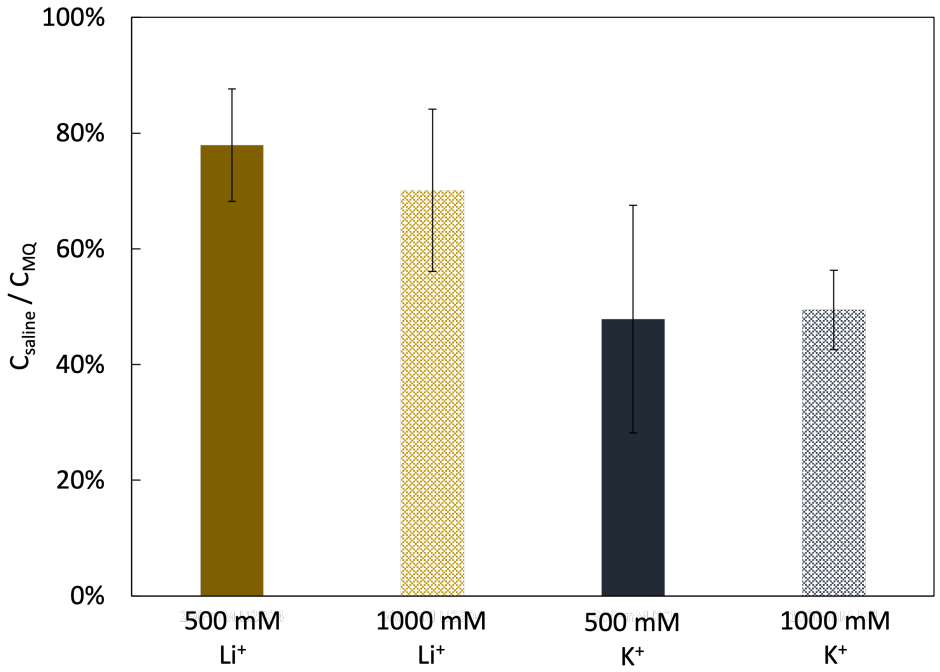

Figure 2.13: Decrease in detectable aqueous phase PFOS concentration with addition of 500- and 1000-mM Li^+ (as Li_2SO_4) and K^+ (as KCl). K^+ results in greater losses of PFOS in bulk solution compared to Li^+, due to differences in the bulk water structure and resulting hydrophobic interactions with the fluorocarbon chain of PFOS. Error bars represent standard deviations for duplicate reactors.

Addressing Bulk Sampling and Sample Preparation Artifacts

In the process of evaluating salting-out effects, we addressed questions related to the reactor sampling and sample preparation procedures. Because of the interfacial sorption and aggregation properties of PFAS, we wanted to confirm that we were not losing PFOS in the sample dilution procedure (which was necessary for LC-MS/MS analysis), or in the centrifugation procedure which was required for solid-containing samples. Results of sample dilution in MeOH (Figure 2.16), and of tests to determine the effect of centrigutaion force and temperature on detected PFOA and PFOS concentrations (Figures 2.17, 2.18, 2.19) are summarized.

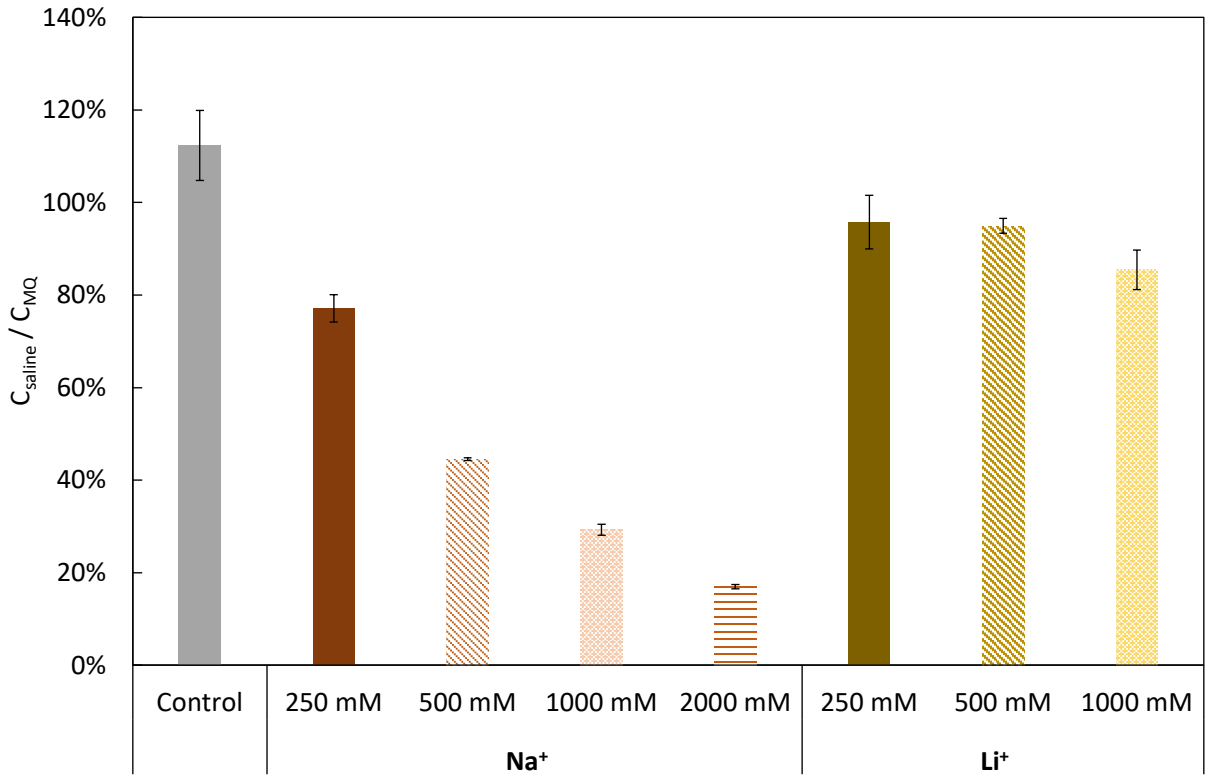

Figure 2.14: Decrease in detectable aqueous phase PFOS concentration with addition of 250-2000-mM Na^+ (as NaCl) and Li^+ (as LiCl). Aqueous phase concentrations were measured 5-minutes after salt addition in a centrifuged sample aliquot. Error bars represent standard deviations of duplicate samples.

Effects of pH and high ionic strength on detected PFOA concentration in bulk solution

Upon observing decreased detection of PFOS in high ionic strength matrices, we initially evaluated both PFOA and PFOS to try to understand the mechanism of the effect. In submitting PFOA to HAPO-like conditions, we did not observe significant changes in detected PFOA concentration over a 'treatment-course', unlike the PFOS losses observed (Figure 2.4). We therefore focused on evaluating PFOS salt effects in the investigation that followed.

Surface tension studies for PFOS in 50-mM specific salt solutions

In addition to the surface tension studies presented in the main text, we evaluated the surface tension isotherms of PFOS in 50-mM salt solutions. The surface tension isotherms

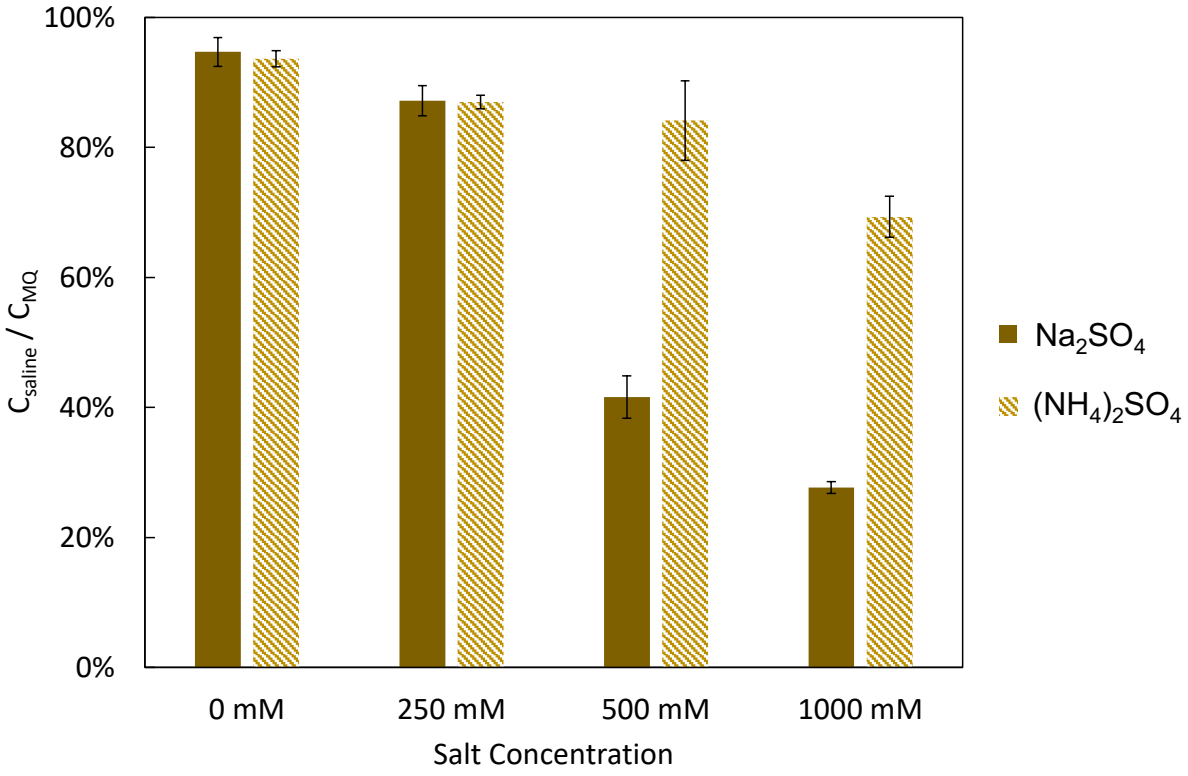

Figure 2.15: Decrease in detectable aqueous phase PFOS concentration with addition of 250-1000-mM Na_2SO_4 and $(NH_4)_2SO_4$. Only at the highest $(NH_4)_2SO_4$ concentrations tested (i.e., 1000-mM), were significant decreases in PFOS concentration observed. Samples were taken 1 hour after salt addition, and the aqueous sample was centrifuged prior to dilution for analysis.

(Figure 2.21), linear fits in the range in which the surface tension decreases (Figure 2.22, and parameters determined from fitting the Langmuir-Szyszkowski equation (Table 2.4) are included for the 50-mM salt data. Note that the trends are the same as those observed in the 500-mM salt conditions, but the aggregation effect is magnified at higher salt concentrations. Also note that the following experiments were done with PFOS solutions prepared from the potassium salt of PFOS (K-PFOS), but are not expected to deviate significantly from experiments performed with the free-acid PFOS because of the high acidity dissociation constants of both forms (Costanza 2019).

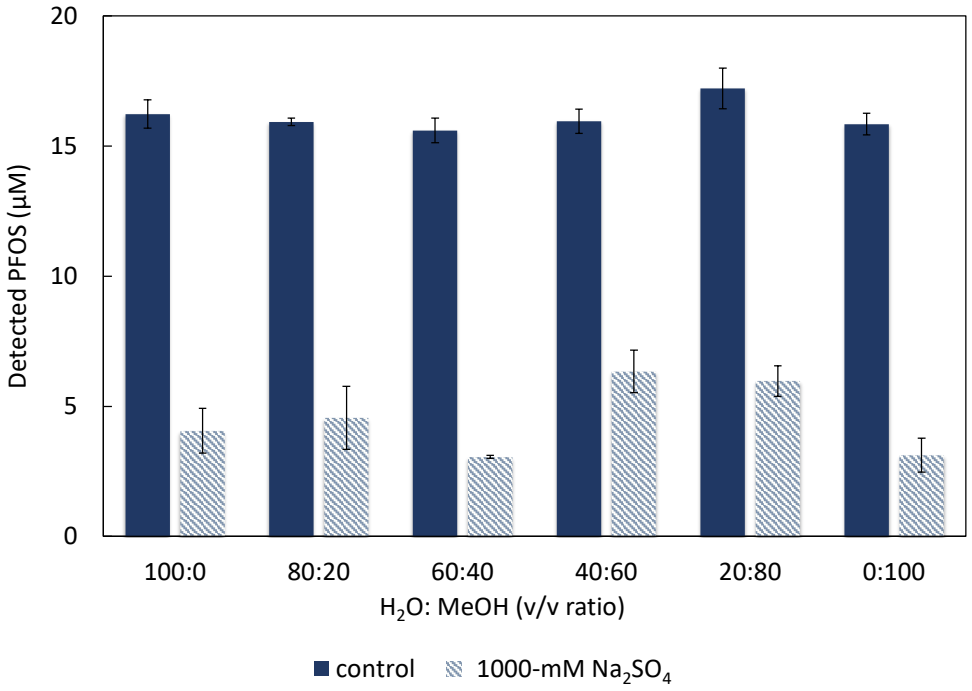

Figure 2.16: Effect of the methanol/water dilution ratio on detected PFOS concentration. After sampling and centrifuging an aqueous PFOS containing sample, an aliquot was diluted into the specified ratios of methanol/water. The low detection in the salt containing samples (1000-mM Na_2SO_4), regardless of the dilution matrix, indicates that PFOS losses were occurring primarily before subsequent dilution. However, the dilutions containing 60% methanol also yielded the highest PFOS detection levels, emphasizing the importance of proper dilution procedures to avoid artificial losses during sample preparation.

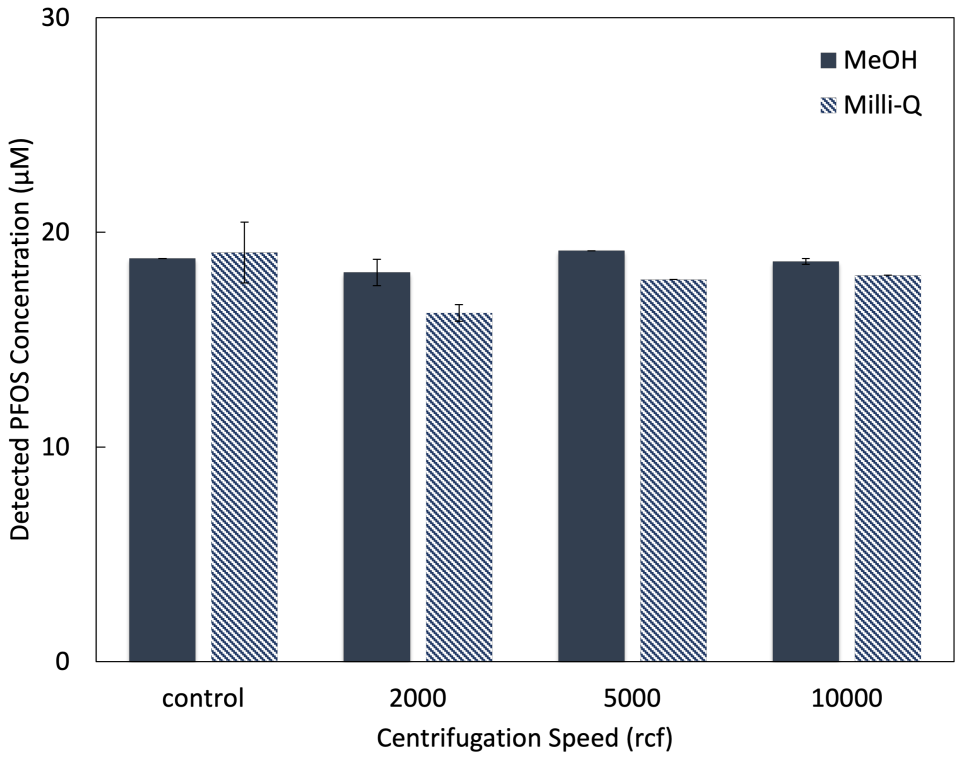

Figure 2.17: Effect of centrifugation force (2,000-10,000 rcf) compared a non-centrifuged control on detected aqueous PFOS concentration in samples diluted in 50/50 MeOH/H2O (v/v). Samples were centrifuged at room temperature. Results indicated that after dilution in MeOH/H2O, recovery is consistent across the centrifugation forces tested.

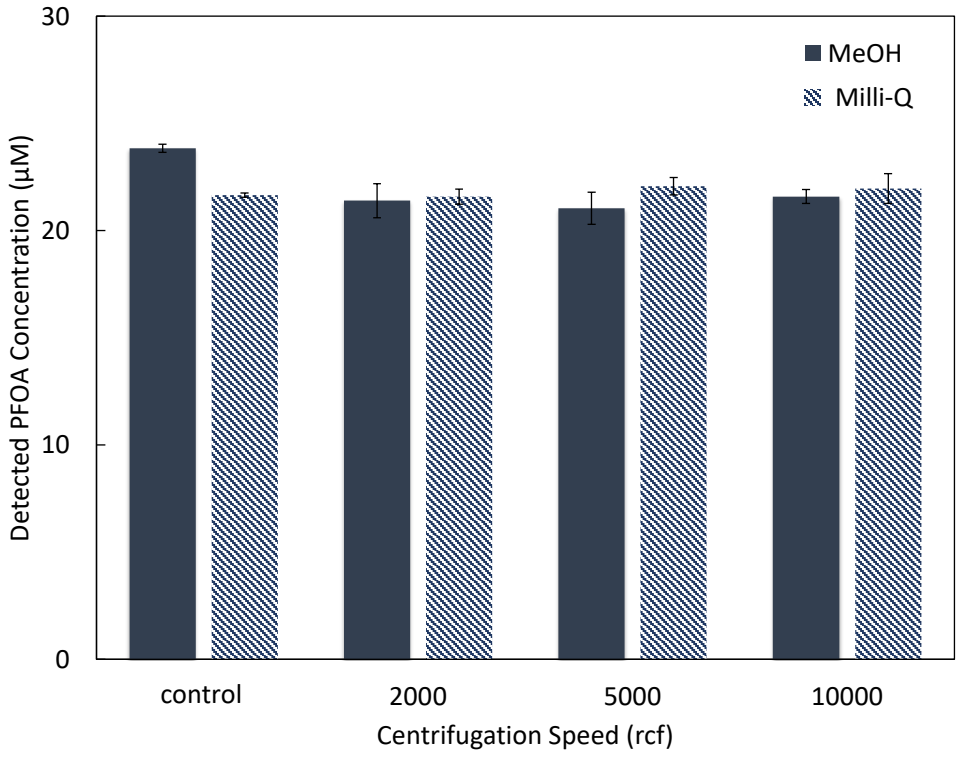

Figure 2.18: Effect of centrifugation force (2,000-10,000 rcf) compared a non-centrifuged control on detected aqueous PFOA concentration in samples diluted in 50/50 MeOH/H2O (v/v). Samples were centrifuged at room temperature. Results indicated that after dilution in MeOH/H2O, recovery is consistent across the centrifugation forces tested.

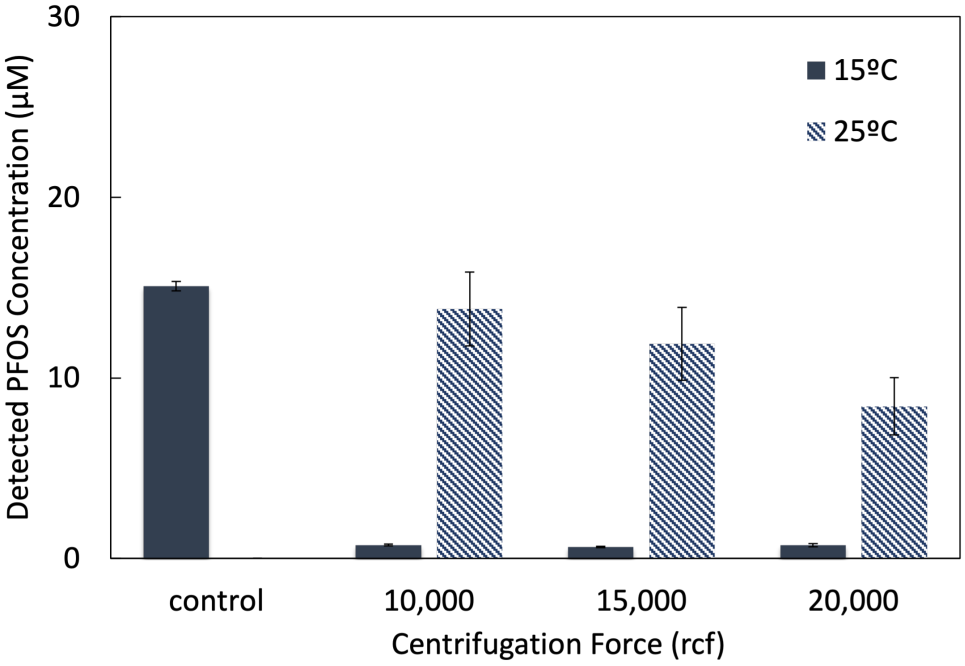

Figure 2.19: Effect of centrifugation temperature (15ºC and 25ºC) and high force (10,000-20,000 rcf) compared to non-centrifuged control on detectable aqueous PFOS concentrations. Samples from aqueous reactors were diluted 2x in MeOH prior to centrifugation. Clearly, low temperature significantly impacts PFOS detection, likely due to reduced solubility at 15ºC.

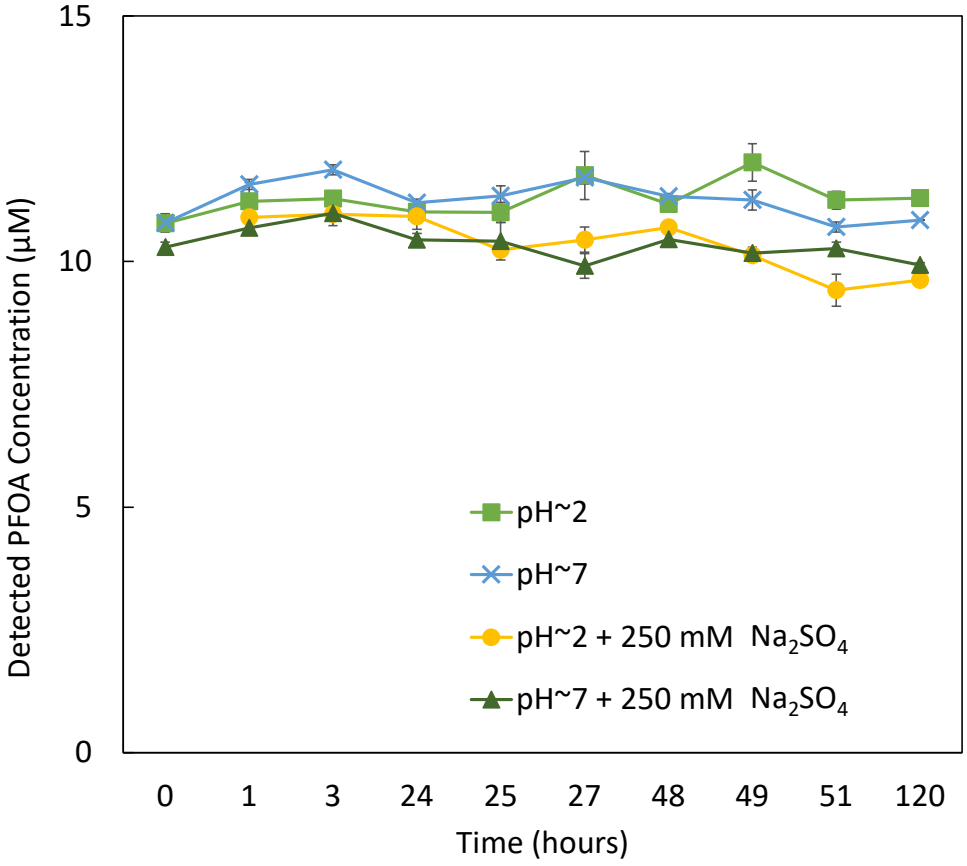

Figure 2.20: Effect of pH and high ionic strength (250-mM Na_2SO_4, I= 0.75 M) on detected PFOA concentration in aqueous solution (PFOA ca. 10 µM). Error bars are standard deviations of duplicate samples.

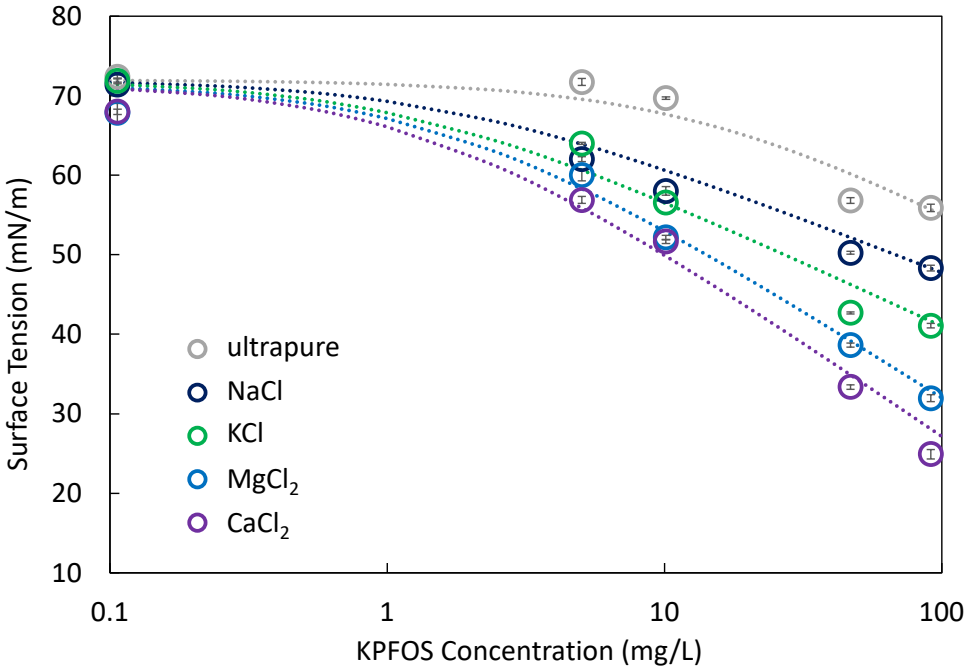

Figure 2.21: The surface tension isotherms of KPFOS (the potassium salt of PFOS) measured by pendant drop tensiometry in 50-mM solutions of NaCl, KCl, $MgCl_2$, and $CaCl_2$.

	a	b (mg/L)	Γ_{max} (mg/m^2)	R^2
ultrapure	0.115	14.82	1.66	0.974
50 mM KCl	0.0959	1.18	1.39	0.982
50 mM NaCl	0.0828	1.75	1.2	0.961
50 mM $MgCl_2$	0.135	1.71	1.96	0.992
50 mM $CaCl_2$	0.146	1.42	2.11	0.985

Table 2.4: Summary of fitted parameters from the Szyszkowski equation and the calculated maximum surface excess values (Γ_{max}) for KPFOS in 50-mM salt solutions. Γ_{max} increases from monovalent to divalent cations, indicating the enhanced surface accumulation due to the decreased electrostatic repulsion between PFOS sulfonate head groups in the presence of the divalent cations, which act as a bridging ion between head groups.

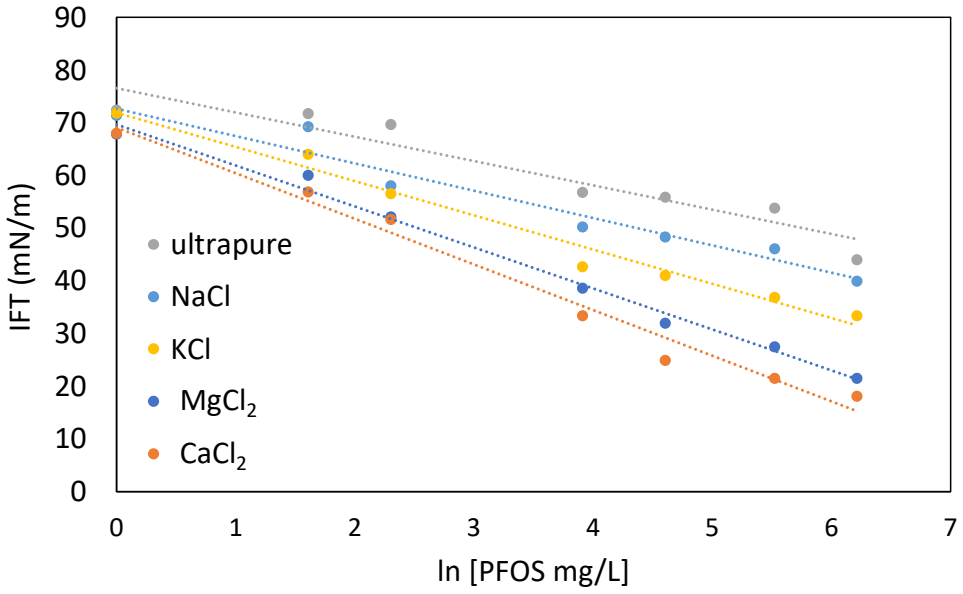

Figure 2.22: In order to determine the CMC of PFOS in the specific salt conditions studies, a linear regression to the surface tension data for PFOS in 50-mM NaCl, KCl, $MgCl_2$ and $CaCl_2$ was performed. The order of the cation effect in solution, as observable by the slopes of the linear fit, follows the order $Ca^{2+} > Mg^{2+} > K^{+} > Na^{+}$. As a result, the CMCs follow the same order.

Chapter 3

Interfacial mass accumulation of per- and polyfluorinated alkyl substances (PFAS) in AFFF in saline environments

Parts of this chapter are included in the manuscript in preparation, "Enhanced interfacial accumulation of AFFF in high salinity conditions" (Steffens et al.)

3.1 Synopsis

Use of AFFF leads to contamination matrices consisting of fluorocarbon and hydrocarbon surfactants rather than singular PFAS. The surface activity of PFAS mixtures in the presence of salts causes phenomena not observed for individual compounds alone. This chapter addresses some of those phenomena, including decreases in surface tension minima and increased interfacial mass accumulation.

3.2 Complexities of interfacial accumulation associated with AFFF

Aqueous film-forming foam (AFFF) contamination has challenged conventional approaches to environmental contaminant monitoring and requires comprehensive analysis of the relationship between environmental characteristics and the contaminant physicochemical properties. Historic AFFF formulations contain per- and polyfluoroalkyl substances (PFAS), a class of surfactants that imbue the film-forming properties and fire extinction performance in AFFF application [178, 179]. PFAS in AFFF formulations vary by manufacturer and age [149, 180, 181] and some PFAS are transformed in the environment [182–184] which compli-

cates characterization of contamination sites. Furthermore, individual PFAS vary in their physicochemical properties and exhibit different transport behavior in the environment [20, 23, 27, 185]. Considering that over 240 individual PFAS have been associated with AFFF [149], a thorough understanding of PFAS environmental behavior is essential for accurate monitoring of fate and transport.

Specifically complicating the picture is that conditions at the contamination source zone, such as water pH, salinity, temperature, hardness, redox conditions, dissolved organic carbon (DOC) content, and even the presence of co-contaminating non-aqueous phase liquids/dense non-aqueous phase liquids (NAPLs/DNAPLs), can markedly alter the physicochemical behavior of PFAS [21, 25, 28, 36, 50, 109, 184]. Thus far, researchers have primarily focused on site properties affecting the sorption and interfacial behavior of PFAS, as these processes are known to alter the accumulation and distribution of PFAS at and near a source zone [24, 28, 49, 186]. Mainly, the effects of salinity [36, 37, 187], DOC [25], and NAPL presence [28, 46, 188] have been evaluated and related quantitatively to sorption and distribution coefficients. Additionally, the critical micelle concentration (CMC) of certain PFAS (e.g., PFOA and PFOS) and AFFF have been measured in the presence of background salts to identify how aggregation or micellization of PFAS, a phenomena unique to surfactants, might affect transport and detection [45, 46, 187].

The relationship between distribution of PFAS and site characteristics is specifically unique to PFAS contamination due to their surfactant properties. Parameters such as air-water interfacial sorption coefficients and critical micelle concentration (CMC) vary based on PFAS structure (e.g., chain length, head group, isomeric form), and the degree of interfacial sorption and micellization is concentration dependent [24, 189]. The number of variables relating to both the PFAS chemistry and the site conditions makes prediction of PFAS behavior and distribution extremely challenging. Apart from source zones where PFAS may be highly concentrated, the implications of sorption and interfacial behavior are relevant in dilute matrices as well and may significantly affect retention processes and detection, particularly in saline waters [39–41, 47].

Building on our work in the previous chapter, which demonstrates PFOS behavior and specific salt effects on micelle formation and interfacial behavior, this chapter serves as an investigation into the aggregation and interfacial behavior of an AFFF in saline matrices. The previous chapter demonstrates an investigation of PFOS-specific behavior and the mechanism of the salt effect on both micelle formation and interfacial behavior. Given the nature of PFAS contamination, in that PFOS never exists as a single contaminant, these studies serve to expand on our understanding of how salinity affects PFAS in mixtures. The effect of high salinity on PFAS detection in an AFFF mixture was evaluated, specifically with regards to detection of PFSAs. We evaluated the CMC of an AFFF formulation in artificial brackish and artificial seawater, and determined surface excess using the Langmuir model. In order to further assess differences attributable to specific cation or anion effects, we evaluated the measurable interfacial mass accumulation of individual PFAS in a bench scale study with different salts. Furthermore, we considered different models of interfacial sorption behavior (i.e., the Langmuir model and the Freundlich model) and the relevance of these models to

typical contamination sites or conditions.

3.3 Materials & Methods

Chemicals

PFAS containing solutions were prepared in 50-mL Corning HDPE centrifuge tubes with Milli-Q water and specified salt concentrations. Reagent grade NaCl and $CaCl_2$ purchased from Sigma-Aldrich were used in mass accumulation experiments. Artificial brackish (ABW) and artificial seawater (ASW) solutions were prepared as 1 L solutions containing salt quantities based on a published preparation protocol (see Supporting Information Table 3.3) [190].

AFFF solutions were prepared using a legacy 3M Guardian AFFF concentrate (manufactured prior to 2002). Dilution series were prepared by weighing out portions of the 3M concentrate and diluting with Milli-Q water; the lowest dilutions were prepared by dilution of higher concentration solutions (see Supporting Information Table 3.4). PFAS analytes were quantified by LC-MS/MS; a detailed list of analytes, transition energies, and the chromatography method can be found in the Supporting Information and Supporting Information Table 3.5.

Surface Tension Measurements

Surface tension isotherms were measured using the pendant drop tensiometry (PDF) method on a KRÜSS tensiometer with a glass syringe and needle attachment. The syringe and needle apparatus were rinsed between each measurement, and cleaned with methanol and water between measurement runs. The instrument was calibrated with Milli-Q water at the beginning of each measurement run to ensure no carryover contamination from previous measurements. Surface tension measurements were taken for three drops to give an average measurement for each solution in the dilution series. The CMC of the 3M AFFF formulation was determined from slope of the surface tension isotherm in the pre-micellar region and the surface tension minima (see Supporting Information Figure 3.5). The data was analyzed using the Langmuir-Szyszkowski (LS) model. The data was fit to the Szyszkowski equation (Equation 3.1 from which the parameters a and b were calculated, constants which are related to the maximum surface excess and surface activity, respectively. The Szyszkowski equation is as follows:

$$\gamma = \gamma_0[1 - a \times ln(\frac{C}{b} + 1)] \tag{3.1}$$

The fitted parameters a and b were determined using a non-linear regression using NumPy, SciPy, and Pandas packages in Python 3.8.5. Surface tension data was imported and the SciPy curve_fit function was used. The R^2 values for the fitted data were calculated using the r2_score function from the sklearn.metrics package. The data was fit for the linear

portion of the CMC curve as researchers have previously shown that the LS equation most accurately describes the relationship between interfacial tension and surface excess parameters in this region; at low solute concentrations, there is some debate as to the use of the Freundlich model for improved accuracy [45, 47, 191, 192]. The maximum surface excess was calculated from the first term in the Langmuir-Szyszkowski equation,

$$\Gamma = \frac{\gamma_0 a}{RT} \frac{C}{C+b} \tag{3.2}$$

where the term Γ represents the maximum surface excess as a function of the parameter a, and the parameter b is the surface activity of the as it relates to the free energy required to transport a surfactant molecule from the bulk solution to the air-water interface. Due to the nature of the analysis of an AFFF solution, rather than individual PFAS analytes, the 'molar mass' of the AFFF can not be used to convert between molar and mass concentration units; therefore, the surface excess is reported only in molar units, and the surface activity (b) is reported in mass units from the Szyszkowski equation fit to the data.

The target AFFF concentrations (mg/L) that were added to the measured solutions were used to fit the surface tension data; validation of the target concentrations was performed by comparing PFOS concentration measured in the AFFF dilution series (see Supporting Information Figure 3.6, Table 3.7).

Bulk Solution Experiments

AFFF solutions were prepared in Milli-Q water in HDPE tubes, to which solid salts were added in the case of single salt experiments (e.g., NaCl and $CaCl_2$); for the experiments in artificial brackish and artificial seawater, diluted solutions of the AFFF were prepared by adding a stock solution directly to centrifuge tubes containing ABW or ASW. Solutions were left to equilibrate in a 37±3°C incubator for at least 3-hours after salt addition. Aqueous samples taken before and after salt addition were diluted in methanol prior to LC-MS/MS analysis.

Interfacial Mass Accumulation Experiments

To assess adsorption of the PFAS in AFFF at the air-water interface (i.e., mass of individual PFAS analytes), we used an experimental procedure described by Schaefer et al. [47] and which we used in the PFOS experiments described in Chapter 2 of this dissertation. Solutions containing 3M AFFF were prepared in 50-mL centrifuge tubes with a small hole drilled at the bottom and temporarily sealed with PFAS-free tape; solutions were prepared in triplicate for each condition studied. Solutions were left to equilibrate on the bench top for 48-hours, and the bulk solution was then drained into a catch tube and the 'film' containing volume (approximately 0.5 mL) was collected in a microcentrifuge tube. From the film volume collected and the concentration detected in the film, the air-water interfacial mass of PFAS was determined.

3.4 Results & Discussion

Detection of PFAS in high ionic strength matrices

In previous work demonstrating the effect of salinity on the interfacial uptake of PFAS, researchers have primarily considered simplified systems containing a single or two analyte(s), and tested a limited range of background salts [45–47, 187]. The interfacial activity of PFCAs as individual analytes [28] and in a AFFF mixture [46] has been evaluated in the presence of NAPL, which is important for understanding field-relevant conditions of AFFF contamination. To expand on this research, we evaluated the interfacial sorption of PFSAs and PFCAs from a 3M AFFF mixture in high salinity matrices. The effect of mixed saline matrices (e.g., an artificial brackish and artificial seawater) as well as individual salts (e.g., NaCl and $CaCl_2$) were evaluated with respect to interfacial mass uptake.

A preliminary study revealed that the apparent concentration of PFSAs in the AFFF mixture decreased upon 200 mM and 500 mM Na_2SO_4 addition. In particular, detected PFOS concentrations decreased on the order of 20-40% in the aqueous phase in the 500 mM Na_2SO_4 solution. This is in agreement with data from the high ionic strength PFOS-only system [187] However, not apparent in the PFOS-only system, was that even at low concentrations (i.e., a 10,000x diluted AFFF solution containing approximately 1 mg/L PFOS), the decrease in detected concentration was around 40% (Figure 3.1. Based on work by Costanza et al. [46] describing the increase in interfacial activity of an AFFF solution, we hypothesized that greater sorption at the air-water interface may be leading to decreased concentrations of aqueous PFOS, even when the bulk solution contains low concentrations of PFAS.

Interfacial activity of AFFF in artificial brackish seawater solutions

In order to evaluate air-water interfacial sorption and critical micelle concentration of the AFFF in saline conditions, we measured surface tension isotherms of a dilution series of 3M AFFF using PDT, as described in the Materials & Methods section. Isotherms were measured in ultrapure, artificial brackish (ABW), and artificial seawater (ASW) solutions to evaluate the effect of salinity on air-water interface activity. From the surface tension isotherms, the apparent CMCs of the 3M AFFF formulation in varying salinity conditions were calculated. In both ABW and ASW, the apparent CMC is lower than in the ultrapure solution (Figure 3.2); for the ABW, the apparent CMC is 1693 mg/L, and for the ASW, the apparent CMC is 1543 mg/L (see Table 3.1). For comparison, a plot including the PFOS-only data in 500-mM NaCl solution as described in Chapter 2, is included in the Supporting Information (see Supporting Information Figure 3.7).

The lowering of the CMC of the 3M AFFF formulation is expected due to the interaction of cations with the negatively charged headgroups of PFCAs and PFSAs. The presence of cations is known to lower the CMC of anionic surfactants by reducing the electrostatic

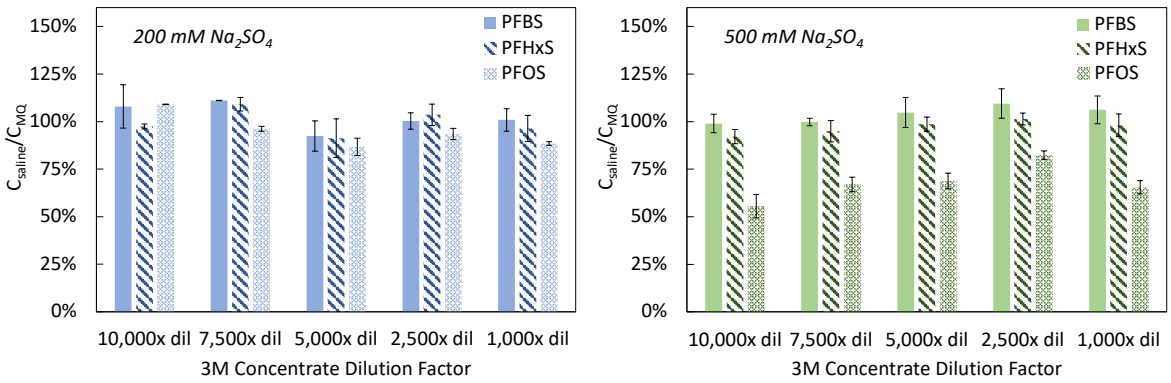

Figure 3.1: Detected aqueous phase concentrations of PFSAs in an AFFF mixture in a saline matrix containing a) 200 mM and b) 500 mM Na_2SO_4. The initial concentrations of the components detected in Milli-Q water (C_{MQ}) are listed in Table 3.8 in the Supporting Information; to give a sense of range, the 10,000x diluted solution contains *ca.* 1 mg/L PFOS, and the 1,000x diluted solution contains *ca.* 10 mg/L PFOS.

	dγ/dC	y-intercept	IFT Minima (mN/m)	ln(CMC)	CMC (mg/L)	R^2
Ultrapure	-13.41	123.8	15.08	8.11	3320	0.971
Brackish	-13.60	113.4	14.52	7.27	1436	0.912
ASW	-12.59	113.4	14.78	7.83	2518	0.912
Ultrapure*	-12.97	121.9	15.08	8.24	3779	0.975
Brackish*	-13.54	115.2	14.51	7.43	1693	0.949
ASW*	-13.69	115.3	14.77	7.34	1543	0.935

Table 3.1: Summary of apparent CMCs of 3M AFFF ultrapure, artificial brackish, and artificial seawater conditions. Linear fits for the dγ/dC curves were obtained in the pre-CMC region after a significant drop in surface tension was observed (i.e., below 70 mN/m) to obtain the best fits. *Notates 'corrected' data, for which 2 data points were extracted in order to optimize the linear fit (see Supporting Information Figure 3.5 for data correction details).

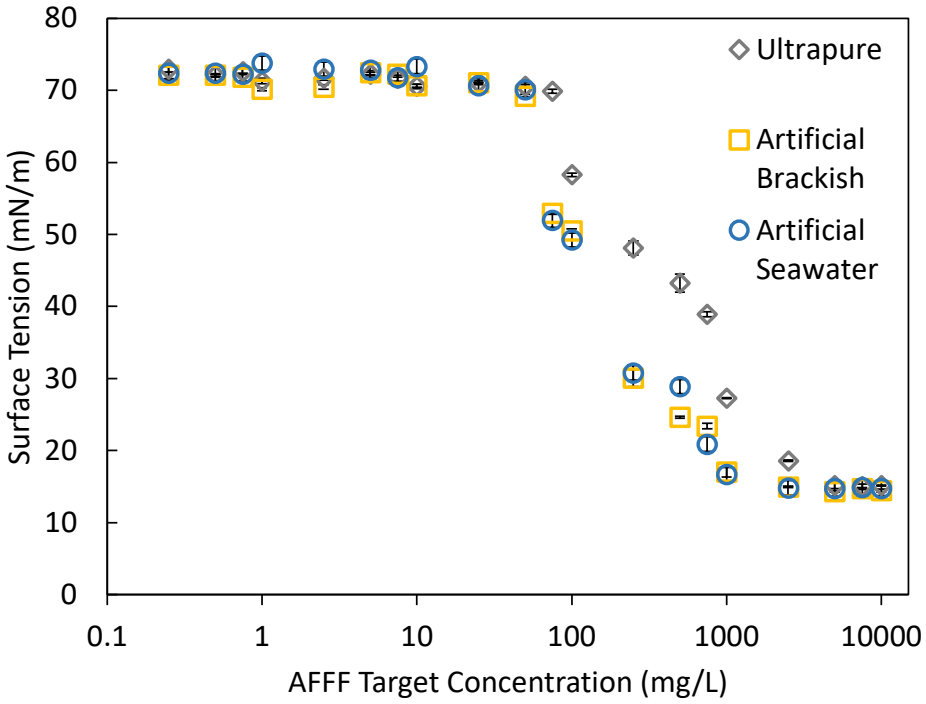

Figure 3.2: Surface tension isotherms for 3M AFFF in ultrapure, artificial brackish, and artificial seawater. AFFF target concentrations were validated by measuring the PFOS concentrations for the AFFF dilution series (see Supporting Information Figure 3.6.)

repulsion among the surfactant headgroups which also can alter the aggregate morphology [145, 160, 166]. The 3M AFFF CMC is similar in the ABW and ASW, despite the higher concentration of cations in the seawater matrix. This may be due to a saturation effect, by which above a certain salt concentration, the cations present pair to a maximum number of PFAS monomers and additional cations cannot further pair or decrease the electrostatic repulsion between the PFAS headgroups [49, 193]. Additionally, we observed that the minimum surface tension achieved by the AFFF solution was consistent across all conditions (14.8 mN/m), suggesting the interfacial uptake maxima are similar among both saline conditions.

Surface excess of AFFF in artificial brackish and artificial seawater solutions

By fitting the Szyszkowski equation to the surface tension isotherms, the parameters related to the surface excess (a) and surface activity (b) can be calculated. The parameter a can be substituted into the first term of the Langmuir-Szyszkowski equation (see Equation

	Surface Activity, *b* (mg/L)	Γ_{max} (x 10^{-7} mol/cm^2)	R^2	PFOS-only Γ_{max} (x 10^{-7} mol/cm^2)*
Ultrapure	116.85	7.32	0.976	6.16
Artificial Brackish	35.81	6.20	0.943	–
Artificial Seawater	35.70	6.24	0.944	–
500 mM NaCl	–	–	–	2.62

Table 3.2: Summary of surface activity and maximum surface excess, Γ_{max}, for the 3M AFFF formulation in ultrapure, brackish, and artificial seawater. PFOS-only* values are from the previous work presented in Chapter 2 of this dissertation. Values were calculated by fitting the Szyszkowski equation to the surface tension isotherms. R^2 values indicate that the saline solutions may be representative of non-ideal behavior given the high ionic strength of the solutions.

3.2) which represents the maximum surface excess. In prior work, we found that for PFOS in a 'two-component system' (e.g., single solute, single salt), the high ionic strength solutions containing 500 mM mono- and divalent salts decreased the maximum surface excess of PFOS compared to ultrapure water. The decrease may be related to the bulk solute effect, by which PFOS monomers are 'salted-out' of solution due to increased hydrophobic interactions of the fluorocarbon chain and bulk water molecules [194]. However, in comparing the surface excess among the salts studied, it was apparent that the divalent cations (Mg^{2+}, Ca^{2+}) resulted in higher surface excess than the monovalent salts (Na^+, K^+). The greater surface excess for the divalent salts is a result of the decreased electrostatic repulsion energy between the anionic sulfonate head groups adsorbed at the interface, due to pairing with the divalent cations [145, 166, 195, 196].

In comparison, the multi-solute 3M AFFF system in ABW and ASW containing a mixture of salts, also indicated a lower maximum surface excess than in the ultrapure water. Most notably, the surface activity represented by the b term from the Szyszkowski equation fit (Eq. 3.1), is significantly lower in the ABW and ASW systems compared to in ultrapure water (Table 3.2). Similar to the observed effect in the single-solute system, the decreased surface activity may be due to the 'salting-out' of the fluorocarbon monomers in the bulk solution. When compared to maximum surface excess in the single-solute PFOS system, the surface activity of the 3M AFFF mixture is higher in both ultrapure water and than in the 500 mM NaCl solution (comparable to the 450 mM NaCl concentration in the ASW solution).

Given that the mixture of fluorocarbon surfactants, in addition to hydrocarbon surfactants and solvents, in an AFFF formulation is optimized in order to achieve the lowest possible interfacial tension and therefore maximize the spreading efficiency and fire-quenching

properties of the foam, it would be expected that the 3M AFFF would exhibit higher surface excess than PFOS alone. However, the significant drop in surface activity in the ABW and ASW saline matrices suggests that spreading behavior of the foam may be dramatically altered in a saline solution. AFFF formulas are typically diluted on site of their intended application [194], and it should be noted that in coastal areas, a saltwater dilution would potentially impact the performance of the formulation in fire-fighting applications.

Measurable interfacial mass accumulation of PFSAs and PFCAs in saline solutions

The Langmuir-Szyszkowski model has been compared to the Freundlich model to evaluate how accurately the two models match the observed air-water interface behavior, and has generally been validated as a more accurate description of the air-water interfacial uptake and surface excess of PFAS in multiple solvent systems [45, 46]. The Freundlich model is suggested to be a better suited model for interfacial accumulation and air-water partitioning coefficients of PFAS in dilute solutions [47, 192], because the Langmuir model fails to predict differences in interfacial accumulation in the range where there are no measurable changes in surface tension (i.e., below 1-5 mg/L PFOS).

Given the complexity of the system being studied– a mixture of fluorocarbon surfactants, hydrocarbon surfactants, and solvents [197] in mixed salt matrices– we wanted to gain insight into the observable interfacial mass accumulation of the individual PFAS components in the 3M AFFF formulation. Using an experimental procedure previously described by Schaefer et al. [47] and used in our work investigating the PFOS-only system [187](see Materials & Methods), we quantified the mass accumulation of PFCAs and PFSAs in various high ionic strength matrices, including the ABW, ASW, and a NaCl and $CaCl_2$ solution and compared the results to those in ultrapure water. In comparing the NaCl and $CaCl_2$ conditions, we evaluated a 500 mM solution of each salt; thus, the NaCl condition is most comparable to the ASW solution (450 mM NaCl) in terms of distinguishing single salt and mixed salt solution effects. The $CaCl_2$ concentration is not relevant to a real water saline matrix, but we hypothesized that the $CaCl_2$ solution may exhibit different behavior than the NaCl system based on findings in our previous work and that of others [40, 49, 187].

Concentrations of the interfacial solution collected from the experiment tubes were quantified by LC-MS/MS, which indicated that the PFSAs made up a higher portion of the total PFAS present in the solution (see Supporting Information Tables 3.9, 3.10, 3.11, 3.12), as was expected from the known AFFF manufacturer and year of production (i.e., 3M pre-2002 formulation) (Place & Field 2012). The results for the mass accumulation are summarized in Figure 3.4. It is challenging to directly assess differences between individual compounds because the compounds are present at varying concentrations in the formulation, and accumulation is concentration dependent [20, 24, 28, 47]. However, some trends can be observed that are indicative of the relationship between structure and relative mass accumulation. Specifically, we compared accumulation of FHxSA, PFHxSAm, and N-TAmP-FHxSA, all of

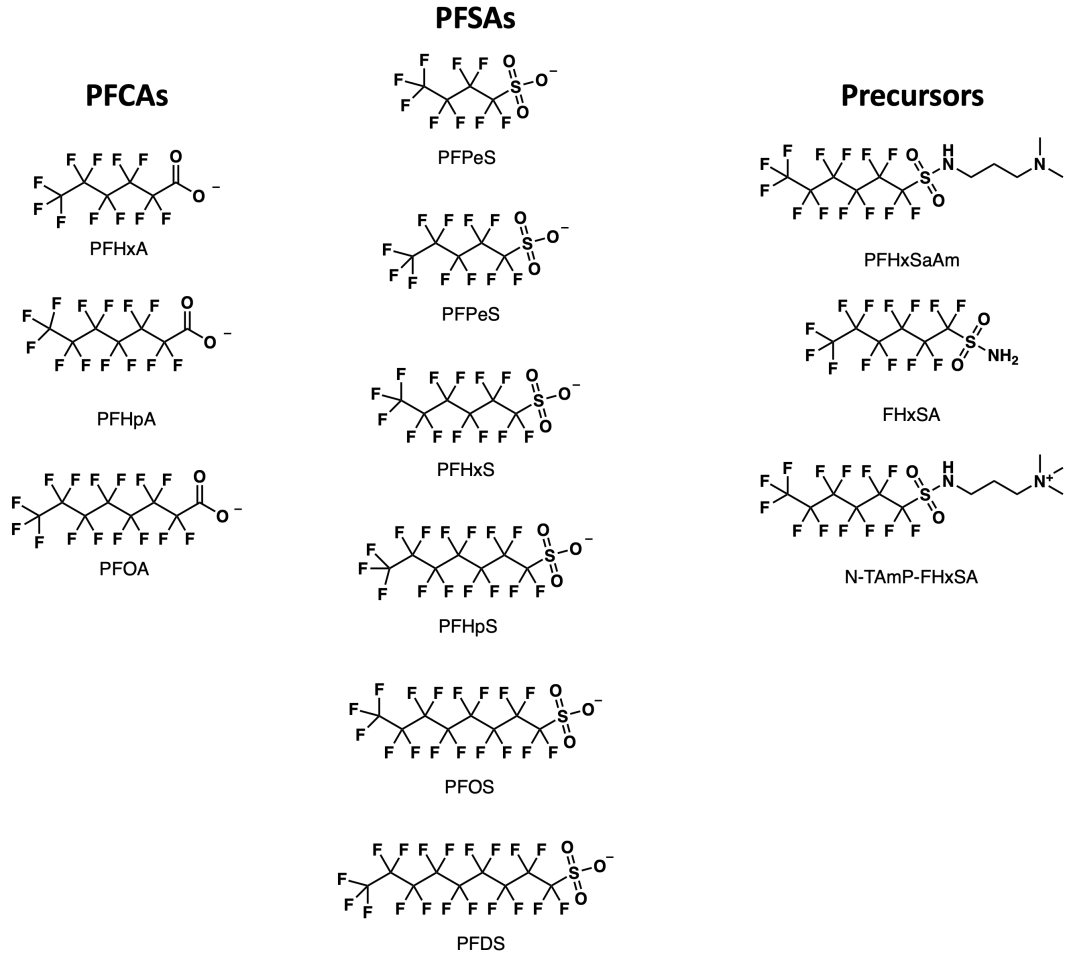

Figure 3.3: Structures of PFCAs, PFSAs, and precursors for which quantitative analysis of the 3M AFFF containing solution was performed.

which are precursor compounds that may be transformed into more mobile and recalcitrant perfluoroalkyl acids, and the two short chain PFSAs, PFBS and PFHxS (Figure 3.3).

The amine functionality, in particular, may increase the propensity for interfacial accumulation in the ASW and $CaCl_2$ matrices, compared to the sulfonate compounds (i.e., PFBS, PFHxS). PFBS and PFHxS, however, exhibit similar mass accumulation in all of the saline matrices, on the order of a two-fold increase compared to the ultrapure solution. The interfacial accumulation of PFOS, which was present at significantly higher concentrations than any of the other PFAS detected in the solutions (see Table 3.12), also exhibited markedly different activity in ASW and $CaCl_2$ solutions. Notably, the mass accumulation in the $CaCl_2$ solution was greater than in the NaCl solution, a similar effect to what was observed in the single-solute PFOS system discussed in Chapter 2.

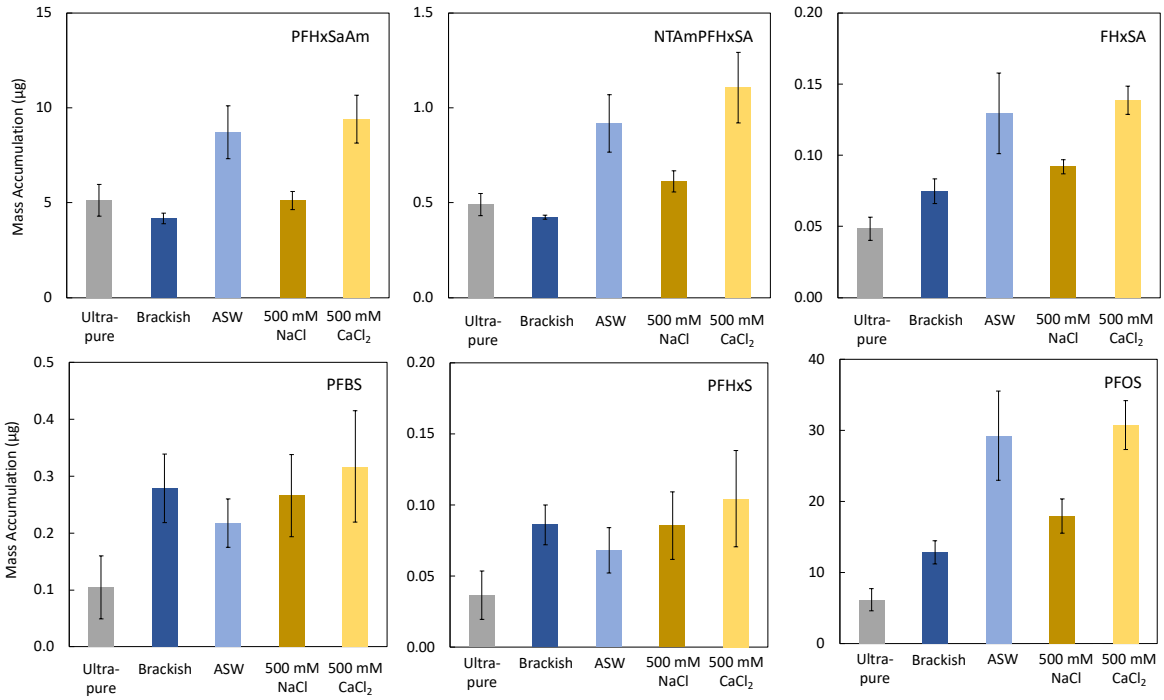

Figure 3.4: Interfacial mass accumulation of precursors and PFSAs in ABW, ASW, 500 mM NaCl, and 500 mM $CaCl_2$ solutions containining diluted AFFF concentrate. Mass accumulation was calculated from interfacial concentration and volume. Error bars are the standard deviations of triplicate samples.

While the ASW and NaCl solutions have similar concentrations of Na^+ ions, the amine-containing compounds as well as PFOS have a higher mass accumulation in the ASW solutions. This indicates that Na^+ alone is not driving the interfacial accumulation in the ASW solution. Likely, the divalent cations present in ASW (46 mM Mg^{2+} and 10 mM Ca^{2+}, see Supporting Information Table 3.3), are a substantial contributor to the increased mass accumulation as we found in investigating the mechanism of monovalent and divalent cations in PFOS interfacial activity (Ch. 2). The increase in interfacial mass accumulation in the matrices evaluated indicates that salinity significantly enhances accumulation and may be a primary mechanism by which PFAS attenuation is affected in the environment.

3.5 Remaining Challenges

As evidenced by the growing body of literature on PFAS interfacial properties and partitioning behavior [24, 28, 41, 45, 46, 109] there is heightened interest in the research community as to how the surfactant properties of PFAS impact their environmental behavior.

	ABW		ASW	
	g/L	mmol	g/L	mmol
NaCl	13.65	225	27.30	450
KCl	0.37	5	0.74	10
$CaCl_2$	0.5	4.5	1	9
$MgCl_2 \cdot 6\,H_2O$	3.05	15	6.1	30
$MgSO_4 \cdot 7H_2O$	1.975	8	3.95	16

Table 3.3: Mass and molar quantities of salts used in preparation of artificial brackish water (ABW) and artificial seawater (ASW).

Interfacial accumulation has significant implications for PFAS fate and transport; it has the potential to affect retention at a source zone and retention during transport downstream, and may result in unexpected accumulation of PFAS beyond the source zone [24, 28, 41, 184]. In evaluating the detection, surface activity, and mass accumulation of PFAS in a 3M AFFF formulation, we observed that high salinity matrices have the ability to decrease detection and decrease the CMC of the formulation, and specifically that divalent salts (e.g., ($CaCl_2$)) have the potential to increase the surface activity and mass accumulation of certain PFAS in solution.

The challenging aspect of this research area is that the interfacial accumulation properties of PFAS vary within the class, depending on the chemical structure (e.g., carboxylic acid or sulfonic acid head group, chain length), and are affected by water properties such as salinity. Additionally, variations in AFFF formulations with respect to relative proportions of fluorocarbon and hydrocarbon surfactants, as well as the proportions of the fluorocarbon surfactants alone, will likely impact interfacial behavior in mixed contaminant systems. As PFAS contamination spreads from a source zone, the characteristics of the mixture will change which may further impact interfacial accumulation. This work demonstrates the enhanced interfacial accumulation of PFAS in saline conditions, and may serve in forming a better understanding of how salinity impacts retention processes of AFFF from contaminated source zones, as well as inspire attention towards natural attenuation mechanisms in the environment which may prove to be a useful mechanism by which to manage PFAS contaminated zones.

Dilution Series

Target mg/L	*From Stock:*	Dilution X	mL 'Stock'	mL ASW
0.25	2.5	10	*1*	9
0.5	5	10	*1*	9
0.75	7.5	10	*1*	9
1	10	10	*1*	9
2.5	25	10	*1*	9
5	50	10	*1*	9
7.5	75	10	*1*	9
10	100	10	*1*	9
25	250	10	*1*	9
50	500	10	*1*	9
75	750	10	*1*	9
100	1000	10	*1*	9
*250	10	**Prepare directly– mg of AFFF conc. added 50 mL centrifuge tube; add 40 mL ASW*		
*500	20			
*750	30			
*1000	40			
**2500	50	***Prepare directly– mg of AFFF conc. added to 50 mL centrifuge tube; add 20 mL ASW*		
**5000	100			
**7500	150			
**10000	200			

Table 3.4: Dilution series of 3M AFFF in ASW (or ABW) water for surface tension isotherm measurements.

3.6 Supporting Information

LC-MS/MS Method for Sample Analysis

Samples for quantification by LC-MS/MS were prepared in 50:50 methanol:H_2O and diluted appropriately such that they were within the calibration range. A target concentration of 2 μg/L of internal standard (MPFAC-MXA from Wellington Laboratories) was added directly to each 2 mL amber LC-MS/MS vial. Per- and polyfluoroalkyl substance (PFAS) analytes were quantified by LC-MS/MS equipped with electrospray ionization in negative mode (Triple Quad 6460A, Agilent Technologies) multiple reaction monitoring (MRM). Gas and Sheath Gas Heater temperatures were 325 and 350°C, respectively. Gas and sheath gas flows were 9 L/min. The nebulizer was kept at 25 psi and the capillary voltage was 3.5

kV. Samples were prepared for analysis by dilution in methanol to a target concentration of 10 μg/L to ensure quantification within the calibration range (0.2-10 μg/L). The isotope dilution method was used to account for any potential matrix effects. Mass labeled [^{13}C]-perfluoroalkyl acids (PFAAs) (2-5 μg/L) were added to LC-MS/MS sample vials for each sample in the final stage of sample preparation. Analytes were separated using a Zinc-Diol guard column coupled to Zorbax C18 XDB guard and analytical columns (Agilent Technologies). The mobile phase (0.4 mL/min) was 5 mM ammonium acetate in water (A) and 5 mM ammonium acetate in methanol (B) with a solvent gradient: hold 0-2 min 95% A, ramp to 10% A by 10 min, hold 10-11.5 min 10% A, ramp to 95% A by 12 min, hold 12-18 min 95% A. The LC-MS/MS setup included a delay C18 column after the purge valve to decrease the effect of possible contamination from upstream polytetrafluoroethylene (PTFE) components. PFAS were quantified by the transitions and collision energies listed in Table 3.5. Mobile phase blanks were run every 10 samples and select calibration samples were re-run every 20 samples to prevent contamination or carryover in the analysis.

Compound	Internal Standard	Precursor Ion	Product Ion	Fragmentor Voltage (V)	Collision Energy (V)	Polarity
MPFBA	-	217	172	50	5	Neg
MPFPeA	-	266	222 221	60	2	Neg
MPFHxA	-	315	270	60	5	Neg
MPFOA	-	417	372	70	2	Neg
MPFNA	-	468	423	70	5	Neg
MPFHxS	-	403	103	150	40	Neg
MPFOS	-	503	80	190	60	Neg
PFBA	MPFBA	213	169	50	2	Neg
PFPeA	MPFPeA	263	219 68.9	60 92	2 8	Neg
PFHxA	MPFHxA	313	269 119	80	2 15	Neg
PFHpA	MPFOA	363	319 169	80	2	Neg
PFOA	MPFOA	413	369 169	80	3 14	Neg
PFNA	MPFNA	463	419 219	80	2 15	Neg
PFBS	MPFHxS	299	99 80	120	30 70	Neg
PFHxS	MPFHxS	399	99 80	125	50 80	Neg
PFOS	MPFOS	499	99 80	122	50 80	Neg
FHxSA	MPFOS	398	78	125	36	Neg
FOSA	MPFOS	498	78	125	36	Neg
6-2 FtS	MPFOS	427	407 80	140	25 35	Neg
AmPr-FHxSA	MPFOS	485	85	135	30	Pos

Table 3.5: PFAS compounds analyzed by LC-MS/MS.

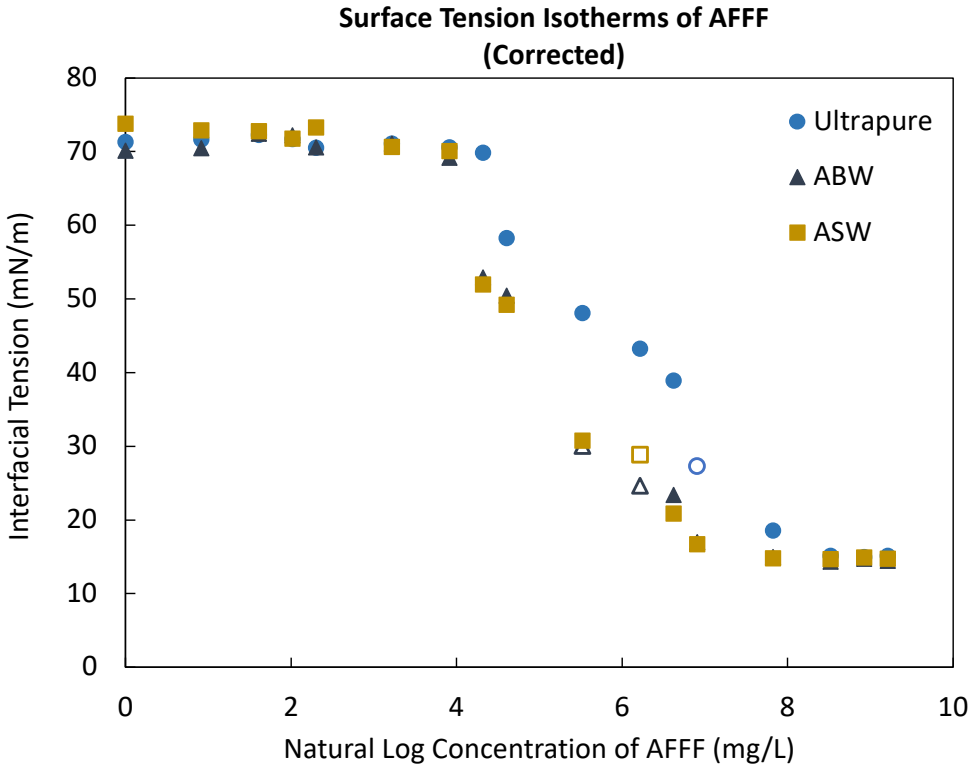

Figure 3.5: Surface tension isotherm data for AFFF in ultrapure, artificial brackish water (Brackish), and artificial seawater (ASW) used to determine the natural logarithmic linear fit for calculation of CMCs under these conditions. Unfilled data points represent the values that were not included in the linear regression in order to improve the linear fit in the pre-micellar region.

	γ_0 (mN/m)	Fit Range (mg/L)	*a*	*b*	Γ_{max} (x 10^{-7} mol/cm^2)	R^2
Ultrapure	72.83	0.25-2500	0.2489	116.85	7.32	0.976
Artificial Brackish	71.76	0.25-2500	0.2139	35.81	6.20	0.943
Artificial Seawater	72.23	0.25-2500	0.2141	35.70	6.24	0.944

Table 3.6: Summary of the fitted parameters a, b and calculated surface excess as determined from the Langmuir-Szyszkowski model.

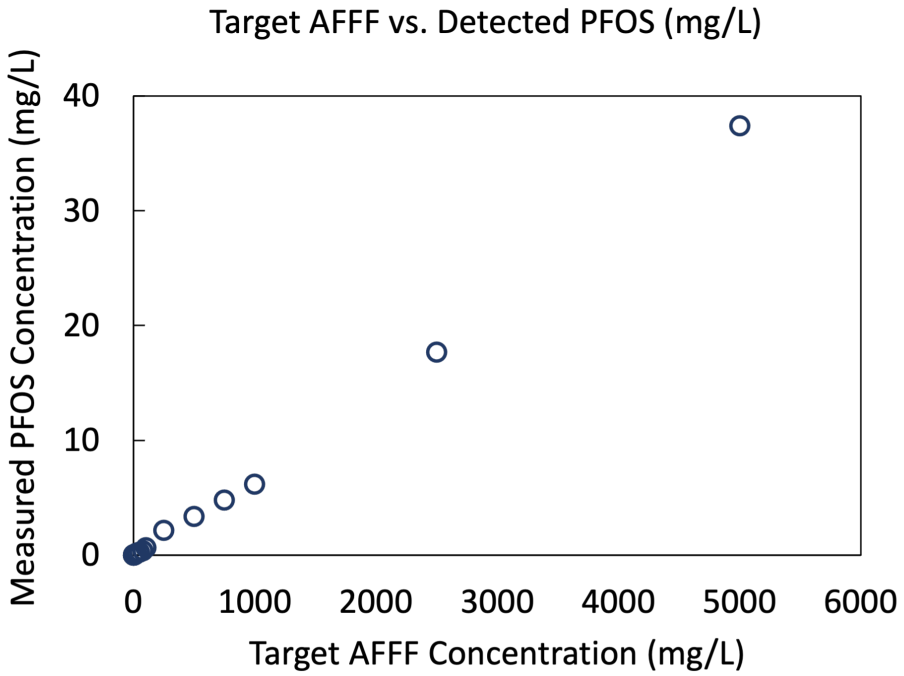

Figure 3.6: Comparison of target 3M AFFF concentration in dilution series solutions and detected PFOS concentrations used for validation. Because we did not analyze for all hydrocarbon and fluorocarbon components of the AFFF formula, AFFF concentration is based on mass measured out for high concentration solutions, and on the subsequent dilutions from those high concentration solutions. The linear relationship between the target and measured PFOS concentration helps to validate the accuracy of the AFFF concentrations in the dilutions series.

Target 3M AFFF Conc. (mg/L)	Detected PFOS Conc. (mg/L)	% PFOS
2.5	0.016	0.65%
5	0.027	0.54%
7.5	0.030	0.40%
10	0.056	0.56%
25	0.189	0.76%
50	0.261	0.52%
75	0.391	0.52%
100	0.644	0.64%
250	2.158	0.86%
500	3.362	0.67%
750	4.812	0.64%
1000	6.167	0.62%
2500	17.693	0.71%
5000	37.403	0.75%
7500	42.755	0.57%

Table 3.7: Target AFFF and measured PFOS concentrations in the 3M AFFF dilution series. The % PFOS concentrations (0.4-0.86%) are in the expected range for a 3M formulation; the data is plotted in Figure 3.6 and the linear relationship between target and measured concentration indicates accuracy in the preparation of the dilution series, despite that not all the analytes could be quantified to determine the total AFFF concentration present in each solution.

C_{MQ} (mM) – Average of Triplicate Samples
Sampled pre- ***200 mM*** *Na_2SO_4 addition*

	PFBS	PFHxS	PFOS
10,000x dil	0.10	0.38	2.40
7,500x dil	0.13	0.49	2.92
5,000x dil	0.18	0.71	4.09
2,500x dil	0.32	1.26	8.09
1,000x dil	0.80	3.14	19.31

C_{MQ} (mM) – Average of Triplicate Samples
Sampled pre- ***500 mM*** *Na_2SO_4 addition*

	PFBS	PFHxS	PFOS
10,000x dil	0.12	0.44	2.93
7,500x dil	0.14	0.54	3.57
5,000x dil	0.20	0.77	5.14
2,500x dil	0.39	1.49	9.69
1,000x dil	0.89	3.34	21.79

Table 3.8: Detected concentrations of PFSAs in 1,000-10,000x diluted AFFF solutions prior to salt addition.

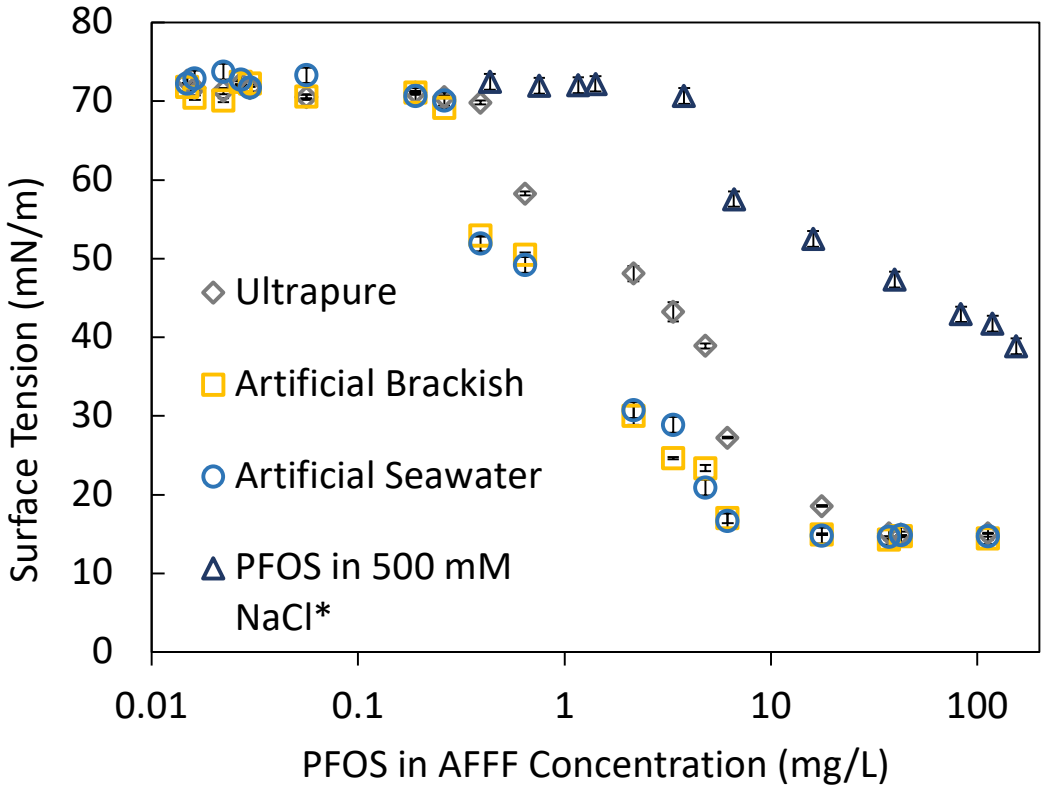

Figure 3.7: Comparison of AFFF surface tension isotherms in ABW, ASW compared to PFOS-only isotherm in 500-mM NaCl. The synergistic effect of the fluorocarbon/hydrocarbon mixture in the AFFF formulation is apparent in the significantly lower surface tensions measure for the AFFF solutions.

	Averages (µg/L)		St. Dev.	
FHxSA	**Bulk**	**Film**	**Bulk**	**Film**
ultrapure	0.0528	0.0965	0.0054	0.0162
Brackish	0.0525	0.1492	0.0077	0.0174
ASW	0.0395	0.2588	0.0045	0.0564
500 mM NaCl	0.0595	0.1839	0.0047	0.0100
500 mM $CaCl_2$	0.0637	0.2771	0.0034	0.0198
PFHxSaAm				
ultrapure	1.241	10.261	0.110	1.659
Brackish	1.332	8.345	0.123	0.544
ASW	1.252	17.416	0.094	2.768
500 mM NaCl	1.480	10.238	0.026	0.966
500 mM $CaCl_2$	1.311	18.822	0.118	2.525
NTAmPFHxSA				
ultrapure	0.080	0.979	0.015	0.115
Brackish	0.077	0.847	0.005	0.022
ASW	0.061	1.835	0.016	0.304
500 mM NaCl	0.087	1.224	0.003	0.113
500 mM $CaCl_2$	0.079	2.213	0.005	0.372
6:2 FtSaB				
ultrapure	0.1858	0.0908	0.0025	0.0011
Brackish	0.1807	0.0932	0.0023	0.0031
ASW	0.1795	0.0981	0.0006	0.0016
500 mM NaCl	0.1795	0.0942	0.0009	0.0027
500 mM $CaCl_2$	0.1807	0.0922	0.0013	0.0013

Table 3.9: Measured concentrations of precursor compounds in bulk and film solutions in high salinity matrices containing 3M AFFF. Standard deviations are reported for the averages of triplicate solutions.

	Averages (µg/L)		St. Dev.	
PFHxA	**Bulk**	**Film**	**Bulk**	**Film**
ultrapure	0.1873	0.0548	0.0120	0.0348
Brackish	0.1740	0.1473	0.0059	0.0290
ASW	0.1655	0.1080	0.0073	0.0173
500 mM NaCl	0.1761	0.1454	0.0063	0.0333
500 mM $CaCl_2$	0.1749	0.1729	0.0031	0.0512
PFHpA				
ultrapure	0.0724	0.0250	0.0015	0.0153
Brackish	0.0647	0.0591	0.0027	0.0150
ASW	0.0674	0.0441	0.0060	0.0046
500 mM NaCl	0.0669	0.0559	0.0013	0.0111
500 mM $CaCl_2$	0.0708	0.0661	0.0046	0.0203
PFOA				
ultrapure	0.2539	0.1006	0.0148	0.0322
Brackish	0.2117	0.1857	0.0090	0.0290
ASW	0.2183	0.1675	0.0113	0.0161
500 mM NaCl	0.2266	0.1919	0.0023	0.0306
500 mM $CaCl_2$	0.2364	0.1973	0.0075	0.0405

Table 3.10: Measured concentrations of PFCAs in bulk and film solutions in high salinity matrices containing 3M AFFF. Standard deviations are reported for the averages of triplicate solutions.

	Averages (µg/L)		St. Dev.	
PFBS	**Bulk**	**Film**	**Bulk**	**Film**
ultrapure	0.707	0.209	0.048	0.111
Brackish	0.680	0.558	0.019	0.120
ASW	0.669	0.435	0.059	0.085
500 mM NaCl	0.677	0.532	0.032	0.144
500 mM $CaCl_2$	0.667	0.634	0.006	0.196
PFPeS				
ultrapure	0.696	0.226	0.033	0.114
Brackish	0.658	0.544	0.005	0.098
ASW	0.635	0.423	0.038	0.063
500 mM NaCl	0.681	0.519	0.010	0.121
500 mM $CaCl_2$	0.669	0.636	0.025	0.186
PFHxS				
ultrapure	0.420	0.073	0.126	0.034
Brackish	0.272	0.172	0.074	0.028
ASW	0.195	0.136	0.016	0.032
500 mM NaCl	0.190	0.171	0.021	0.047
500 mM $CaCl_2$	0.214	0.209	0.001	0.068

Table 3.11: Measured concentrations of short chain PFSAs in bulk and film solutions in high salinity matrices containing 3M AFFF. Standard deviations are reported for the averages of triplicate solutions.

	Averages (µg/L)		St. Dev.	
PFHpS	**Bulk**	**Film**	**Bulk**	**Film**
ultrapure	0.307	0.133	0.032	0.073
Brackish	0.284	0.389	0.022	0.073
ASW	0.264	0.567	0.029	0.119
500 mM NaCl	0.288	0.466	0.003	0.113
500 mM $CaCl_2$	0.295	0.686	0.009	0.071
PFOS				
ultrapure	13.331	12.325	0.710	3.059
Brackish	12.156	25.611	0.362	3.268
ASW	10.843	58.491	0.508	12.516
500 mM NaCl	12.169	35.856	0.152	4.783
500 mM $CaCl_2$	11.634	61.492	0.324	6.924
PFDS				
ultrapure	0.033	0.063	0.024	0.004
Brackish	0.037	0.054	0.027	0.006
ASW	0.054	0.100	0.006	0.016
500 mM NaCl	0.071	0.050	0.003	0.004
500 mM $CaCl_2$	0.056	0.100	0.009	0.018

Table 3.12: Measured concentrations of short (PFHpS) and long chain (PFOS, PFDS) PFSAs in bulk and film solutions in high salinity matrices containing 3M AFFF. Standard deviations are reported for the averages of triplicate solutions.

Chapter 4

Assessing transformation potential of perfluoroalkyl acids (PFAAs) in a laccase mediator system (LMS)

Parts of this chapter are included in the manuscript under review, "A Systematic Investigation of the Potential Oxidation Mechanism of Perfluoroalkylacids (PFAAs) in a Laccase-Mediator System (LMS)" (Steffens et al. 2022)

4.1 Synopsis

Bio-based treatment systems have been proposed to transform PFAAs, but neither transformation pathways nor suspected transformation products have been confirmed. This chapter is an investigation of a proposed enzyme treatment system and the discovery of a sorptive removal process that could be interpreted as an artifact of transformation.

4.2 Efforts towards PFAS bioremediation

Biological treatment has been used for over a century for treatment of wastewater, and more recently for treatment of persistent organic pollutants, which have emerged as a consequence of industrialization and urbanization [198, 199]. Per- and polyfluoroalkyl substances (PFAS) are among the most recalcitrant pollutants, earning the colloquial title "forever chemicals" due to their long half-lives and resistance to biological, thermal, and chemical degradation. While typical removal and destruction technologies for PFAS are chemically and energetically intensive processes such as advanced oxidation/reduction processes, adsorption technology, and incineration [200], the lower energy and chemical requirements of biological treatment strategies are an enticing, yet elusive, alternative for PFAS transformation.

Unlike species of natural chlorinated organics, which number in the thousands, only a small number fluorinated organics are found in nature [201–203]. This perhaps explains the relative success of bioremediation of chlorinated ethenes compared to highly fluorinated compounds such as PFAS, for which few or no naturally occurring analogues exist. Perfluoroalkyl acids (PFAAs) including perfluorooctanoic acid (PFOA) and perfluorooctane sulfonic acid (PFOS), have generally been shown to fail as potential electron acceptors for dehalogenating bacteria [202, 204, 205]. Biotransformation of some polyfluoralkyl substances is possible, but generally requires at least one hydrogen atom at the α-carbon adjacent to the perfluoroalkyl chain in order for a reaction to initiate [204, 206]. For example, fluorotelomer thioether amido sulfonates can biotransform into fluorotelomer sulfonates and fluorotelomer carboxylic acids [99, 207], and fluorotelomer alcohols can biotransform into PFAAs, even undergoing partial chain-shortening [208–210]. In one study, the ammonium oxidizing bacteria *Acidimicrobium sp.* strain A6 was shown defluorinate PFOA and PFOS under iron-reducing conditions, but further investigation is needed to confirm complete mineralization in this system [3]. Currently characterized biotransformation reactions are essential for understanding the fate of PFAS in the environment, but have yet to prove their utility as viable PFAS treatment technologies.

In contrast to isolated bacteria or bacterial communities, enzymatic biotransformation reactions are promising for the transformation of persistent organic pollutants, even PFAS, because of their rapid kinetics and the diversity of enzymes available for use. Horseradish peroxidase (HRP) and fungal laccase enzymes have been reported for biotransformation of PFOA [105, 211, 212] and PFOS [106]. Laccase enzymes are of particular interest because unlike HRP, which requires hydrogen peroxide as a terminal electron acceptor, they utilize molecular oxygen, catalyzing the reduction of O_2 to H_2O [213, 214]. Laccase enzymes are also prevalent in the environment, and can be found in plants, insects, fungi, and [215–217], which could be beneficial for in situ treatment of organic compounds such as PFAS. Laccases are used to catalyze lignin biodegradation via one electron abstraction from phenolic hydroxyl groups [214]. However, the oxidative power of these enzymes is limited by relatively low redox potentials (0.2-0.8 V/NHE) [218]. The addition of small molecule mediators, most commonly bearing nitroxyl or phenolic moieties, can facilitate electron transfer from target substrate to laccase, expanding the scope of laccase-catalyzed reactions to larger substrates with higher redox potentials [218, 219]. This multi-step oxidation cycle, in which laccase oxidizes a chemical mediator, the chemical mediator oxidizes a target substrate, and molecular oxygen is reduced to water, is referred to as the laccase-mediator system (LMS).

LMSs have been investigated for the degradation of pesticides and pharmaceuticals, decolorization of dyes, among other water pollutants [118, 218, 220, 221]. While initial results indicating application of an LMS to transform PFOA and PFOS were promising, the transformation products reported were tentative and the reaction kinetics were inefficient [105, 106]. Additionally, the apparent requirement for copper in the reaction system poses some concern for in situ remediation applications. Therefore, we sought to improve the scope, efficacy, and mechanistic underpinnings of LMSs for PFAS treatment by investigating the following: what other laccase enzymes could catalyze the reaction? What other mediators?

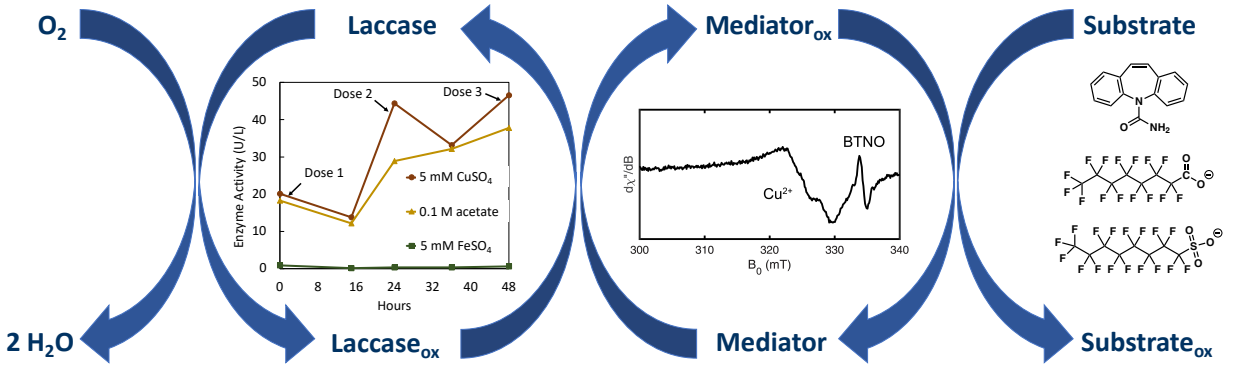

Figure 4.1: A systematic study of the proposed oxidation mechanism for PFAAs in a laccase-mediator system.

Could other metals be used to replace copper? Additionally, could the reaction rate be improved? We began our investigation with a screening of laccase-mediator combinations for PFOS degradation, utilizing the previously published reaction conditions [106]. However, after seeing no signs of PFOS removal, we altered the scope of our investigation to systematically probe the individual oxidation steps of the LMS reaction. Primarily, we focused on characterizing enzyme activity under a variety of conditions, testing the degradation of a proxy compound and prevalent water contaminant, carbamazepine (CBZ), in an LMS, and investigating the generation of the radical mediator species. This led to the discovery of an important removal artifact that may influence the application of enzyme-based treatment strategies to PFAS-contaminated water.

4.3 Materials & Methods

Chemicals

Chemicals used in the experiments were of reagent grade quality or higher, and were purchased from the following suppliers: MilliporeSigma, Fisher Scientific, Spectrum, and VWR. Commercial enzymes were purchased from MilliporeSigma (*Trametes versicolor, Agaricus bisporus, Aspergillus sp.*) and from Creative Enzymes (Native laccase, white rot fungi). Chemicals and enzymes were used without further purification. Mass-labeled internal standard compounds were purchased from Wellington Laboratories. The mass-labeled compounds arrived in glass ampules ranging from 1.0-50 μg/L, and were diluted to make stock solutions for preparation of internal standard solution and standard working solutions for the preparation of a standard curve. For preparation of aqueous buffers for the reactors, Milli-Q water was used. For preparation of mediator stocks for reactor amendments, HPLC-grade acetonitrile (MeCN) was used. Reactors were prepared using 50 mL polypropylene (PP)

Corning centrifuge tubes, or 20 mL glass scintillation vials.

Enzyme Activity Assay

A colorimetric UV-spectrophotometric assay was used to determine the relative enzyme activity among batches and species of commercial laccase enzymes. The assay measures the oxidative conversion of 2,6-dimethoxyphenol (DMP) to the corresponding 3,5,3'5'-tetramethoxydiphenoquinone [222]. The absorbance spectra of the quinone is measured at a wavelength maxima of 468 nm (ε=49,600 $M^{-1}cm^{-1}$) in a citrate-phosphate buffer (pH 3.8) prepared from a 0.1 M solution of citric acid and a 0.2 M solution of Na_2HPO_4. Assays were conducted in 96-well plates at a volume of 200 μL total. Buffer solution was added to the plate followed by the laccase-containing solution; DMP (1 mM) was then quickly added before placing the plate in a Shimadzu UV-vis reader for absorbance measurements. The laccase-containing solution was diluted appropriately (1,000 - 10,000x) in order to achieve an absorbance in the range of 0.1-1 AU for best accuracy. In the majority of experiments, the target enzyme activity was 0.5-2 U/mL; in order to accurately measure enzyme activity of these experiment solutions, a total dilution of approximately 1000x was required to obtain an absorbance reading in the appropriate range. Absorbance was measured continuously over 10 minutes. Solutions were assayed in triplicate from which the average absorbance measurements were calculated. Absorbance data was related to enzyme activity using the Beer-Lambert law,

$$A = \varepsilon b C \tag{4.1}$$

where ε=molar extinction coefficient, b=path length, and C=concentration. Path length was calibrated to 1 cm from a matrix blank using Gen5 Version 3.02 processing software. The change in concentration of substrate per minute (μmol/minute) was used to determine the enzyme activity, adjusted for dilution. The following equation was used,

$$Activity(U/mL) = \frac{\Delta A}{\varepsilon} \times 10^6 \times \frac{1}{D} \tag{4.2}$$

with a factor of 10^6 to convert from mol of product to µmol of product, and a factor of 1/D to correct for total dilution from the original enzyme containing solution.

Batch Transformation Experiments

Reactors were prepared in triplicate, unless noted otherwise. Reactor solutions consisted of the target substrate in a selected buffer, to which a selected mediator and enzyme was added. Reactors were prepared either in Corning 50 mL PP centrifuge tubes, with up to 10 mL solution volume, or 20 mL glass scintillation vials, with up to 5 mL solution volume, to ensure oxygenated headspace. Solutions were prepared in the following order: 1) Buffer was added to the tube/vial (e.g., sodium malonate); 2) A small volume of concentrated substrate stock was added to the buffer (e.g., 100 μL of aqueous PFOS, PFOA, or carbamazepine);

3) A small volume of concentrated mediator stock was added to the buffer (e.g., 50-100 μL of 1-hydroxybenzotriazole (HBT) in MeCN); 4) Laccase enzyme was added to the reactor solution, either as a solid powder or from a concentrated stock diluted in the same buffer used in the reactors. For control reactors (i.e., those without mediator, without enzyme, or without both), equivalent volumes of MeCN and/or buffer were added to the reactors such that volume changes throughout the course of the experiment were as consistent as possible for all reactors.

Reactors were placed in a floor shaker incubator (New Brunswick Excella E25) set to 30^{o}C and 130 rpm, unless noted otherwise. All reactions were aqueous phase only, unless noted otherwise. Following the protocol established by Luo et al. [105, 106], the reactors were amended with mediator and enzyme throughout the course of the experiment. The purpose of this protocol was to maintain enzyme activity and continue stimulating the reaction. Reactors were amended using a predetermined schedule, ranging from two-times daily to once a week, depending on the experimental set-up. The quantity and frequency of enzyme and mediator doses was one of the variables evaluated in this study, and the specifics of the dosing schedule is described for individual experiments.

Reactors were sampled to monitor target substrate concentration as frequently as once per day, up to once a week, depending on the length of the experiment as well as the mediator/enzyme amendment schedule. At the sampling time, all reactors were opened to promote aeration. Reactors were kept open for a minimum of 10 minutes to ensure oxygen was replenished in the reactor container. Sample aliquots were removed from reactors and immediately diluted into methanol (MeOH) or basic methanol (2% ammonium hydroxide) to terminate the reaction. A minimum of 100 μL aqueous sample was removed for dilution. For sacrificial extraction experiments, the aqueous solution volume at the end of the experiment was weighed and the equivalent volume of MeOH was added directly to the reactor (i.e., 2x dilution, 5 mL of MeOH added to 5 mL aqueous reaction solution) to ensure complete 'extraction' from the reactor in the case that substrate had sorbed to the container walls. This extract was measured and compared to a sample taken just prior to extraction to quantify sorptive effects.

Statistical analysis was performed using the Stats, NumPy, and one-way ANOVA modules in the SciPy package of Python 3.8.5. A paired, two-tailed T-test was used to determine P-values between two data sets; the one-way ANOVA test was used to determine P-values across multiple reactor conditions.

Analytical Methods

Samples were prepared for analysis by dilution in MeOH to a target concentration of 10 μg/L to ensure quantification within the calibration range (0.2-10 μg/L). The isotope dilution method was used to account for any potential matrix effects. Mass labeled [^{13}C]-PFAAs (2-5 μg/L) were added to LC-MS/MS sample vials for each sample in the final stage of sample preparation. Analytes were separated using a Zinc-Diol guard column coupled to Zorbax C18 XDB guard and analytical columns (Agilent Technologies). The mobile phase (0.4 mL/min)

was 5 mM ammonium acetate in water (A) and 5 mM ammonium acetate in MeOH (B) with a solvent gradient: hold 0-2 min 95% A, ramp to 10% A by 10 min, hold 10-11.5 min 10% A, ramp to 95% A by 12 min, hold 12-18 min 95% A. The LC-MS/MS setup included a delay C18 column after the purge valve to decrease the effect of possible contamination from upstream PTFE components. PFAS analytes were quantified by LC-MS/MS equipped with electrospray ionization in negative mode (Triple Quad 6460A, Agilent Technologies) multiple reaction monitoring (MRM). Gas and Sheath Gas Heater temperatures were 325 and 350°C, respectively. Gas and sheath gas flows were 9 L/min. The nebulizer was kept at 25 psi and the capillary voltage was 3.5 kV. PFAS were quantified by the transitions and collision energies listed in Table 3.5. Mobile phase blanks were run every 10 samples and select calibration samples were re-run every 20 samples to prevent contamination or carryover in the analysis.

EPR Spectroscopy

Electron paramagnetic resonance (EPR) spectroscopy studies were performed in the CalEPR center in the University of California, Davis with Dr. Guodong Rao and Dr. David Britt. X-band (9.4 GHz) continuous-wave (CW) EPR spectra were recorded on a Bruker Biospin EleXsys E500 spectrometer with a super high Q resonator (ER4122SHQE), an ESR900 liquid helium cryostat with a temperature controller (Oxford Instruments ITC503) and gas flow meter. CW EPR spectra were recorded under slow-passage, non-saturating conditions. Spectral simulations were performed in Matlab 2018a with Easyspin 5.2.35 toolkit [223].

The EPR sample of BTNO (benzotriazole-N-oxyl) radical in CH_3CN was prepared by mixing 100 μL 20 mM cerium (IV) ammonium nitrate in CH_3CN and 100 μL 20 mM HBT in CH_3CN. The spectrum was recorded at room temperature, using the following spectrometer settings: conversion time = 120 ms, modulation frequency = 100 kHz, modulation amplitude = 0.025 mT, and simulated using previously reported parameters [224]. EPR samples of HBT radicals generated by laccase enzymes were prepared by incubating aqueous solutions containing 1 mM HBT, 12 mg/mL Tv laccase, 10 μM $CuSO_4$, and 1 mM of different substrates for varying periods. The spectra were recorded at 50 K using the following spectrometer settings: conversion time = 120 ms, modulation frequency = 100 kHz, modulation amplitude = 0.5 mT.

4.4 Results & Discussion

Screening of laccase-mediator combinations for PFOS transformation

Multiple laccase enzymes were screened with five nitroxyl radical mediators for PFOS transformation. While the white rot laccase *Pleurotus ostreatus* previously reported for

PFAA degradation [105, 106] is no longer commercially available, we evaluated an alternative Native white rot laccase (Creative Enzymes) and *Agaricus bisporus* (Sigma), both of which are 'high-redox' laccases capable of oxidizing nitroxyl mediator compounds [213, 225]. In the proposed mechanism, the key species for initiating oxidation of the target substrates (i.e. PFOA, PFOS) is the BTNO radical. Therefore, the species of laccase should be interchangeable, as long as the enzyme has a high enough redox potential to oxidize HBT to the reactive radical BTNO, which mediates the electron transfer to the substrate. With the aim of expanding the relevance of LMSs for PFAS degradation, we sought to evaluate other laccase species and mediator compounds capable of catalyzing PFOS transformation. Based on previously reported mediator species capable of oxidizing PFOA and PFOS [211, 226], we chose to screen a variety of mediator compounds in order to optimize the transformation reaction. Of particular interest were nitroxyl compounds similar in structure to HBT, violuric acid, and ABTS, which were shown to decrease PFOA and PFOS concentrations in soil slurries [226]. Additionally, PFOA degradation was observed without a mediator in laccase systems containing soil slurries as well as soybean meal, perhaps indicating that natural mediators present in the soybean meal could promote degradation [227].

We selected five nitroxyl-bearing mediators (Figure 4.2) based on LMSs previously reported in literature. Because the nature of electron transfer mediated by the nitroxyl groups may differ, we wanted to evaluate the impact of the mechanism on degradation efficiency. Compounds such as HBT, violuric acid, and N-hydroxyphthalimide (HPI) generally perform oxidation through a hydrogen atom transfer (HAT) mechanism by abstracting a hydrogen atom from the substrate, but can also perform electron transfer (ET) in some cases [224]. Alternatively, compounds such as TEMPO and AZADO generally perform oxidation through an ionic mechanism, through which the radical forms a positive charge and the mediator initiates a typical nucleophilic-type reaction mechanism. Given that our primary target substrates, PFOS and PFOA, contain no hydrogen atoms at relevant pH ranges, we hypothesized that the reaction with HAT/ET type mediators should proceed via the ET route.

Additionally, in a previous study [106], it was shown that copper was essential to PFOS degradation in the LMS with *Pleurotus ostreatus* and HBT. It was hypothesized that the Cu^{2+} could induce a structural change in PFOS, 'unlocking' the helical CF_2 backbone of PFOS. While density functional theory (DFT) calculations reported in this study did not indicate a significant change in the C–C bond strength in the backbone units, they showed a change in the dihedral bond angles in the chain. It was suggested that the decrease in the dihedral angles allowed for greater accessibility for attack by the oxidized HBT radical, facilitating the breaking of the CF_2 backbone. While it is interesting that copper may induce this change in the helical structure of PFOS, which has been similarly shown for other metal cations [228], it is not immediately clear how a change in dihedral angle would facilitate the oxidative reaction.

Screening PFOS degradation with two laccase enzymes and five nitroxyl mediators, with weekly dosing of each, resulted in no significant PFOS degradation (Figure 4.3). The apparent decrease in PFOS concentration across the 28 day reaction is similar among the treatment conditions and the enzyme-only control, suggesting that the laccase-mediator re-

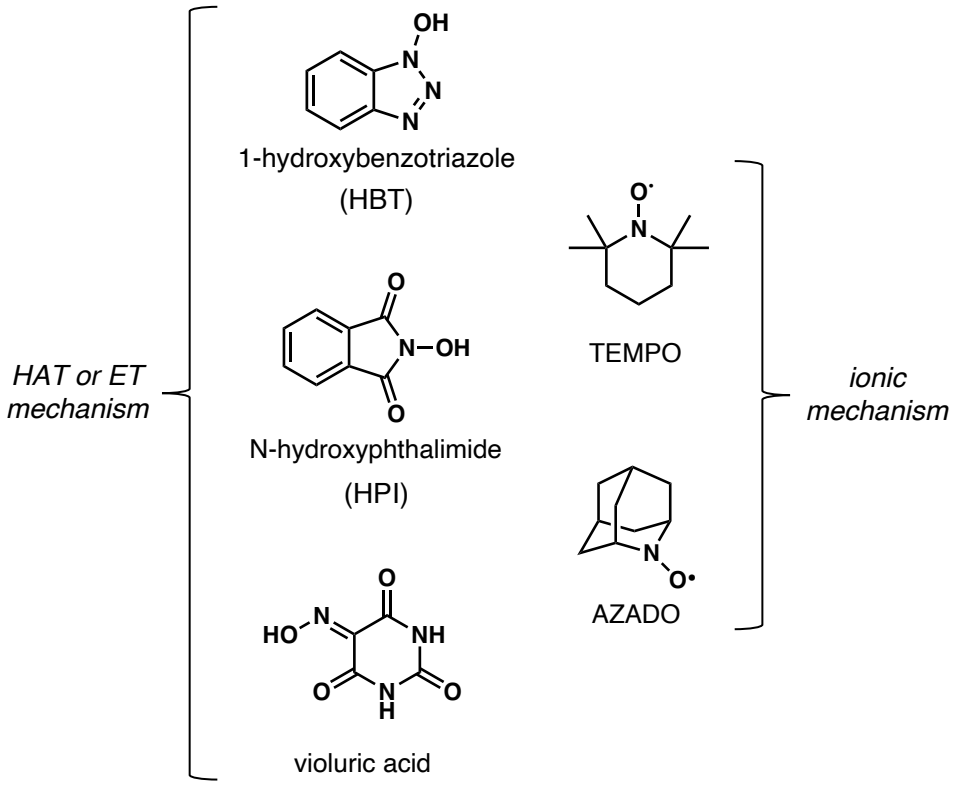

Figure 4.2: Nitroxyl (N-OH) mediator compounds selected for screening.

action is not initiating detectable PFOS degradation. Additionally, no detectable differences were observed between the mediator compounds screened. This suggested that the LMS was not effectively degrading PFOS among the conditions studied. Because the main difference in this system and the previously reported reaction [106] was the enzyme itself, we decided to further evaluate the enzyme-mediator reaction via evaluation of reactivity towards a proxy compound.

Evaluating degradation of a proxy compound

Upon observing no apparent degradation of PFOS or PFOA in the LMSs initially screened, we chose to evaluate the degradation of a proxy compound, carbamazepine (CBZ), in order to probe the reactivity of the system. CBZ is an antiepileptic drug and persistent aqueous pollutant. It is one of the most frequently detected pharmaceuticals in surface and groundwater [229], as well as in wastewater treatment plant effluents [220]. Though non-fluorinated, CBZ is hydrophobic ($\log K_{ow} > 2$) [230] and generally requires a strong oxidizing agent (e.g., hydroxyl radical) for complete mineralization [231]. Multiple other researchers have investigated LMS treatment for CBZ as an environmentally benign approach that requires lower

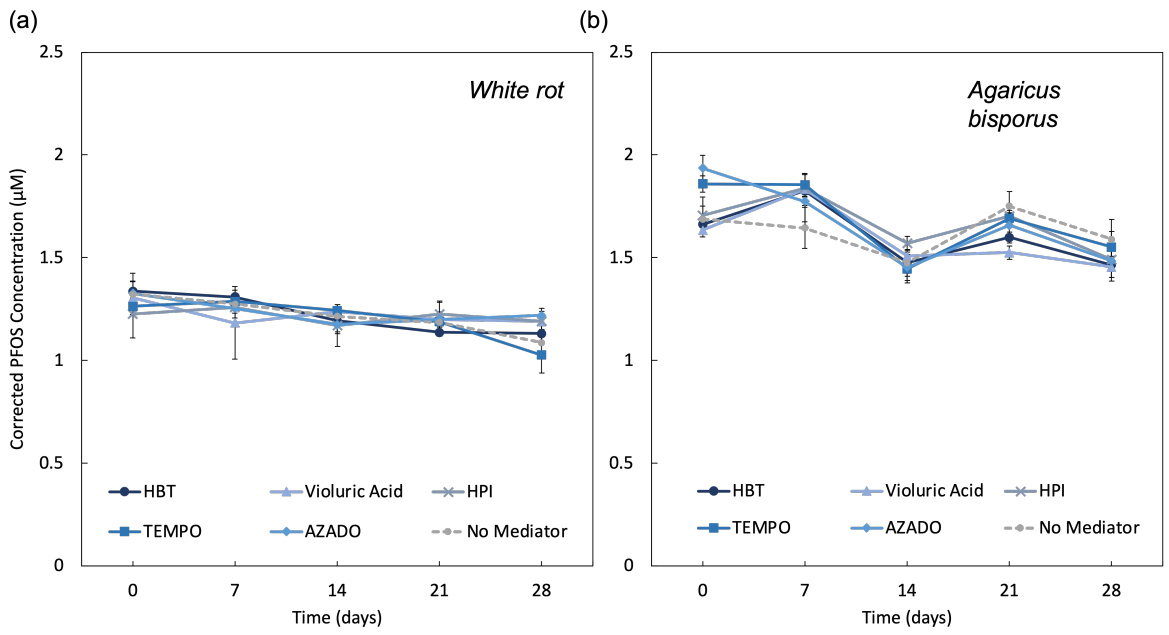

Figure 4.3: Screening of laccase-mediator combinations for reactivity towards PFOS. PFOS concentrations do not appear to decrease significantly compared to the no mediator control over the 28 day period (p=0.58 white rot, p=0.24 *Agaricus bisporus*. Concentrations were normalized to a control (No laccase, No mediator) to account for possible evaporation (see Supporting Information Figure 4.11). Laccase and mediator were added weekly at the time of sampling.

energy inputs and avoids accumulation of a waste stream [220, 229]. It has been shown that *Trametes versicolor* laccase (TvL) and HBT can result in CBZ removal of up to 60% [220]. In theory, the oxidation of the mediator, HBT, and its subsequent reaction with the target compound, PFOS or PFOA, is critical for driving the degradation reaction. We reasoned that by evaluating CBZ degradation using *Trametes versicolor* laccase and HBT we could confirm that the laccase-mediator reaction was in fact occurring. Both *Trametes versicolor* and *Pleurotus ostreatus* are considered high redox potential species, with redox potentials of 800 mV (vs. NHE) [232] and 650-740 mV (vs. NHE) [225], respectively. With this assumption, submitting PFOS and PFOA to the reaction conditions capable of CBZ transformation, should result in oxidation of the perfluorinated substrates as well.

We conducted preliminary experiments to evaluate the effect of enzyme dosage and mediator compound on CBZ degradation, and screened an additional high redox laccase enzyme, *Aspergillus* (770 mV vs. NHE) [233] and a *Pycnoporus* species (see Supporting Information Figure 4.14, 4.15) with multiple buffers in addition to *Trametes versicolor*. We observed CBZ removal with the *Aspergillus* laccase, but not in the *Pynoporus* system. We also eval-

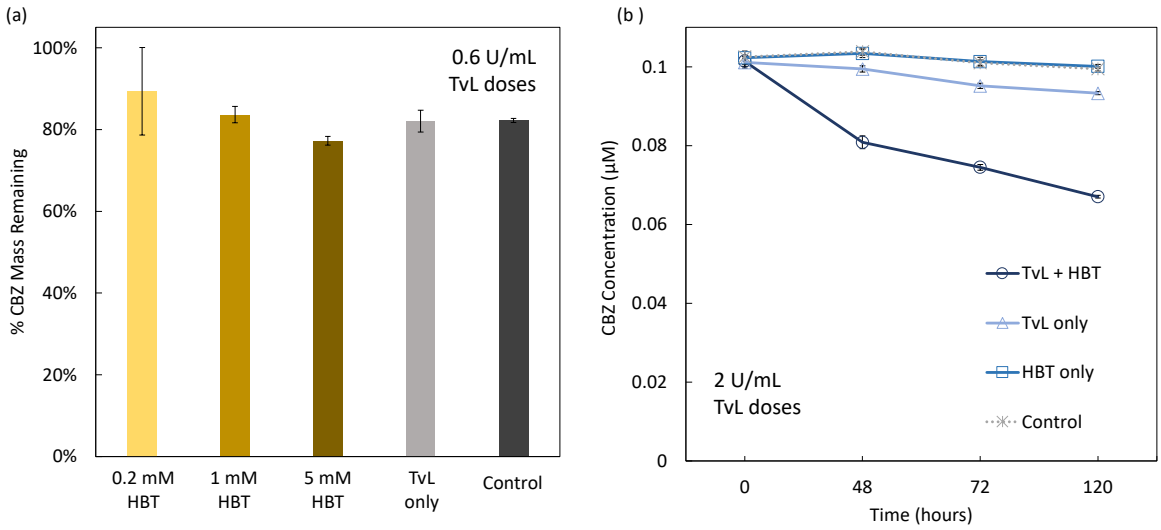

Figure 4.4: CBZ degradation with TvL and HBT treatment. Left panel a) Effect of mediator dosage (0.2 - 5 mM HBT) with 0.6 U/mL TvL dosage on CBZ mass removal over 48 hours; Right panel b) CBZ degradation with 1 mM HBT + 2 U/mL TvL dosage over 120 hours. Averages and standard deviations represent triplicate reactor conditions.

uated enzyme activity in various buffers (see Supporting Information Figures 4.12 4.13. In evaluating the effect of mediator dosage with *Trametes versicolor*, we observed that higher mediator doses (1 mM, 5 mM) may slightly improve the removal efficiency of CBZ compared to the 'No Mediator' control (Figure 4.4-a).

To improve the removal efficiency, we increased the enzyme dose from 0.6 U/mL to 2 U/mL and decreased the initial concentration of CBZ 0.1 µM. Treatment with TvL and HBT resulted in approximately 35% removal of CBZ over the course of 120 hours ($p < 0.001$) (Figure 4.4-b). While we were satisfied with these results as an indication that the laccase-mediator reaction was occurring, it should be noted that we were not able to achieve the 60-95% removal levels reported previously [220, 229].

EPR Study of nitroxy-radical species

To further assess the enzyme-mediator reaction, we investigated the generation of the BTNO radical with EPR. Following a previous report [224], we were able to generate the BTNO radical in the CH_3CN solution by oxidizing HBT with Ce (IV). The room-temperature CW EPR spectrum of the resulting dark solution showed a hyperfine-split feature that can be simulated using previously reported ^{14}N and ^{1}H hyperfine parameters (Figure 4.5-a) [224].

Formation of the BTNO radical in aqueous solution was also observed by incubating TvL laccase and HBT at the presence of Cu^{2+} (Figure 4.5-b). However, the hyperfine patterns

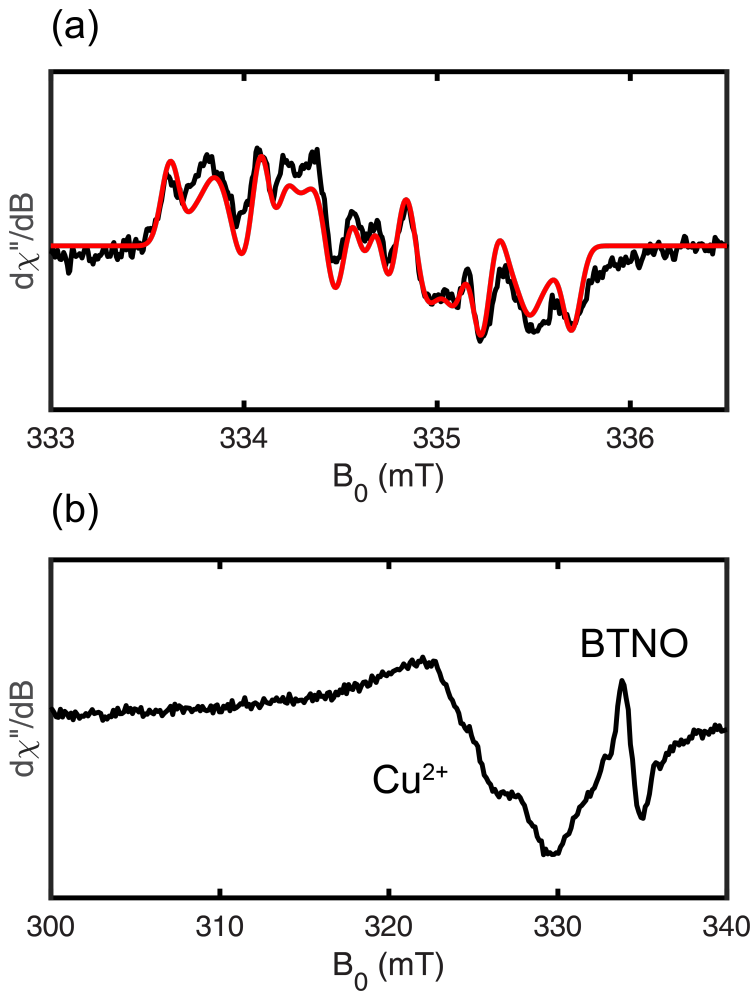

Figure 4.5: X-band CW EPR spectra. (a) Room temperature EPR spectrum of BTNO radical generated in CH_3CN (black trace) and simulation (red trace). Simulation parameters: g = 2.0069, three ^{1}H with a (^{1}H) = 1.0, 5.7 and 12.8 MHz, three ^{14}N a (^{14}N) = 1.6, 4.3 and 13.3 MHz. (b) EPR spectrum of BTNO radical generated in the laccase system. The feature on the left is due to Cu^{2+} EPR signal.

were not resolved in the EPR spectrum of the frozen aqueous solution, likely due to the line broadening caused by anisotropies in the latter. Similar EPR signals for N-oxide radicals in aqueous solutions have been documented previously [234].

We hypothesized that EPR may give some indication as to whether the HBT radical interacted with the target perfluorinated substrates. We evaluated the EPR reaction under similar conditions used in the aqueous reactors monitored via LC-MS/MS (2 U/mL TvL, 1 mM HBT); we chose to use a lower copper concentration (10 μM rather than 10 mM) to avoid interference with the organic radical signal. The decrease in the radical signal within 20 minutes upon PFOA and PFOS addition could suggest an interaction between BTNO and the substrate; however, the signal increased to the initial level for both substrates after 120 minutes (see Supporting Information Figure 4.17). While it is unclear why the addition of PFOA or PFOS causes the radical signal to decrease, a parallel experiment monitoring PFOA and PFOS concentration by LC-MS/MS confirmed that no removal was detected under these conditions (see Supporting Information Figure 4.18).

Treatment of PFOA and PFOS with Trametes versicolor and HBT

Upon confirming the reactivity of the *Trametes versicolor* and HBT system towards a proxy compound, we evaluated the reactivity towards another previously reported LMS substrate, PFOA, the carboxylic acid analogue of PFOS. The degradation of PFOA was previously reported by an LMS system [105, 226]. As a typically easier to oxidize substrate than PFOS using other destructive technologies [150], we considered that we might have greater success in reproducing PFOA removal and degradation. Additionally, reports of PFOA degradation in some iterations of the LMS studied included solids in the reaction matrix, and we hypothesized that the addition of solids may have impacted laccase reactivity.

To evaluate this hypothesis, we compared treatment of a solution spiked with 1 µM PFOA in soil and soil-free reactors. The treatment conditions included an enzyme-only control, as well as an untreated control to account for potential sorption effects to the soil or the reactor containers. We chose to dose reactors more frequently over a shorter period of time– 6 doses over two weeks– based on the previously reported conditions [226] as well as the loss of enzyme activity we observed throughout the dosing regimen.

At each timepoint, triplicate reactors were sampled sacrificially by adding MeOH directly to the vial such that the volume was doubled; the solution was then allowed to equilibrate overnight before an aliquot was taken for LC-MS/MS analysis. As shown in Figure 4.6, neither the enzyme-mediator treatment nor the enzyme-only treatment resulted in removal of PFOA compared to the control. Additionally, no difference in removal was observed between the soil and soil-free conditions. However, the soil did impact the retention of enzyme activity. Between doses (approximately 48-hours), the enzyme activity decreased nearly to zero in the soil-free reactors dosed with laccase and mediator, while it decreased by roughly 60% in the soil-containing reactors. Similarly, in the reactors dosed with enzyme-only, the enzyme lost approximately 56% of its activity in the soil-free reactors, and only 35% in the soil-containing reactors. While the higher enzyme activity retention in the soil-

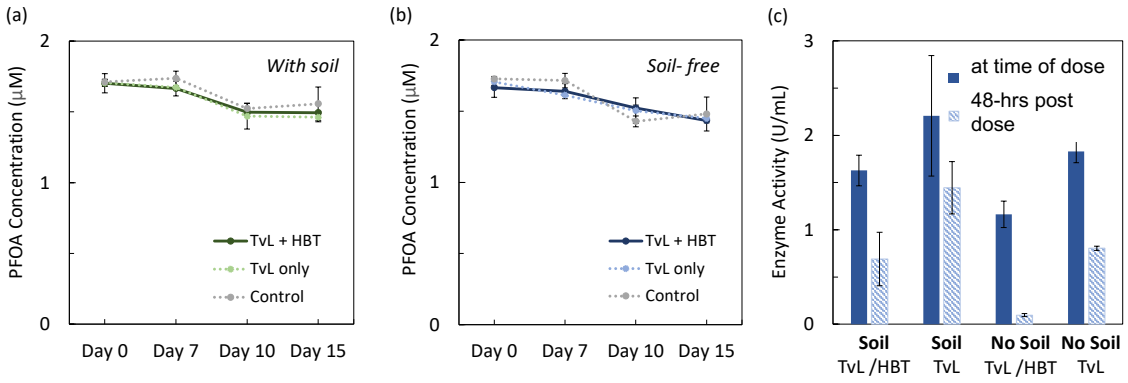

Figure 4.6: PFOA removal is not substantial compared to control reactors in a) soil or b) soil- free conditions over the course of 15 days; TvL and HBT were added every 2-3 days, ($6x$ total). c) Enzyme activity is better retained in soil containing reactors.

containing reactors did not apparently improve PFOA removal, this observation did provide us with important insight for the dosing regimen. The near complete loss of activity within 48 hours in the soil-free reactors suggested that dosing frequency could be increased to minimize the amount of time that laccase was inactive during experiments.

We also applied a near identical treatment regimen to a parallel set of aqueous phase reactors containing a target concentration of either 0.1 μM PFOA or 0.1 μM PFOS in a 10 mM $CuSO_4$ buffer. It was previously reported that the addition of copper, in the form of $CuSO_4$, was essential to the reactivity of the LMS [106, 212]. It was suggested that the Cu^{2+} cation could form a complex with the negatively charged head group of PFOA or PFOS (the carboxylate or sulfonate, respectively), bridging the enzyme and substrate allowing for faster transfer of the radical HBT. The reactors were treated with 1 U/mL *Trametes versicolor* and 1 mM HBT; doses of enzyme and mediator were added twice daily, for four days. We increased the frequency of dosing because we observed that enzyme activity decreased nearly to zero over the course of 6-8 hours (see Supporting information Figure 4.19). Aliquots were removed daily to measure concentration.

While there is an apparent concentration decrease in both PFOA and PFOS concentration after the first two doses of enzyme and mediator (within the first 24 hours), the concentration then appears to level off (Figure 4.7-a,b). Additionally, at the end of the experiment, the reactors were extracted with MeOH. Upon analyzing the total mass contained in the reactors at the beginning and end of the experiment, and comparing it to the mass determined from the 'extract' concentration, both PFOA and PFOS can be fully recovered (Figure 4.7-c,d). The recovery of PFOS and PFOA suggests that the initial decrease in concentration is likely due to physical processes in the system (e.g. sorption). Despite full recovery in all the conditions tested, the significant difference in the enzyme-mediator and enzyme-only

treated reactors suggests that the enzyme may be adsorbing PFOA and PFOS. Both PFOA and PFOS have been shown to have a strong affinity for proteins, namely human serum albumin (HSA) [235–237] and bovine serum albumin (BSA) [238]. Recently, one group of researchers even investigated proteins as adsorbents for PFOA, including BSA, casein, egg white albumin, and lysozyme [239], and found that these proteins could achieve up to 93% removal depending on the aqueous conditions. The adsorption mechanism in proteins is understood to be primarily due to hydrophobic interactions, and specific protein binding sites have been reported for proteins of interest such as HSA [240].

The enzyme-only conditions do not appear to promote significant sorption of PFOA compared to PFOS, while the enzyme-mediator conditions appear to promote sorption of both substrates. Molecular docking studies have shown that changes in the enzyme oxidation state significantly change certain structural characteristics of the protein [241]. It is possible that the binding mechanism of PFOS is relatively unaltered regardless of the enzyme oxidation state, while the binding affinity of PFOA is affected by the enzyme oxidation state, hence indicating sorptive behavior only in the presence of the enzyme and mediator. The apparent increase in PFOA and PFOS, particularly in the enzyme-free treatment conditions, may be due to incomplete desorption from the protein upon basic MeOH extraction.

Interestingly, when CBZ was subjected to these treatment conditions (i.e., 10 mM $CuSO_4$ buffer), we did not achieve as high of removal rates as observed in the sodium malonate buffer. Only 10% CBZ mass loss was observed compared to the control (see Supporting Information Figure 4.20, while we observed over 30% removal compared to the control in the sodium malonate buffer. One potential cause of this is that a lower enzyme activity was used per dose in this experiment (1 U/mL), although the same quantity of enzyme was added per 24 hr period. Importantly, we did not observe recovery of CBZ in the extracted reactors at the end of the experiment, as was observed in the PFOA and PFOS reactors, supporting that CBZ was in fact degrading in the treatment conditions containing TvL and HBT.

4.5 Precautions in assessment of enzymatic treatment systems

While attractive as a bio-based treatment method for PFAS remediation, laccase-mediator systems appear to be unsuccessful at degrading the perfluorinated compounds PFOA and PFOS. Despite prior studies which indicated promising transformation results via treatment with a high redox laccase species, we were unable to reproduce transformation with an alternative high redox species *Trametes versicolor*, despite the multiple literature reports of *Trametes versicolor* and HBT systems for contaminant degradation [118, 220, 229]. Investigation by EPR confirmed the generation of the radical species, however, no reaction between HBT and the target perfluorinated substrates was apparent. Additionally, our results indicated that substrate sorption by the protein was likely causing concentration fluctuations in the treatment conditions, that could appear as a transformation artifact in enzyme-based

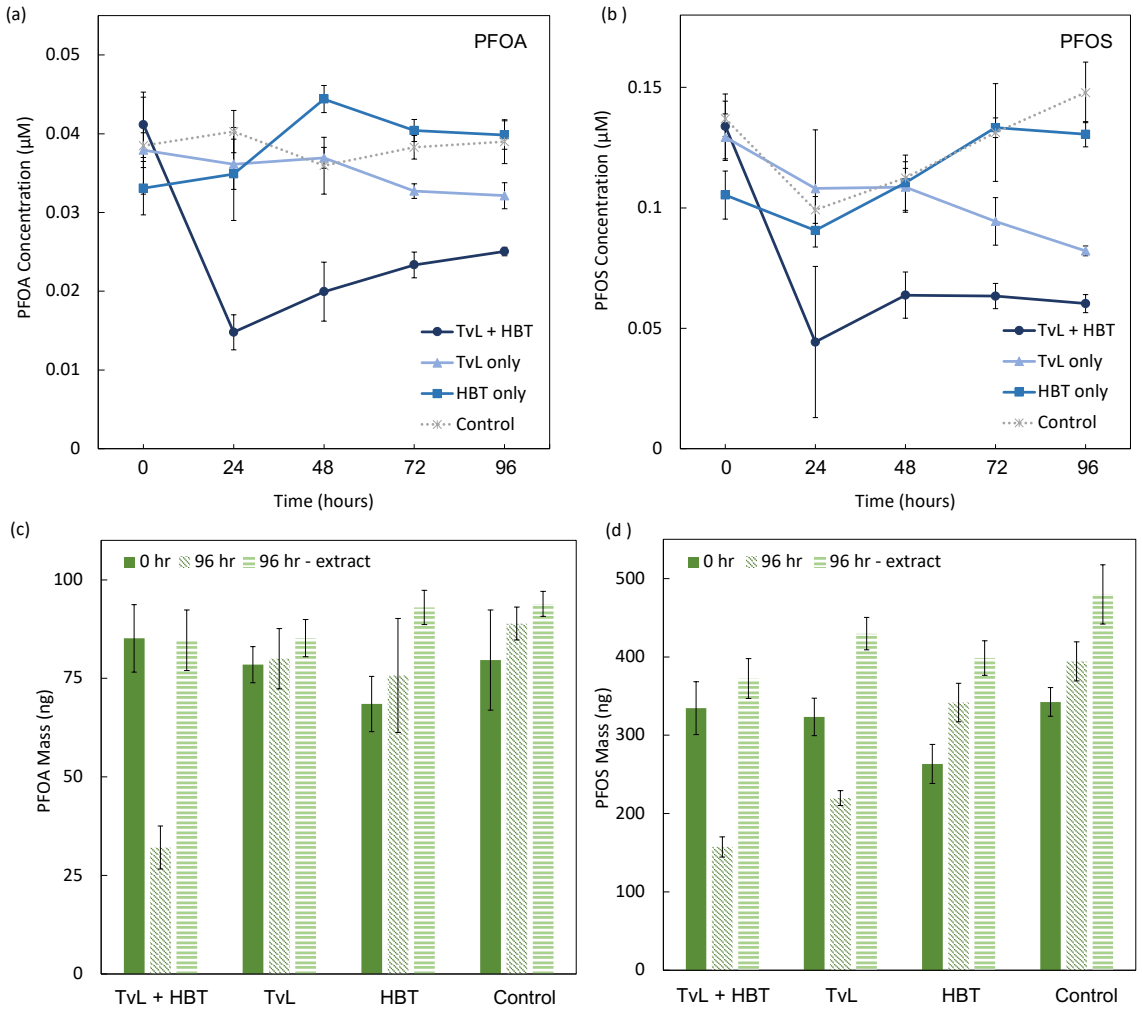

Figure 4.7: Reactors were amended with TvL and HBT twice daily. a) Concentration of PFOA and b) Concentration of PFOS monitored via removal of an aqueous aliquot from the reactors; c) Mass of PFOA and d) Mass of PFOS in reactors calculated from detected concentration and total solution volume at the beginning of the experiment, at the 96 hour time point, and in the extracted solution volume at the 96 hour time point. Error bars are standard deviations of triplicate reactors.

treatment systems.

The adsorption of PFAS to proteins is not novel and may be a viable remediation strategy in and of itself, although the quantity of enzyme needed may be prohibitive. However, the study of PFAS-protein binding mechanisms could provide insight to bio-inspired adsorptive materials to selectively target PFAS removal from complex waste streams. Given the ubiquity of PFAS contamination, bioremediation is an attractive treatment strategy but extremely challenging due to the strength of the C–F bond and lack of defluorinating bacteria [202]. Innovations in chemical treatment strategies, along with bio-based strategies, will be necessary to address PFAS contamination.

Despite our findings, laccase-mediator systems may be useful for treatment of certain polyfluorinated substances that are common precursors to PFAAs. Some researchers have demonstrated success in using a *Trametes versicolor* system to degrade 6:2 and 7:3 fluorotelomers [242, 243]. However, further research is needed to evaluate whether fungal remediation is a viable strategy for environmental remediation of polyfluorinated substances.

4.6 Supporting Information

Determination of enzyme activity of commercial laccases

Enzyme activity may vary batch by batch in the case of commercially purchased enzymes, or in the case of enzymes isolated in the lab, may vary isolate to isolate. In order to standardize the relative quantity of enzyme used across experiments, or compare enzyme 'doses' across experiments, a quantitative enzyme activity assay was used. Laccase enzyme activity assays were performed using previously published methods for spectrophotometric assays, which make use of UV-visible compounds that can be oxidized by laccase. The two assays used in this work used ABTS and dimethoxyphenol (DMP) as indicator compounds. In the assay, as in most enzymatic assays, formation of 1 μmol of oxidized substrate is considered equivalent to 1 U/mL enzyme activity. Activity can be calculated by plotting the slope of the absorbance curve for different dilutions of the enzyme; an example for the DMP assay is shown in Figure 4.8; an example of activity calculation from the ABTS assay is shown in Figure 4.9. Different indicator compounds can result in different activity calculations. Given that both ABTS and DMP are often cited in laccase literature, we compared both assays for determining the activity of *Trametes versicolor*. As evidenced in Figure 4.10, ABTS indicates a 100-fold greater activity for the enzyme than DMP. Because the system we were attempting to replicate cited use of the DMP assay, we chose to base our target activity 'dosage' on the DMP assay rather than the ABTS assay.

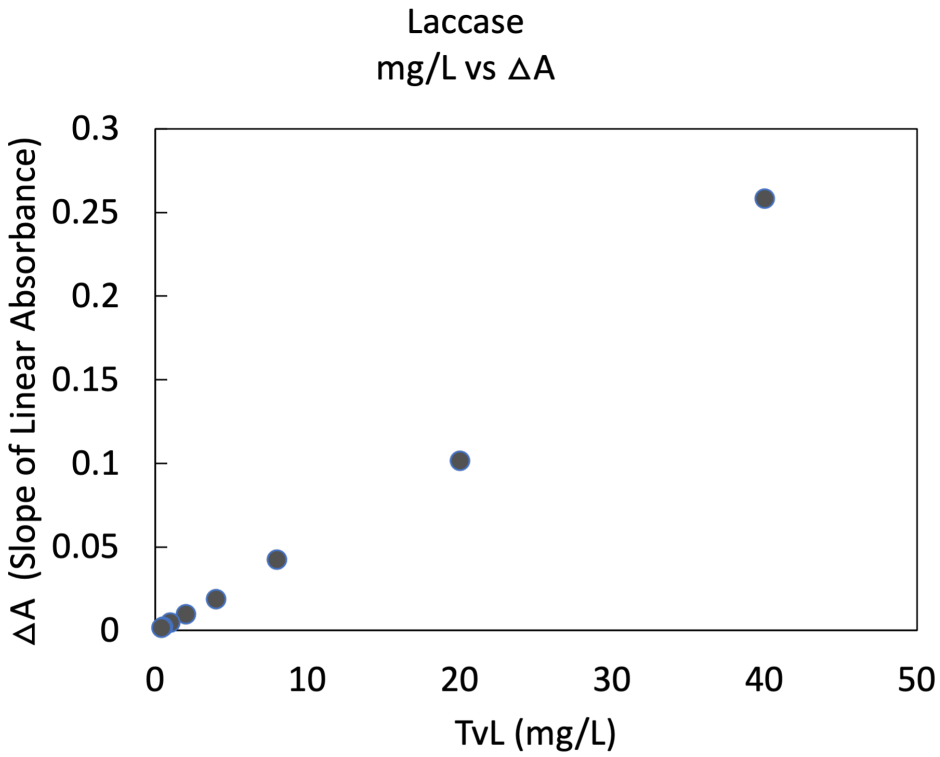

Figure 4.8: From the raw data generated by the continuous absorbance assay, a plot of Δ A versus mass of enzyme can be generated to show the relative mass of enzyme required for the desired enzymatic activity.

Corrected concentration calculations for enzyme-mediator screening

In the preliminary enzyme-mediator screening conditions, summarized in Figure 4.3, we observed increases in PFOS concentration across all the treatment conditions that we attributed to evaporation through filter caps over the 28-day treatment period (Figure 4.11). To correct for evaporation, we compared the detected concentrations ($C_{detected-Day\ X}$) in the treatment reactors between sampling time points to the concentration in the control reactor ($C_{control-Day\ X}$), which contained no enzyme and no mediator. Specifically, $C_{detected-Day\ X}$ in each treatment reactor for Day 0, 7, 14, 21, 28 was divided by the quotient of the concentrations in the control on Day 0 and Day 0, 7, 14, 21, 28 to give $C_{corrected-Day\ X}$:

$$C_{corrected-Day\ X} = \frac{C_{detected-Day\ X}}{C_{Control-Day\ 0}/C_{Control-Day\ X}} \tag{4.3}$$

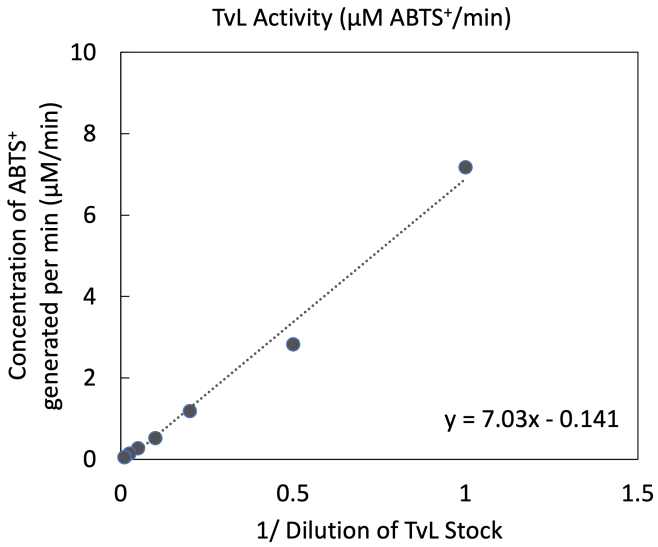

LINEST Fit	7.0300154	-0.1409768		
Dilution for 1 U/mL activity (from og. stock):	0.16230075	6.16140109		
Stock	20	mg		
	0.5	L		
Target	6.49202988	mg/L		
	6.5	mg/mL		
	in each 10 mL solution, 65 mg of TV			

Figure 4.9: A stock solution of *Trametes versicolor* laccase was prepared in the buffer solution (i.e., 50 mM sodium malonate) and diluted sequentially, in order to determine the relative concentration required for 1 U/mL activity.

Additionally, to the control reactor set, 'doses' of 10 mM $CuSO_4$ buffer and CH_3CN were added weekly at the same time as enzyme (in buffer solution) and mediator (in CH_3CN) to maintain as consistent of volume addition to all the reactors as possible.

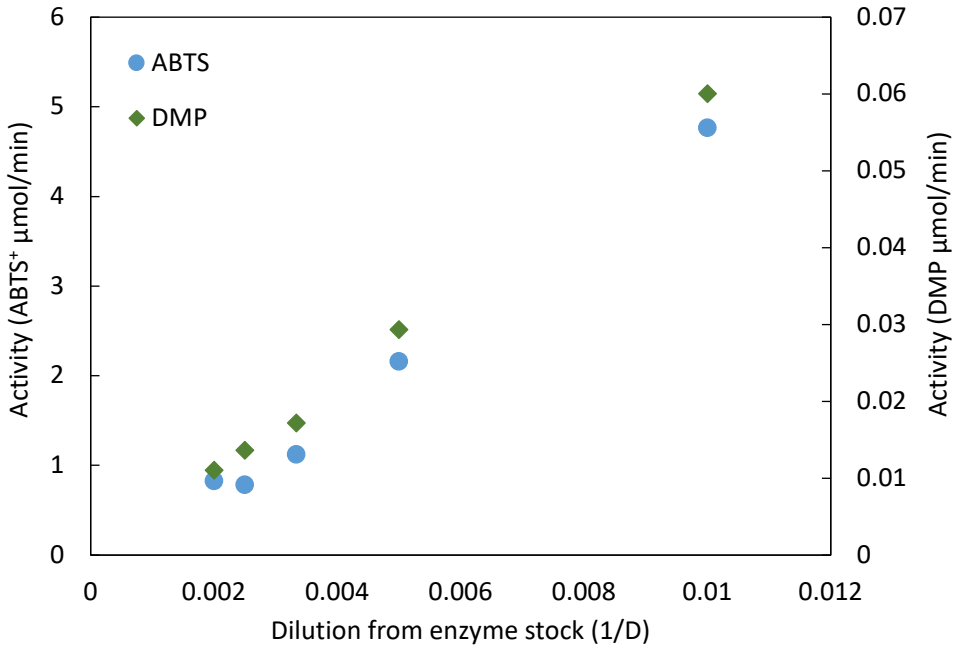

Figure 4.10: Activity calculated from the ABTS assay and DMP assay. Dilution series from the same enzyme stocks were prepared in order to determine activity; the only difference in the assays was the substrate added (e.g., 1 mM ABTS or 1 mM DMP). The nearly 100-fold increase in enzyme activity indicated by the ABTS assay demonstrates the importance of a consistent assay technique between interlaboratory experiments, and intralaboratory experiments when evaluating the role of enzyme activity in system reactivity.

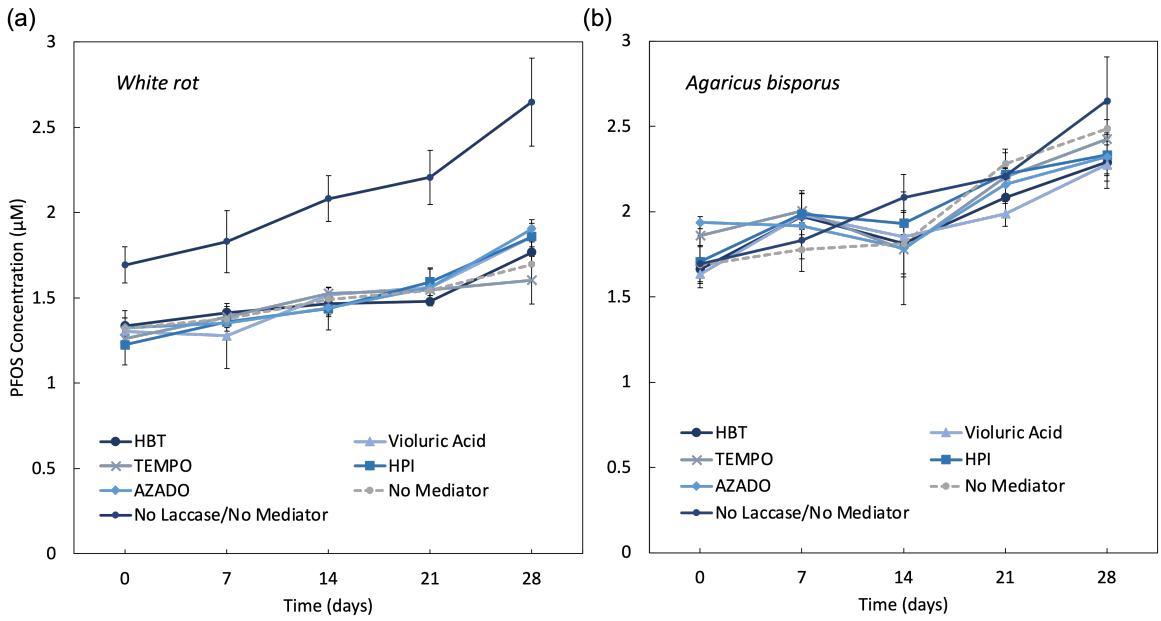

Figure 4.11: PFOS concentrations in reactors over the 28-day period. Increases in concentration were observed due to evaporation, thus concentrations were corrected using the No Laccase, No Mediator control.

p-values PFOA treated reactors	Conc. (t_0 and t_f)	Mass (t_0 and t_f)	C_f (treated*) compared to C_f (control)	M_f (treated*) compared to M_f (control)
TvL + HBT*	0.472	0.940	0.447	0.331
TvL only*	0.812	0.329	0.069	0.0293
HBT only*	0.0350	0.0062	0.126	0.565
Control	0.469	0.318		

p-values PFOS treated reactors	Conc. (t_0 and t_f)	Mass (t_0 and t_f)	C_f (treated*) compared to C_f (control)	M_f (treated*) compared to M_f (control)
TvL + HBT*	0.555	0.360	0.057	0.0470
TvL only*	0.0352	0.0219	0.0501	0.0627
HBT only*	0.0199	0.0357	0.0738	0.0504
Control	0.0364	0.0078		

Table 4.1: Standard two-tailed T-tests were used to determine p-values for the data, as described in the Materials & Methods section.

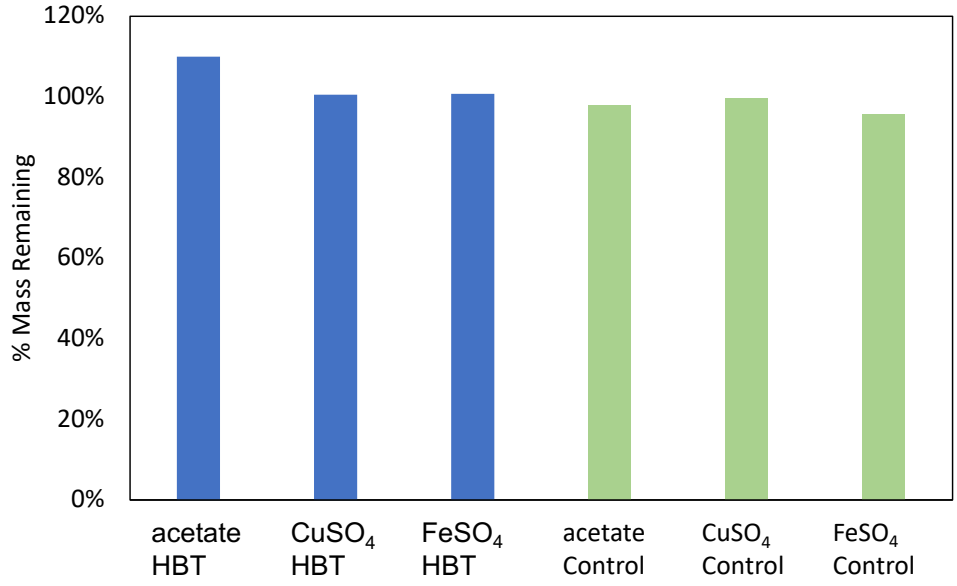

Figure 4.12: Degradation of PFOS (10 μM) with 1 U/mL TvL and 1 mM HBT treatment in different buffers, with and without mediator (30^{o}C, 150 rpm). Three doses of TvL/HBT were added over the course of 48-hours. Values shown are averages of duplicate reactor conditions; no observable differences were seen among the different buffers screened.

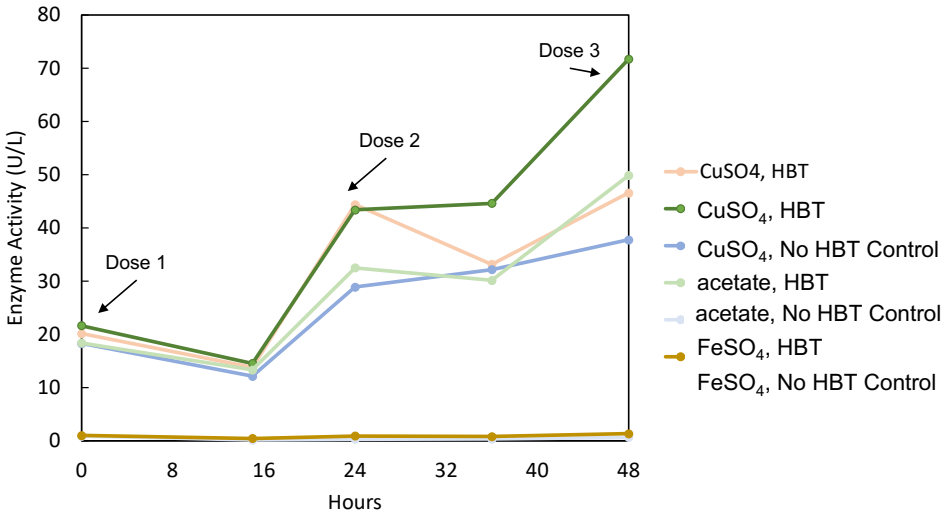

Figure 4.13: Activity monitored by DMP assay (oxidation of 2,6-dimethoxyphenol monitored by UV-vis) during experiment evaluating potential removal in different buffers; enzyme activity is retained in copper and acetate buffers (5 mM $CuSO_4$, 100 mM NaAc), but no enzyme activity is observed in the 5 mM $FeSO_4$ buffer indicating that Fe^{2+} may inhibit enzyme activity.

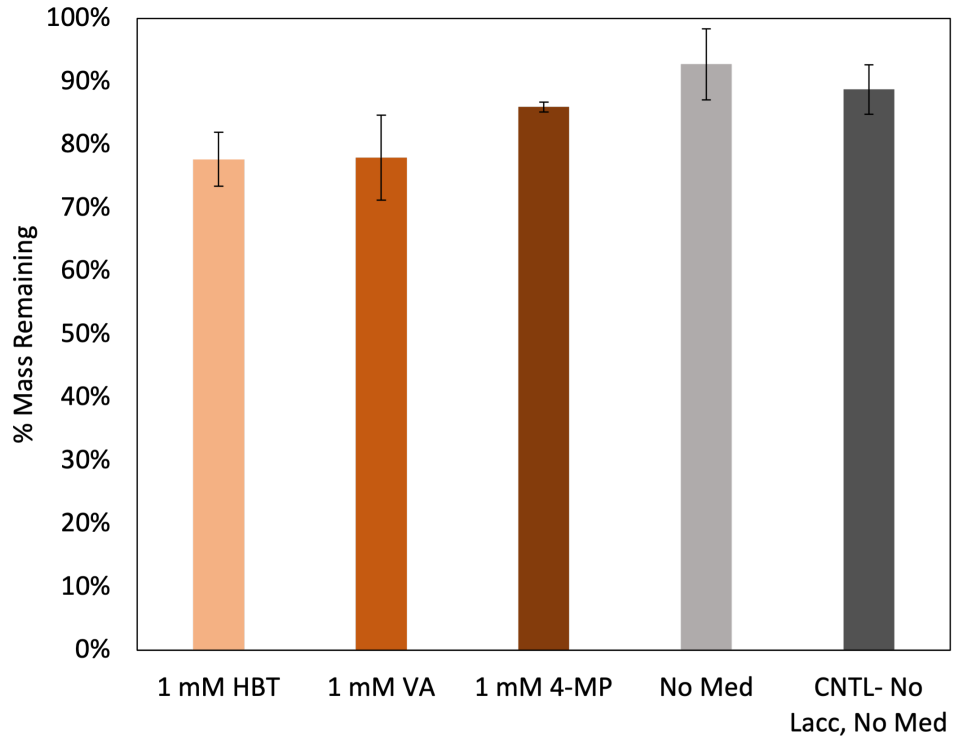

Figure 4.14: Degradation of CBZ with 2.5 U/mL Aspergillus and 1 mM mediator over 72 hours; reactors were placed on a shaker incubator set to 30^{o}C and 130 rpm; reactors were treated 3 times over the reaction time course. Three mediators were screened in a 50 mM sodium malonate buffer. Data shown is for averages of duplicate conditions.

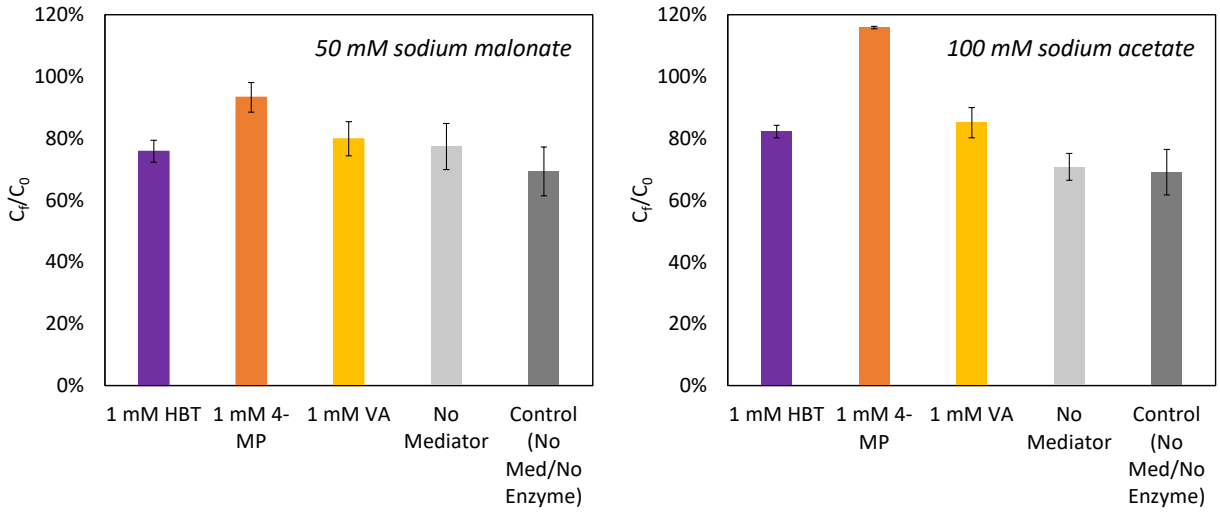

Figure 4.15: Degradation of CBZ with 1 U/mL Pycnoporus enzyme (crude) and 1 mM mediator over 120 hours; reactors were placed on a shaker incubator set to 30^{o}C and 130 rpm; reactors were treated 3 times over the reaction time course. Three mediators were screened in two different buffers, in a) 50 mM sodium malonate buffer, pH 4.5 and b) 100 mM sodium acetate buffer (pH 5). Error bars represent the standard deviation of concentrations measured in duplicate reactors. Neither set of reactors indicated observable degradation of CBZ.

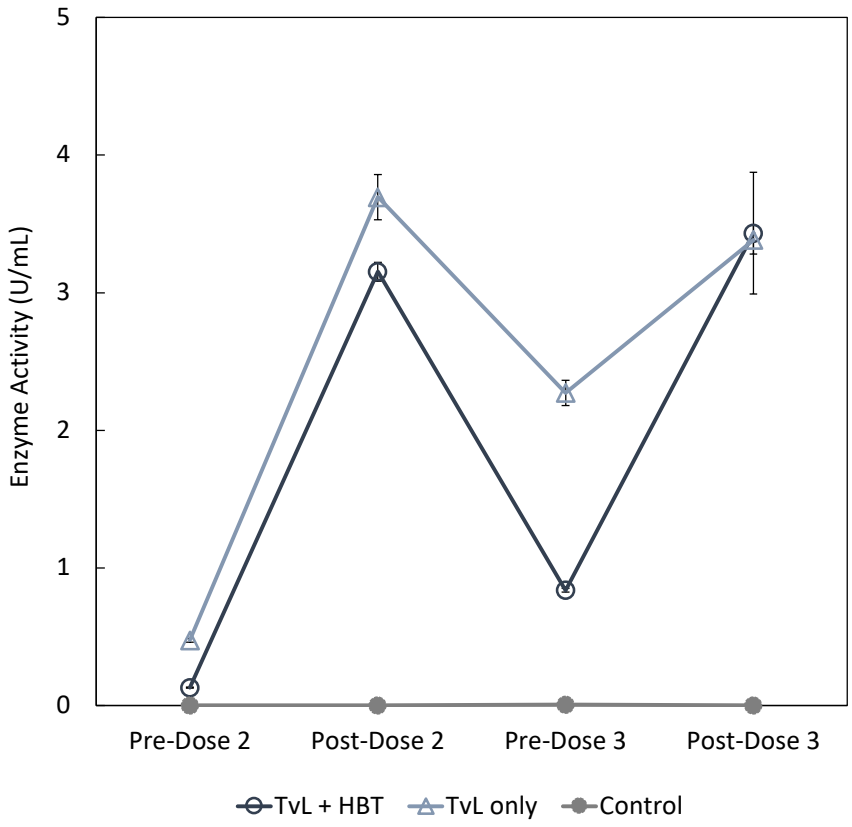

Figure 4.16: TvL activity monitored between doses by the DMP assay. CBZ reactors treated with 2 U/mL TvL and 1 mM HBT in a 50 mM sodium malonate buffer (adjusted to pH 5). Doses of enzyme and mediator were added 0 hours, 48 hours, and 72 hours (3 doses total).

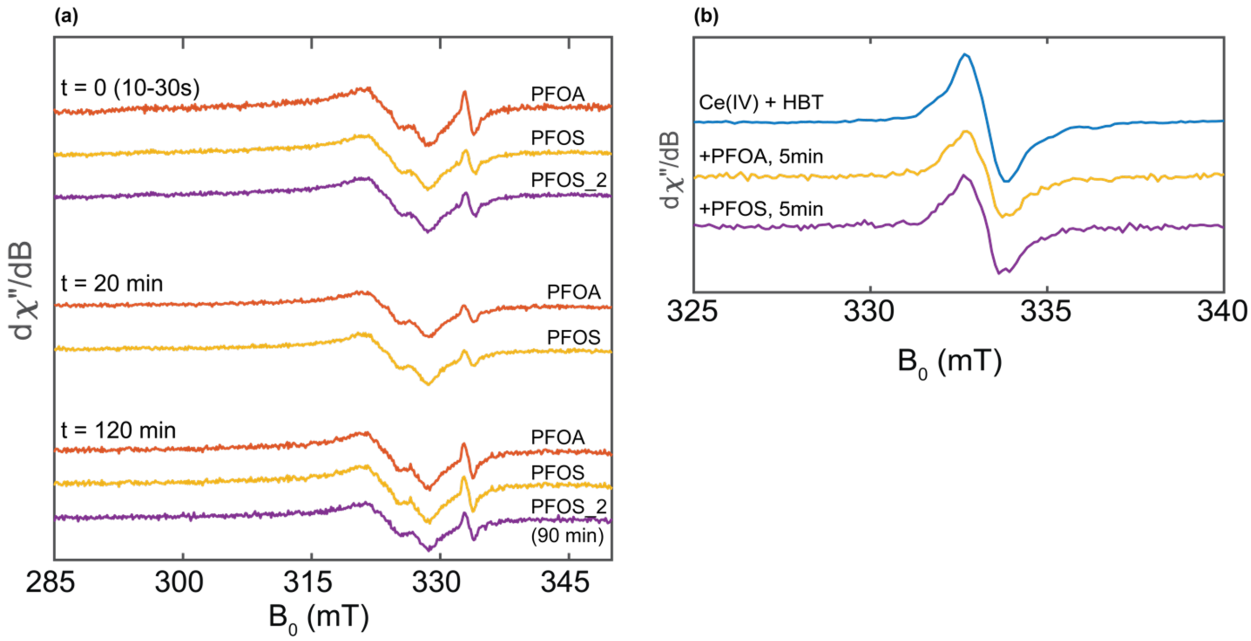

Figure 4.17: a) HBT radical generated in a 10 μM $CuSO_4$ matrix with 2 U/mL TvL and 1 mM HBT; radical signal decreases within 60 seconds of PFOS addition and within 20 minutes after PFOA, PFOS addition but then increases to the same level in the presence of both substrates. b) HBT radical generated in acetonitrile with Ce (IV); radical signal remains constant immediately after PFOA, PFOS addition.

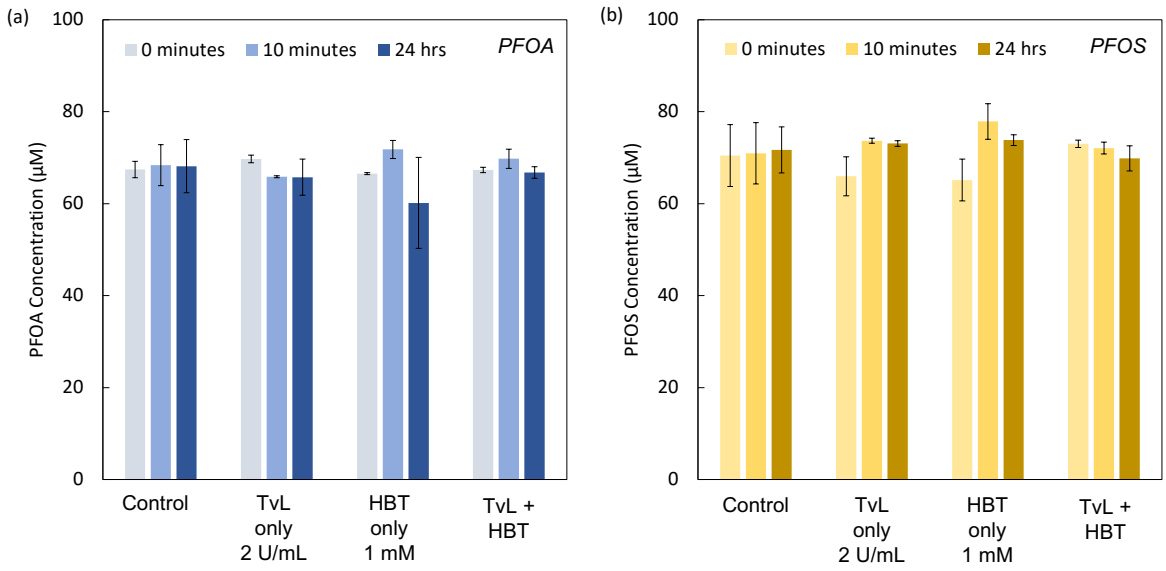

Figure 4.18: a) PFOA and b) PFOS concentrations monitored by LC-MS/MS in reaction conditions replicated from the EPR experiment. A reactor containing 2 U/mL TvL and 1 mM HBT in 10 µM $CuSO_4$ was incubated for 45 minutes to allow for substantial radical generation; 200 μL aliquots were then taken and added to microcentrifuge tubes to which 50 μM PFOA, PFOS were added to directly. Reactions were quenched by addition of 200 μL MeOH directly to the microcentrifuge tubes and diluted for LC-MS/MS analysis. Averages and standard deviations represent triplicate reactor conditions.

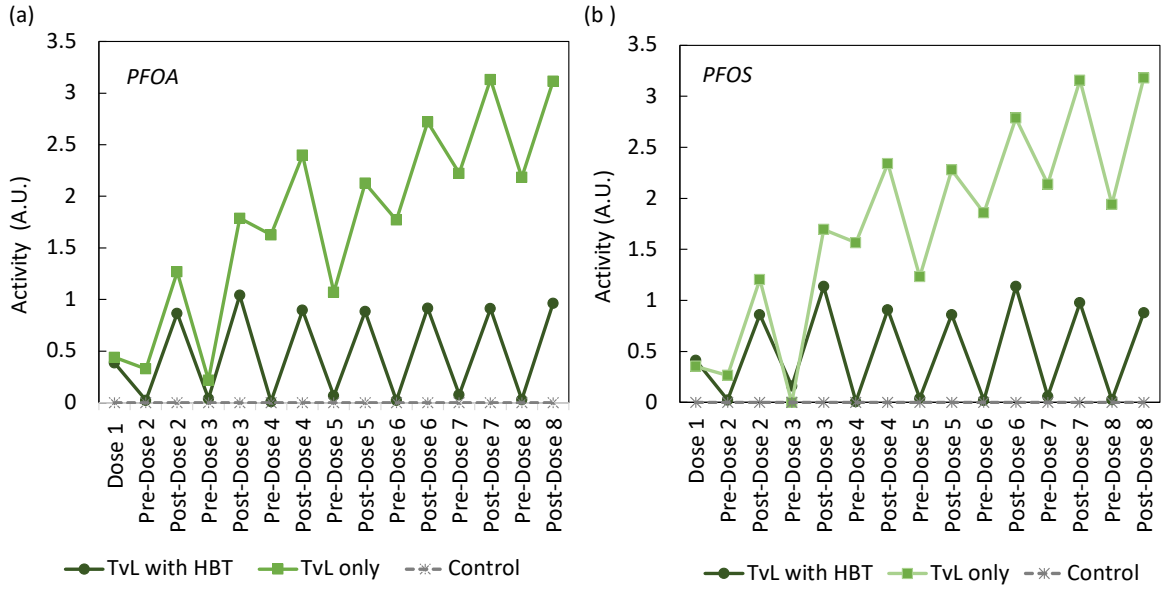

Figure 4.19: Enzyme activity monitored by the DMP assay over the course of the reaction in reactors treated with 1 U/mL TvL and 1 mM HBT. Doses were added twice daily, with approximately 6-8 hours in between doses.

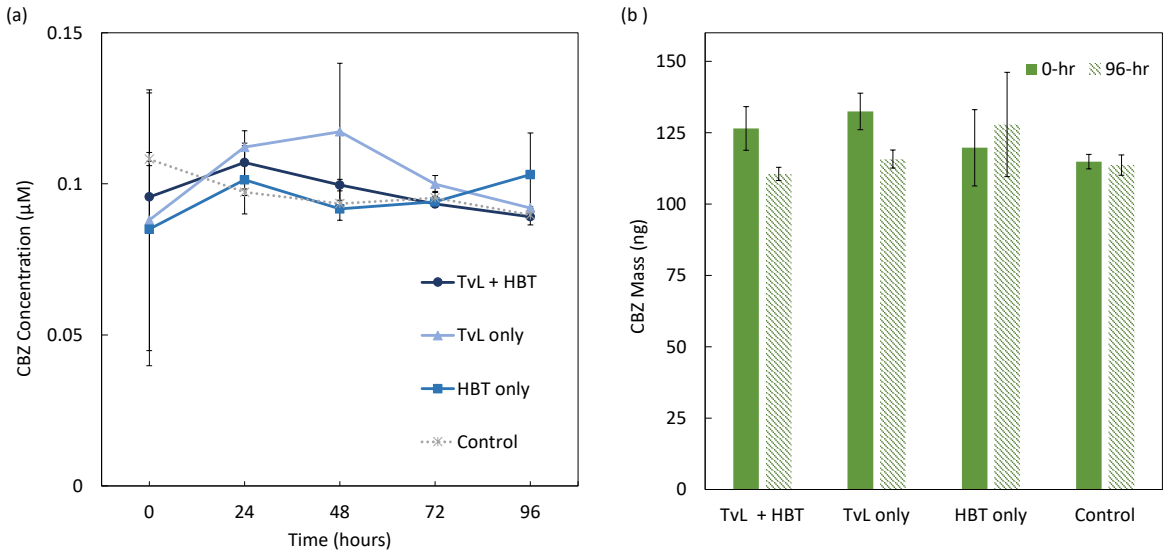

Figure 4.20: CBZ a) Concentration and b) Mass removal in enzyme-mediator and enzyme-only treated conditions; removal is substantially less that in sodium malonate buffer, potentially due to the copper present in the reactor solution.

Chapter 5

Conclusions

5.1 Learnings

The chemistry of PFAS and their environmental fate are inextricably linked. The implications of this relationship have begun to emerge as researchers investigate the surfactant physicochemical properties of PFAS in the context of their environmental behavior. By interpreting the physicochemical properties of PFAS, we can begin to uncover the entirety of the PFAS story, from their first industrial uses, to the challenges we now face in addressing their environmental remediation and human health consequences.

In this work, we investigated artifacts of PFAS removal that are caused by their surfactant nature. Specifically, we uncovered the relationship between 'salting-out' and aggregation of PFOS in high ionic strength matrices representative of HAPO-treated sites or coastal sites contaminated by repeated AFFF fire fighting training activities (Chapter 2). We found that the salting-out effect can lead to under-reporting of PFOS concentrations due to detection losses in the case of groundwater relevant monovalent cations (e.g., Na^+, K^+); in the case of divalent cations (i.e. Mg^{2+}, Ca^{2+}), increases in aggregation and interfacial activity lead to decreased critical micelle concentrations and increased surface excess, potentially impacting fate and transport characteristics. As one of the most well studied PFAS, PFOS as a representative case indicates the importance of understanding the role between cations present in natural waters and the aggregation, surface activity, and interfacial sorption of PFOS in addressing detection, monitoring, and evaluation of treatment technologies for salt-impacted matrices.

PFAS contamination is complex, in that it cannot be defined by a single compound, nor a confined site of contamination. Particularly, the use of AFFFs, which contain a mixture of fluorocarbon surfactants, has resulted in contaminated matrices containing a mixture of AFFF-components and products of their partial degradation, both at a point source and downstream from the source. To expand on our study of PFOS salting-out effects, we evaluated the aggregation and interfacial properties of an ECF-derived 3M AFFF formulation; namely, we determined salinity effects on AFFF component detection, changes to the crit-

ical micelle concentration of the formulation, and interfacial mass accumulation of AFFF components in high salinity matrices (i.e., artificial brackish, artificial seawater, mono- and divalent salt solutions) (Chapter 3). We found that similarly to the single-component system (i.e., PFOS only), high salinity caused decreases in PFOS detection in bulk solution, while the effect was less apparent for shorter-chain PFSAs. However, the inherent concentration differences of PFSA components in the AFFF solution may relate to this observation; for example, if PFHxS concentrations were sufficiently high, the salting-out effect might become apparent. The critical micelle concentration of the AFFF formula decreased in both artificial brackish and artificial seawater; critical micelle concentration in this context is most related to the performance of AFFF (i.e., foaming, spreading properties), and indicates that dilution of AFFF formulas at the site of their use, such as on a ship or coastal military base, would be impacted depending on the dilution matrix. In the lens of environmental remediation, the effect of salinity on increasing mass accumulation of PFAS at the air-water interface may impact the retention and transport properties of AFFF-components.

Another artifact of PFAS removal was revealed in the investigation of an enzyme-based treatment system for PFAAs (Chapter 4). Upon carrying out a systematic investigation of the oxidative reaction sequence proposed for the transformation of PFOA and PFOS, which requires a cascade of reactions between a laccase enzyme, a nitroxyl mediator compound, and the target substrate, we discovered that apparent 'removal' of PFOA and PFOS from aqueous reactor systems was caused by sorption to the enzyme itself. While unanticipated, this was not surprising given the affinity of PFAS for proteins that has been studied in the context of their human health endpoints (i.e., concentration in human serum and liver tissues), and even in the context of their removal. While ultimately we deemed the reaction system under investigation as unable to successfully degrade PFAAs, the strong affinity of PFAAs for laccase enzymes and further investigation of the binding mechanism could inspire membrane or other adsorbent removal technologies specifically targeted towards PFAS, even in complex contamination matrices.

Primarily, this work serves to bridge the gap between the study of perfluorocarbon chemistry and the study of their treatment in the environment. The reasons that they are so valuable as molecules in such a diverse set of applications is ultimately what has led to their widespread distribution; their persistence and resistance to treatment is why they were used across applications in the first place. Careful consideration of their behavior in the environment and its relationship to surfactant properties such as aggregation, surface activity, and interfacial accumulation, will help in the thorough understanding of the efficacy of treatment technologies and in the management of their environmental fate and transport.

5.2 Persistence is not an accident

PFAS contamination is not an 'accident'. After over seven decades of manufacturing, and use of over 1400 unique PFAS in over 200 applications [5], it is unsurprising that we are now tasked with their clean up. The reason that we now face the extreme persistence of PFAS in

the environment is the exact reason that they were first commercialized. Manhattan Project scientists had been searching for materials that could resist degradation by a highly volatile, highly reactive uranium derivative during the processes used to concentrate U-235, and perfluorocarbons became the clear winner [244]. The high thermal and chemical stability of perfluorocarbons contribute to environmental accumulation and challenges remediation research in finding appropriate ways to break them down.

The persistence of PFAS can be taken as a lesson when considering the future of the chemical industry. One approach to avoid future reversible contamination impacts of currently known and yet to be discovered chemistries is to use the "P-sufficient" approach. This approach, as outlined by Cousins et al. in their 2019 perspective [245], argues that high persistence alone and its correlation with increased environmental concentrations and increased probabilities of side effects of chemicals should be established as a basis for chemical management. They argue this based on the historical and ongoing problems that chemical classes such as PFAS have caused. While this approach may be precautionary, it may also be necessary to avoid the immense challenges we now face in trying to reverse impacts of chemical contamination.

In general, class-based management systems for PFAS are gaining traction in the research community– the sheer number of known PFAS compounds makes any other approach seem impractical. Recently, the surfactant physicochemical properties of PFAS have been evaluated in relation to monitored natural attenuation processes as a strategy for PFAS-class remediation [107, 108]. Regulation efforts could also benefit from treating PFAS as a chemical class, rather than the using a round-about approach of approaching each regulation of each individual compound [68, 70] which relies on studying individual toxicity mechanisms, and can promote regrettable substitution as has already occurred in the case of replacing legacy PFAS with GenX [68–70, 246, 247]. Ultimately, we need to steer away from our heavy reliance on fluorocarbon chemistry all together. But what can serve as a replacement?

5.3 Looking Forward

PFAS may indeed prove to be "irreplaceable" in the roles we've assigned them, in which case we need to evaluate their replacement by asking a different set of questions. Those questions might look like this: do we need Teflon-coated cookware that is so repellent, we never need to scrape it clean? Do we need PTFE-coated rain jackets or weekend camping tents that will survive hundreds of wash cycles [248]? Do we need fluoropolymer-based steel coatings, so that bridges can withstand 30 years of weather exposure [249]? There are some that are more challenging, such as, can non-fluorinated AFFFs meet the performance criteria for fire-extinguishing [250]? And, can non-PTFE coated firefighting gear keep firefighters safe from burn hazards [251]? Clearly, the challenges are also related to policy and regulation, and will not be solved in the context of environmental management and remediation alone. The broader the perspective that we can take in understanding the causes and consequences of PFAS use, the broader the context for solutions might become. Addressing remediation,

preventing exposure, and promoting ingenuity in PFAS-replacement technologies is a multi-disciplinary problem that requires a multi-disciplinary solution.

Bibliography

(1) Budisa, N.; Kubyshkin, V.; Schulze-Makuch, D. Fluorine-rich planetary environments as possible habitats for life. *Life* **2014**, *4*, 374–385.

(2) Seong, H. J.; Kwon, S. W.; Seo, D.-C.; Kim, J.-H.; Jang, Y.-S. Enzymatic defluorination of fluorinated compounds. *Applied Biological Chemistry* **2019**, *62*, 1–8.

(3) Huang, S.; Jaffé, P. R. Defluorination of Perfluorooctanoic Acid (PFOA) and Perfluorooctane Sulfonate (PFOS) by Acidimicrobium sp. Strain A6. *Environ. Sci. Technol.* **2019**, *53*, 11410–11419.

(4) Dalvi, V. H.; Rossky, P. J. Molecular origins of fluorocarbon hydrophobicity, 2010.

(5) Evich, M. G.; Davis, M. J. B.; McCord, J. P.; Acrey, B.; Awkerman, J. A.; Knappe, D. R. U.; Lindstrom, A. B.; Speth, T. F.; Tebes-Stevens, C.; Strynar, M. J.; Wang, Z.; Weber, E. J.; Henderson, W. M.; Washington, J. W. Per- and polyfluoroalkyl substances in the environment. *Science* **2022**, *375*.

(6) Garnett, J.; Halsall, C.; Winton, H.; Joerss, H.; Mulvaney, R.; Ebinghaus, R.; Frey, M.; Jones, A.; Leeson, A.; Wynn, P. Increasing Accumulation of Perfluorocarboxylate Contaminants Revealed in an Antarctic Firn Core (1958–2017). *Environ. Sci. Technol.* **2022**, *56*, 11246–11255.

(7) Mokra, K. Endocrine Disruptor Potential of Short- and Long-Chain Perfluoroalkyl Substances (PFASs)-A Synthesis of Current Knowledge with Proposal of Molecular Mechanism. *Int. J. Mol. Sci.* **2021**, *22*.

(8) Ducatman, A.; Fenton, S. E. Invited Perspective: PFAS and Liver Disease: Bringing All the Evidence Together. *Environ. Health Perspect.* **2022**, *130*, 41303.

(9) Anderko, L.; Pennea, E. Exposures to per-and polyfluoroalkyl substances (PFAS): Potential risks to reproductive and children's health. *Curr. Probl. Pediatr. Adolesc. Health Care* **2020**, *50*, 100760.

(10) Peden-Adams, M. M.; Keller, J. M.; Eudaly, J. G.; Berger, J.; Gilkeson, G. S.; Keil, D. E. Suppression of humoral immunity in mice following exposure to perfluorooctane sulfonate. *Toxicol. Sci.* **2008**, *104*, 144–154.

(11) Fenton, S. E.; Ducatman, A.; Boobis, A.; DeWitt, J. C.; Lau, C.; Ng, C.; Smith, J. S.; Roberts, S. M. Per- and Polyfluoroalkyl Substance Toxicity and Human Health Review: Current State of Knowledge and Strategies for Informing Future Research. *Environ. Toxicol. Chem.* **2021**, *40*, 606–630.

(12) Nelson, J. W.; Hatch, E. E.; Webster, T. F. Exposure to polyfluoroalkyl chemicals and cholesterol, body weight, and insulin resistance in the general U.S. population. *Environ. Health Perspect.* **2010**, *118*, 197–202.

(13) Blake, B. E.; Fenton, S. E. Early life exposure to per- and polyfluoroalkyl substances (PFAS) and latent health outcomes: A review including the placenta as a target tissue and possible driver of peri- and postnatal effects. *Toxicology* **2020**, *443*, 152565.

(14) Okazoe, T. Overview on the history of organofluorine chemistry from the viewpoint of material industry. *Proc. Jpn. Acad. Ser. B Phys. Biol. Sci.* **2009**, *85*, 276.

(15) Buck, R. C.; Franklin, J.; Berger, U.; Conder, J. M.; Cousins, I. T.; de Voogt, P.; Jensen, A. A.; Kannan, K.; Mabury, S. A.; van Leeuwen, S. P. J. Perfluoroalkyl and polyfluoroalkyl substances in the environment: terminology, classification, and origins. *Integr. Environ. Assess. Manag.* **2011**, *7*, 513–541.

(16) Comptox Chemicals Dashboard: Master List of PFAS Substances (Version2), `https://comptox.epa.gov/dashboard/chemical_lists/pfasmaster`, Accessed: 2022-11-14.

(17) Lindstrom, A. B.; Strynar, M. J.; Libelo, E. L. Polyfluorinated compounds: Past, present, and future. *Environmental Science and Technology* **2011**, *45*, 7954–7961.

(18) Robert Mueller, V. Y. *History and Use of Per- and Polyfluoroalkyl Substances (PFAS)*; tech. rep.; Interstate Technology Regulatory Council, 2020.

(19) Leeson, A.; Thompson, T.; Stroo, H. F.; Anderson, R. H.; Speicher, J.; Mills, M. A.; Willey, J.; Coyle, C.; Ghosh, R.; Lebrón, C.; Patton, C. Identifying and Managing Aqueous Film-Forming Foam-Derived Per- and Polyfluoroalkyl Substances in the Environment. *Environ. Toxicol. Chem.* **2021**, *40*, 24–36.

(20) Guo, B.; Zeng, J.; Brusseau, M. L. A Mathematical Model for the Release, Transport, and Retention of Per- and Polyfluoroalkyl Substances (PFAS) in the Vadose Zone. *Water Resour. Res.* **2020**, *56*.

(21) Brusseau, M. L. Assessing the potential contributions of additional retention processes to PFAS retardation in the subsurface. *Sci. Total Environ.* **2018**, *613-614*, 176–185.

(22) Hansen, K. J.; Clemen, L. A.; Ellefson, M. E.; Johnson, H. O. Compound-specific, quantitative characterization of organic fluorochemicals in biological matrices. *Environ. Sci. Technol.* **2001**, *35*, 766–770.

(23) Brusseau, M. L. The influence of molecular structure on the adsorption of PFAS to fluid-fluid interfaces: Using QSPR to predict interfacial adsorption coefficients. *Water Res.* **2019**, *152*, 148–158.

(24) Brusseau, M. L.; Van Glubt, S. The influence of surfactant and solution composition on PFAS adsorption at fluid-fluid interfaces. *Water Res.* **2019**, *161*, 17–26.

(25) Schwichtenberg, T.; Bogdan, D.; Carignan, C. C.; Reardon, P.; Rewerts, J.; Wanzek, T.; Field, J. A. PFAS and Dissolved Organic Carbon Enrichment in Surface Water Foams on a Northern U.S. Freshwater Lake. *Environmental Science and Technology* **2020**, *54*, 14455–14464.

(26) McKenzie, E. R.; Siegrist, R. L.; McCray, J. E.; Higgins, C. P. Effects of chemical oxidants on perfluoroalkyl acid transport in one-dimensional porous media columns. *Environmental Science and Technology* **2015**, *49*, 1681–1689.

(27) McGuire, M. E.; Schaefer, C.; Richards, T.; Backe, W. J.; Field, J. A.; Houtz, E.; Sedlak, D. L.; Guelfo, J. L.; Wunsch, A.; Higgins, C. P. Evidence of remediation-induced alteration of subsurface poly- and perfluoroalkyl substance distribution at a former firefighter training area. *Environmental Science and Technology* **2014**, *48*, 6644–6652.

(28) Silva, J. A. K.; Martin, W. A.; Johnson, J. L.; McCray, J. E. Evaluating air-water and NAPL-water interfacial adsorption and retention of Perfluorocarboxylic acids within the Vadose zone. *J. Contam. Hydrol.* **2019**, *223*.

(29) Du, Z.; Deng, S.; Bei, Y.; Huang, Q.; Wang, B.; Huang, J.; Yu, G. Adsorption behavior and mechanism of perfluorinated compounds on various adsorbents—A review. *J. Hazard. Mater.* **2014**, *274*, 443–454.

(30) Milinovic, J.; Lacorte, S.; Vidal, M.; Rigol, A. Sorption behaviour of perfluoroalkyl substances in soils. *Sci. Total Environ.* **2015**, *511*, 63–71.

(31) Chen, Y.-C.; Lo, S.-L.; Li, N.-H.; Lee, Y.-C.; Kuo, J. Sorption of perfluoroalkyl substances (PFASs) onto wetland soils. *Desalination Water Treat.* **2013**, *51*, 7469–7475.

(32) Nassi, M.; Sarti, E.; Pasti, L.; Martucci, A.; Marchetti, N.; Cavazzini, A.; Di Renzo, F.; Galarneau, A. Removal of perfluorooctanoic acid from water by adsorption on high surface area mesoporous materials. *J. Porous Mater.* **2014**.

(33) Chandramouli, B.; Benskin, J. P.; Hamilton, M. C.; Cosgrove, J. R. Sorption of per- and polyfluoroalkyl substances (PFASs) on filter media: implications for phase partitioning studies. *Environ. Toxicol. Chem.* **2015**, *34*, 30–36.

(34) Wang, T. C.; Bury, W.; Gómez-Gualdrón, D. A.; Vermeulen, N. A.; Mondloch, J. E.; Deria, P.; Zhang, K.; Moghadam, P. Z.; Sarjeant, A. A.; Snurr, R. Q.; Stoddart, J. F.; Hupp, J. T.; Farha, O. K. Ultrahigh Surface Area Zirconium MOFs and Insights into the Applicability of the BET Theory. *J. Am. Chem. Soc.* **2015**, *137*, 3585–3591.

(35) Yu, Q.; Zhang, R.; Deng, S.; Huang, J.; Yu, G. Sorption of perfluorooctane sulfonate and perfluorooctanoate on activated carbons and resin: Kinetic and isotherm study. *Water Res.* **2009**, *43*, 1150–1158.

(36) Munoz, G.; Budzinski, H.; Labadie, P. Influence of environmental factors on the fate of legacy and emerging per- and polyfluoroalkyl substances along the salinity/turbidity gradient of a macrotidal estuary. *Environmental Science and Technology* **2017**, *51*, 12347–12357.

(37) Chen, H.; Zhang, C.; Yu, Y.; Han, J. Sorption of perfluorooctane sulfonate (PFOS) on marine sediments. *Mar. Pollut. Bull.* **2012**, *64*, 902–906.

(38) Jeon, J.; Kannan, K.; Lim, B. J.; An, K. G.; Kim, S. D. Effects of salinity and organic matter on the partitioning of perfluoroalkyl acid (PFAs) to clay particles. *J. Environ. Monit.* **2011**, *13*, 1803–1810.

(39) Hong, S.; Khim, J. S.; Park, J.; Kim, M.; Kim, W. K.; Jung, J.; Hyun, S.; Kim, J. G.; Lee, H.; Choi, H. J.; Codling, G.; Giesy, J. P. In situ fate and partitioning of waterborne perfluoroalkyl acids (PFAAs) in the Youngsan and Nakdong River Estuaries of South Korea. *Sci. Total Environ.* **2013**, *445-446*, 136–145.

(40) Li, C.; Zhang, C.; Gibbes, B.; Wang, T.; Lockington, D. Coupling effects of tide and salting-out on perfluorooctane sulfonate (PFOS) transport and adsorption in a coastal aquifer. *Adv. Water Resour.* **2022**, *166*, 104240.

(41) Newell, C. J.; Javed, H.; Li, Y.; Johnson, N. W.; Richardson, S. D.; Connor, J. A.; Adamson, D. T. Enhanced attenuation (EA) to manage PFAS plumes in groundwater. *Remediation* **2022**, *32*, 239–257.

(42) Mussabek, D.; Ahrens, L.; Persson, K. M.; Berndtsson, R. Temporal trends and sediment–water partitioning of per- and polyfluoroalkyl substances (PFAS) in lake sediment. *Chemosphere* **2019**, *227*, 624–629.

(43) Munoz, G.; Budzinski, H.; Babut, M.; Lobry, J.; Selleslagh, J.; Tapie, N.; Labadie, P. Temporal variations of perfluoroalkyl substances partitioning between surface water, suspended sediment, and biota in a macrotidal estuary. *Chemosphere* **2019**, *233*, 319–326.

(44) Munoz, G.; Ray, P.; Mejia-Avendaño, S.; Vo Duy, S.; Tien Do, D.; Liu, J.; Sauvé, S. Optimization of extraction methods for comprehensive profiling of perfluoroalkyl and polyfluoroalkyl substances in firefighting foam impacted soils. *Anal. Chim. Acta* **2018**, *1034*, 74–84.

(45) Costanza, J.; Arshadi, M.; Abriola, L. M.; Pennell, K. D. Accumulation of PFOA and PFOS at the Air-Water Interface. *Environmental Science and Technology Letters* **2019**, *6*, 487–491.

(46) Costanza, J.; Abriola, L. M.; Pennell, K. D. Aqueous Film-Forming Foams Exhibit Greater Interfacial Activity than PFOA, PFOS, or FOSA. *Environ. Sci. Technol.* **2020**, *54*, 13590–13597.

(47) Schaefer, C. E.; Culina, V.; Nguyen, D.; Field, J. Uptake of Poly- And Perfluoroalkyl Substances at the Air-Water Interface. *Environmental Science and Technology* **2019**, *53*, 12442–12448.

(48) Le, S.-T.; Kibbey, T. C. G.; Weber, K. P.; Glamore, W. C.; O'Carroll, D. M. A group-contribution model for predicting the physicochemical behavior of PFAS components for understanding environmental fate. *Sci. Total Environ.* **2021**, *764*, 142882.

(49) Lyu, Y.; Brusseau, M. L.; Chen, W.; Yan, N.; Fu, X.; Lin, X. Adsorption of PFOA at the AirWater Interface during Transport in Unsaturated Porous Media. *Environmental Science & Technology* **2018**, *52*, 7745–7753.

(50) Schaefer, C. E.; Lavorgna, G. M.; Lippincott, D. R.; Nguyen, D.; Christie, E.; Shea, S.; O'Hare, S.; Lemes, M. C. S.; Higgins, C. P.; Field, J. A field study to assess the role of air-water interfacial sorption on PFAS leaching in an AFFF source area. *J. Contam. Hydrol.* **2022**, *248*.

(51) Kannan, K.; Christian Franson, J.; Bowerman, W. W.; Hansen, K. J.; Jones, P. D.; Giesy, J. P. Perfluorooctane Sulfonate in Fish-Eating Water Birds Including Bald Eagles and Albatrosses. *Environ. Sci. Technol.* **2001**, *35*, 3065–3070.

(52) Appleman, T. D.; Higgins, C. P.; Quiñones, O.; Vanderford, B. J.; Kolstad, C.; Zeigler-Holady, J. C.; Dickenson, E. R. V. Treatment of poly- and perfluoroalkyl substances in U.S. full-scale water treatment systems. *Water Res.* **2014**, *51*, 246–255.

(53) Domingo, J. L.; Nadal, M. Per- and polyfluoroalkyl substances (PFASs) in food and human dietary intake: A review of the recent scientific literature. *J. Agric. Food Chem.* **2017**, *65*, 533–543.

(54) Domingo, J. L.; Nadal, M. Human exposure to per- and polyfluoroalkyl substances (PFAS) through drinking water: A review of the recent scientific literature. *Environ. Res.* **2019**, *177*, 108648.

(55) Ghisi, R.; Vamerali, T.; Manzetti, S. Accumulation of perfluorinated alkyl substances (PFAS) in agricultural plants: A review. *Environ. Res.* **2019**, *169*, 326–341.

(56) Crone, B. C.; Speth, T. F.; Wahman, D. G.; Smith, S. J.; Abulikemu, G.; Kleiner, E. J.; Pressman, J. G. Occurrence of per- and polyfluoroalkyl substances (PFAS) in source water and their treatment in drinking water. *Crit. Rev. Environ. Sci. Technol.* **2019**, *49*, 2359–2396.

(57) Conder, J. M.; Hoke, R. A.; De Wolf, W.; Russell, M. H.; Buck, R. C. Are PFCAs bioaccumulative? A critical review and comparison with regulatory criteria and persistent lipophilic compounds. *Environmental Science and Technology* **2008**, *42*, 995–1003.

(58) Poothong, S.; Papadopoulou, E.; Padilla-Sánchez, J. A.; Thomsen, C.; Haug, L. S. Multiple pathways of human exposure to poly- and perfluoroalkyl substances (PFASs): From external exposure to human blood. *Environ. Int.* **2020**, *134*, 105244.

(59) Zheng, G.; Boor, B. E.; Schreder, E.; Salamova, A. Indoor exposure to per- and polyfluoroalkyl substances (PFAS) in the childcare environment. *Environ. Pollut.* **2020**, *258*, 113714.

(60) Ragnarsdóttir, O.; Abdallah, M. A.-E.; Harrad, S. Dermal uptake: An important pathway of human exposure to perfluoroalkyl substances? *Environ. Pollut.* **2022**, *307*, 119478.

(61) Abercrombie, S. A.; de Perre, C.; Iacchetta, M.; Flynn, R. W.; Sepúlveda, M. S.; Lee, L. S.; Hoverman, J. T. Sublethal effects of dermal exposure to poly- and perfluoroalkyl substances on postmetamorphic amphibians. *Environ. Toxicol. Chem.* **2021**, *40*, 717–726.

(62) Nadal, M.; Domingo, J. Indoor Dust Levels of Perfluoroalkyl Substances (PFASs) and the Role of Ingestion as an Exposure Pathway: A Review. *Curr. Org. Chem.* **2014**, *18*, 2200–2208.

(63) Winkens, K.; Vestergren, R.; Berger, U.; Cousins, I. T. Early life exposure to per- and polyfluoroalkyl substances (PFASs): A critical review. *Emerging Contaminants* **2017**, *3*, 55–68.

(64) Dreyer, A.; Kirchgeorg, T.; Weinberg, I.; Matthias, V. Particle-size distribution of airborne poly- and perfluorinated alkyl substances. *Chemosphere* **2015**, *129*, 142–149.

(65) Pérez, F.; Nadal, M.; Navarro-Ortega, A.; Fàbrega, F.; Domingo, J. L.; Barceló, D.; Farré, M. Accumulation of perfluoroalkyl substances in human tissues. *Environ. Int.* **2013**, *59*, 354–362.

(66) La Merrill, M.; Emond, C.; Kim, M. J.; Antignac, J.-P.; Le Bizec, B.; Clément, K.; Birnbaum, L. S.; Barouki, R. Toxicological function of adipose tissue: focus on persistent organic pollutants. *Environ. Health Perspect.* **2013**, *121*, 162–169.

(67) Cao, Y.; Ng, C. Absorption, distribution, and toxicity of per- and polyfluoroalkyl substances (PFAS) in the brain: a review. *Environ. Sci. Process. Impacts* **2021**, *23*, 1623–1640.

(68) Kwiatkowski, C. F.; Andrews, D. Q.; Birnbaum, L. S.; Bruton, T. A.; DeWitt, J. C.; Knappe, D. R. U.; Maffini, M. V.; Miller, M. F.; Pelch, K. E.; Reade, A.; Soehl, A.; Trier, X.; Venier, M.; Wagner, C. C.; Wang, Z.; Blum, A. Scientific Basis for Managing PFAS as a Chemical Class. *Environ Sci Technol Lett* **2020**, *7*, 532–543.

(69) Cousins, I. T.; Vestergren, R.; Wang, Z.; Scheringer, M.; McLachlan, M. S. The precautionary principle and chemicals management: The example of perfluoroalkyl acids in groundwater. *Environ. Int.* **2016**, *94*, 331–340.

(70) Bălan, S. A.; Mathrani, V. C.; Guo, D. F.; Algazi, A. M. Regulating PFAS as a Chemical Class under the California Safer Consumer Products Program. *Environ. Health Perspect.* **2021**, *129*, 25001.

(71) Epa, U. S. EPA Announces New Drinking Water Health Advisories for PFAS Chemicals, $1 Billion in Bipartisan Infrastructure Law Funding to Strengthen Health Protections, en, `https://www.epa.gov/newsreleases/epa-announces-new-drinking-water-health-advisories-pfas-chemicals-1-billion-bipartisan`, Accessed: 2022-11-18, 2022.

(72) Salvatore, D.; Mok, K.; Garrett, K. K.; Poudrier, G.; Brown, P.; Birnbaum, L. S.; Goldenman, G.; Miller, M. F.; Patton, S.; Poehlein, M.; Varshavsky, J.; Cordner, A. Presumptive Contamination: A New Approach to PFAS Contamination Based on Likely Sources. *Environmental Science & Technology Letters* **2022**, *9*, 983–990.

(73) Andrews, D. Q.; Naidenko, O. V. Population-Wide Exposure to Per- and Polyfluoroalkyl Substances from Drinking Water in the United States. *Environ. Sci. Technol. Lett.* **2020**, *7*, 931–936.

(74) Stoiber, T.; Evans, S.; Naidenko, O. V. Disposal of products and materials containing per- and polyfluoroalkyl substances (PFAS): A cyclical problem. *Chemosphere* **2020**, *260*, 127659.

(75) Eschauzier, C.; Beerendonk, E.; Scholte-Veenendaal, P.; De Voogt, P. Impact of Treatment Processes on the Removal of Perfluoroalkyl Acids from the Drinking Water Production Chain. *Environ. Sci. Technol.* **2012**, *46*, 1708–1715.

(76) Xiao, F.; Simcik, M. F.; Gulliver, J. S. Mechanisms for removal of perfluorooctane sulfonate (PFOS) and perfluorooctanoate (PFOA) from drinking water by conventional and enhanced coagulation. *Water Res.* **2013**, *47*, 49–56.

(77) Xiao, X.; Ulrich, B. A.; Chen, B.; Higgins, C. P. Sorption of Poly- and Perfluoroalkyl Substances (PFASs) Relevant to Aqueous Film-Forming Foam (AFFF)-Impacted Groundwater by Biochars and Activated Carbon. *Environmental Science and Technology* **2017**, *51*, 6342–6351.

(78) Banks, D.; Jun, B. M.; Heo, J.; Her, N.; Park, C. M.; Yoon, Y. Selected advanced water treatment technologies for perfluoroalkyl and polyfluoroalkyl substances: A review. *Sep. Purif. Technol.* **2020**, *231*, 115929.

(79) Léniz-Pizarro, F.; Vogler, R. J.; Sandman, P.; Harris, N.; Ormsbee, L. E.; Liu, C.; Bhattacharyya, D. Dual-Functional Nanofiltration and Adsorptive Membranes for PFAS and Organics Separation from Water. *ACS ES T Water* **2022**, *2*, 863–872.

(80) Lee, T.; Speth, T. F.; Nadagouda, M. N. High-pressure membrane filtration processes for separation of Per- and polyfluoroalkyl substances (PFAS). *Chem. Eng. J.* **2022**, *431*, 134023.

(81) Carter, K. E.; Farrell, J. Removal of perfluorooctane and perfluorobutane sulfonate from water via carbon adsorption and ion exchange. *Sep. Sci. Technol.* **2010**, *45*, 762–767.

(82) Wiberg, K.; McCleaf, P.; Ahrens, L.; Lindegren, K.; Englund, S.; Östlund, A. Removal efficiency of multiple poly- and perfluoroalkyl substances (PFASs) in drinking water using granular activated carbon (GAC) and anion exchange (AE) column tests. *Water Res.* **2017**, *120*, 77–87.

(83) Zaggia, A.; Conte, L.; Falletti, L.; Fant, M.; Chiorboli, A. Use of strong anion exchange resins for the removal of perfluoroalkylated substances from contaminated drinking water in batch and continuous pilot plants. *Water Res.* **2016**, *91*, 137–146.

(84) Maimaiti, A.; Deng, S.; Meng, P.; Wang, W.; Wang, B.; Huang, J.; Wang, Y.; Yu, G. Competitive adsorption of perfluoroalkyl substances on anion exchange resins in simulated AFFF-impacted groundwater. *Chem. Eng. J.* **2018**, *348*, 494–502.

(85) Dudley, L. A.; Arevalo, E. C.; Knappe, D. R. Removal of perfluoroalkyl substances by PAC adsorption and anion exchange. *Water Research Foundation* **2015**, 152.

(86) Wohlin, D. Analysis of PFAS in ash from incineration facilities from Sweden, en, Ph.D. Thesis, 2020.

(87) Altarawneh, M.; Almatarneh, M. H.; Dlugogorski, B. Z. Thermal decomposition of perfluorinated carboxylic acids: Kinetic model and theoretical requirements for PFAS incineration. *Chemosphere* **2022**, *286*, 131685.

(88) Ross, I.; McDonough, J.; Miles, J.; Storch, P.; Thelakkat Kochunarayanan, P.; Kalve, E.; Hurst, J.; S. Dasgupta, S.; Burdick, J. A review of emerging technologies for remediation of PFASs. *Remediation Journal* **2018**, *28*, 101–126.

(89) Vecitis, C. D.; Park, H.; Cheng, J.; Mader, B. T.; Hoffmann, M. R. Treatment technologies for aqueous perfluorooctanesulfonate (PFOS) and perfluorooctanoate (PFOA). *Front. Environ. Sci. Eng. China* **2009**, *3*, 129–151.

(90) Bentel, M. J.; Yu, Y.; Xu, L.; Li, Z.; Wong, B. M.; Men, Y.; Liu, J. Defluorination of Per- and Polyfluoroalkyl Substances (PFASs) with Hydrated Electrons: Structural Dependence and Implications to PFAS Remediation and Management. *Environmental Science and Technology* **2019**, *53*, 3718–3728.

(91) Qu, Y.; Zhang, C.; Li, F.; Chen, J.; Zhou, Q. Photo-reductive defluorination of perfluorooctanoic acid in water. *Water Res.* **2010**, *44*, 2939–2947.

(92) Sun, Z.; Zhang, C.; Xing, L.; Zhou, Q.; Dong, W.; Hoffmann, M. R. UV/Nitrilotriacetic Acid Process as a Novel Strategy for Efficient Photoreductive Degradation of Perfluorooctanesulfonate. *Environmental Science and Technology* **2018**, *52*, 2953–2962.

(93) Trojanowicz, M.; Bojanowska-Czajka, A.; Bartosiewicz, I.; Kulisa, K. Advanced Oxidation/Reduction Processes treatment for aqueous perfluorooctanoate (PFOA) and perfluorooctanesulfonate (PFOS) – A review of recent advances. *Chem. Eng. J.* **2018**, *336*, 170–199.

(94) Yang, L.; He, L.; Xue, J.; Ma, Y.; Xie, Z.; Wu, L.; Huang, M.; Zhang, Z. Persulfate-based degradation of perfluorooctanoic acid (PFOA) and perfluorooctane sulfonate (PFOS) in aqueous solution: Review on influences, mechanisms and prospective. *J. Hazard. Mater.* **2020**, *393*, 122405.

(95) McDonough, J. T.; Kirby, J.; Bellona, C.; Quinnan, J. A.; Welty, N.; Follin, J.; Liberty, K. Validation of supercritical water oxidation to destroy perfluoroalkyl acids. *Remediation* **2022**, *32*, 75–90.

(96) Li, J.; Austin, C.; Moore, S.; Pinkard, B. R.; Novosselov, I. V. PFOS destruction in a continuous supercritical water oxidation reactor. *Chem. Eng. J.* **2023**, *451*, 139063.

(97) Krause, M. J.; Thoma, E.; Sahle-Damesessie, E.; Crone, B.; Whitehill, A.; Shields, E.; Gullett, B. Supercritical water oxidation as an innovative technology for PFAS destruction. *J. Environ. Eng.* **2022**, *148*.

(98) Pinkard, B. R.; Shetty, S.; Stritzinger, D.; Bellona, C.; Novosselov, I. V. Destruction of perfluorooctanesulfonate (PFOS) in a batch supercritical water oxidation reactor. *Chemosphere* **2021**, *279*, 130834.

(99) Harding-Marjanovic, K. C.; Houtz, E. F.; Yi, S.; Field, J. A.; Sedlak, D. L.; Alvarez-Cohen, L. Aerobic Biotransformation of Fluorotelomer Thioether Amido Sulfonate (Lodyne) in AFFF-Amended Microcosms. *Environ. Sci. Technol.* **2015**, *49*, 7666–7674.

(100) Hamid, H.; Li, L. Y.; Grace, J. R. Aerobic biotransformation of fluorotelomer compounds in landfill leachate-sediment. *Sci. Total Environ.* **2020**, *713*, 136547.

(101) Mejia-Avendaño, S.; Vo Duy, S.; Sauvé, S.; Liu, J. Generation of Perfluoroalkyl Acids from Aerobic Biotransformation of Quaternary Ammonium Polyfluoroalkyl Surfactants. *Environ. Sci. Technol.* **2016**, *50*, 9923–9932.

(102) Mejia Avendaño, S.; Liu, J. Production of PFOS from aerobic soil biotransformation of two perfluoroalkyl sulfonamide derivatives. *Chemosphere* **2015**, *119*, 1084–1090.

(103) Yang, S. H.; Shi, Y.; Strynar, M.; Chu, K. H. Desulfonation and defluorination of 6:2 fluorotelomer sulfonic acid (6:2 FTSA) by Rhodococcus jostii RHA1: Carbon and sulfur sources, enzymes, and pathways. *J. Hazard. Mater.* **2022**, *423*, 127052.

(104) Yi, S.; Harding-Marjanovic, K. C.; Houtz, E. F.; Gao, Y.; Lawrence, J. E.; Nichiporuk, R. V.; Iavarone, A. T.; Zhuang, W. Q.; Hansen, M.; Field, J. A.; Sedlak, D. L.; Alvarez-Cohen, L. Biotransformation of AFFF Component 6:2 Fluorotelomer Thioether Amido Sulfonate Generates 6:2 Fluorotelomer Thioether Carboxylate under Sulfate-Reducing Conditions. *Environmental Science and Technology Letters* **2018**, *5*, 283–288.

(105) Luo, Q.; Lu, J.; Zhang, H.; Wang, Z.; Feng, M.; Chiang, S. Y. D.; Woodward, D.; Huang, Q. Laccase-Catalyzed Degradation of Perfluorooctanoic Acid. *Environmental Science and Technology Letters* **2015**, *2*, 198–203.

(106) Luo, Q.; Yan, X.; Lu, J.; Huang, Q. Perfluorooctanesulfonate Degrades in a Laccase-Mediator System. *Environmental Science and Technology* **2018**, *52*, 10617–10626.

(107) Newell, C. J.; Adamson, D. T.; Kulkarni, P. R.; Nzeribe, B. N.; Connor, J. A.; Popovic, J.; Stroo, H. F. Monitored natural attenuation to manage PFAS impacts to groundwater: Scientific basis. *Ground Water Monit. Remediat.* **2021**, *41*, 76–89.

(108) Newell, C. J.; Adamson, D. T.; Kulkarni, P. R.; Nzeribe, B. N.; Stroo, H. Comparing PFAS to other groundwater contaminants: Implications for remediation. *Remediation Journal* **2020**, *30*, 7–26.

(109) Adamson, D. T.; Nickerson, A.; Kulkarni, P. R.; Higgins, C. P.; Popovic, J.; Field, J.; Rodowa, A.; Newell, C.; Deblanc, P.; Kornuc, J. J. Mass-Based, Field-Scale Demonstration of PFAS Retention within AFFF-Associated Source Areas. *Environmental Science and Technology* **2020**, *54*, 15768–15777.

(110) Sonawane, S.; Rayaroth, M. P.; Landge, V. K.; Fedorov, K.; Boczkaj, G. Thermally activated persulfate-based Advanced Oxidation Processes — recent progress and challenges in mineralization of persistent organic chemicals: a review. *Curr. Opin. Chem. Eng.* **2022**, *37*, 100839.

(111) Yang, S.; Chen, Y.; Xu, H.; Wang, P.; Liu, Y.; Zhang, W.; Wang, M. A novel advanced oxidation technology: Activated persulfate. *Prog. Inorg. Chem.* **2008**, *20*, 1433.

(112) Eberle, D.; Ball, R.; Boving, T. B. Impact of ISCO Treatment on PFAA Co-Contaminants at a Former Fire Training Area. *Environmental Science and Technology* **2017**, *51*, 5127–5136.

(113) Chen, J.; Qian, Y.; Liu, H.; Huang, T. Oxidative degradation of diclofenac by thermally activated persulfate: implication for ISCO. *Environ. Sci. Pollut. Res. Int.* **2016**, *23*, 3824–3833.

(114) Ahmadi, S.; Igwegbe, C. A.; Rahdar, S. The application of thermally activated persulfate for degradation of Acid Blue 92 in aqueous solution. *International Journal of Industrial Chemistry* **2019**, *10*, 249–260.

(115) Li, S.; Hong, D.; Chen, W.; Wang, J.; Sun, K. Extracellular laccase-activated humification of phenolic pollutants and its application in plant growth. *Sci. Total Environ.* **2022**, *802*, 150005.

(116) Brogioni, B.; Biglino, D.; Sinicropi, A.; Reijerse, E. J.; Giardina, P.; Sannia, G.; Lubitz, W.; Basosi, R.; Pogni, R. Characterization of radical intermediates in laccase-mediator systems. A multifrequency EPR, ENDOR and DFT/PCM investigation. *Phys Chem Chem Phys* **2008**, *10*, 7284–7292.

(117) Jin, X.; Yu, X.; Zhu, G.; Zheng, Z.; Feng, F.; Zhang, Z. Conditions Optimizing and Application of Laccase-mediator System (LMS) for the Laccase-catalyzed Pesticide Degradation. *Sci. Rep.* **2016**, *6*, 1–7.

(118) Kupski, L.; Salcedo, G. M.; Caldas, S. S.; de Souza, T. D.; Furlong, E. B.; Primel, E. G. Optimization of a laccase-mediator system with natural redox-mediating compounds for pesticide removal. *Environ. Sci. Pollut. Res.* **2019**, *26*, 5131–5139.

(119) Mukerjee, P.; Chan, C. C. Effects of high salt concentrations on the micellization of octyl glucoside: Salting-out of monomers and electrolyte effects on the micelle-water interfacial tension. *Langmuir* **2002**, *18*, 5375–5381.

(120) Endo, S.; Pfennigsdorff, A.; Goss, K. U. Salting-out effect in aqueous NaCl solutions: Trends with size and polarity of solute molecules. *Environmental Science and Technology* **2012**, *46*, 1496–1503.

(121) Gross, P. M. The Salting Out of Non-Electrolytes from Aqueous Solutions. *Chem. Rev.* **1933**, *13*, 91–101.

(122) Hyde, A. M.; Zultanski, S. L.; Waldman, J. H.; Zhong, Y. L.; Shevlin, M.; Peng, F. General Principles and Strategies for Salting-Out Informed by the Hofmeister Series. *Org. Process Res. Dev.* **2017**, *21*, 1355–1370.

(123) Long, F. A.; McDevit, W. F. Activity coefficients of nonelectrolyte solutes in aqueous salt solutions. *Chem. Rev.* **1952**, *51*, 119–169.

(124) Maeda, H.; Muroi, S.; Kakehashi, R. Effects of Ionic Strength on the Critical Micelle Concentration and the Surface Excess of Dodecyldimethylamine Oxide. *J. Phys. Chem. B* **2002**, *101*, 7378–7382.

(125) Ray, A.; Némethy, G. Effects of Ionic Protein Denaturants on Micelle Formation by Nonionic Detergents. *J. Am. Chem. Soc.* **1971**, *93*, 6787–6793.

(126) Ren, Z. H. Mechanism of the Salt Effect on Micellization of an Aminosulfonate Amphoteric Surfactant. *Ind. Eng. Chem. Res.* **2015**, *54*, 9683–9688.

(127) Okur, H. I.; Hladılková, J.; Rembert, K. B.; Cho, Y.; Heyda, J.; Dzubiella, J.; Cremer, P. S.; Jungwirth, P. Beyond the Hofmeister Series: Ion-Specific Effects on Proteins and Their Biological Functions. *J. Phys. Chem. B* **2017**, *121*, 1997–2014.

(128) Kissa, E., *Fluorinated Surfactants and Repellents, Second Edition,* CRC Press: 2001.

(129) Shinoda, K.; Hatö, M.; Hayashi, T. The physicochemical properties of aqueous solutions of fluorinated surfactants. *J. Phys. Chem.* **1972**, *76*, 909–914.

(130) Hoffmann, H.; Würtz, J. Unusual phenomena in perfluorosurfactants. *J. Mol. Liq.* **1997**, *72*, 191–230.

(131) Guo, W.; Brown, T. A.; Fung, B. M. Micelles and aggregates of fluorinated surfactants. *J. Phys. Chem.* **1991**, *95*, 1829–1836.

(132) Kostarelos, K.; Sharma, P.; Christie, E.; Wanzek, T.; Field, J. Viscous Microemulsions of Aqueous Film-Forming Foam (AFFF) and Jet Fuel A Inhibit Infiltration and Subsurface Transport. *Environmental Science and Technology Letters* **2021**, *8*, 142–147.

(133) Prevedouros, K.; Cousins, I. T.; Buck, R. C.; Korzeniowski, S. H. Sources, fate and transport of perfluorocarboxylates. *Environmental Science and Technology* **2006**, *40*, 32–44.

(134) Martin, J. W.; Asher, B. J.; Beesoon, S.; Benskin, J. P.; Ross, M. S. PFOS or PreFOS? Are perfluorooctane sulfonate precursors (PreFOS) important determinants of human and environmental perfluorooctane sulfonate (PFOS) exposure? *J. Environ. Monit.* **2010**, *12*, 1979–2004.

(135) Nakayama, S. F.; Yoshikane, M.; Onoda, Y.; Nishihama, Y.; Iwai-Shimada, M.; Takagi, M.; Kobayashi, Y.; Isobe, T. Worldwide trends in tracing poly- and perfluoroalkyl substances (PFAS) in the environment. *TrAC - Trends in Analytical Chemistry* **2019**, *121*, 115410.

(136) Lau, C.; Butenhoff, J. L.; Rogers, J. M. The developmental toxicity of perfluoroalkyl acids and their derivatives. *Toxicol. Appl. Pharmacol.* **2004**, *198*, 231–241.

(137) Jian, J. M.; Chen, D.; Han, F. J.; Guo, Y.; Zeng, L.; Lu, X.; Wang, F. A short review on human exposure to and tissue distribution of per- and polyfluoroalkyl substances (PFASs). *Sci. Total Environ.* **2018**, *636*, 1058–1069.

(138) Weathers, T. S.; Harding-Marjanovic, K.; Higgins, C. P.; Alvarez-Cohen, L.; Sharp, J. O. Perfluoroalkyl Acids Inhibit Reductive Dechlorination of Trichloroethene by Repressing Dehalococcoides. *Environmental Science and Technology* **2016**, *50*, 240–248.

(139) Tang, C. Y.; Fu, Q. S.; Robertson, A. P.; Criddle, C. S.; Leckie, J. O. Use of reverse osmosis membranes to remove perfluorooctane sulfonate (PFOS) from semiconductor wastewater. *Environmental Science and Technology* **2006**, *40*, 7343–7349.

(140) Ahdab, Y. D.; Thiel, G. P.; Böhlke, J. K.; Stanton, J.; Lienhard, J. H. Minimum energy requirements for desalination of brackish groundwater in the United States with comparison to international datasets. *Water Res.* **2018**, *141*, 387–404.

(141) Liu, Y.; Robey, N. M.; Bowden, J. A.; Tolaymat, T. M.; Da Silva, B. F.; Solo-Gabriele, H. M.; Townsend, T. G. From Waste Collection Vehicles to Landfills: Indication of Per- And Polyfluoroalkyl Substance (PFAS) Transformation. *Environmental Science and Technology Letters* **2021**, *8*, 66–72.

(142) Wei, Z.; Xu, T.; Zhao, D. Treatment of per- And polyfluoroalkyl substances in landfill leachate: Status, chemistry and prospects. *Environmental Science: Water Research and Technology* **2019**, *5*, 1814–1835.

(143) Department of Defense Installations Conducting Assessments for PFAS Use or Potential Release, 2020.

(144) F. Houtz, E.; P. Higgins, C.; A. Field, J.; L. Sedlak, D. Persistence of Perfluoroalkyl Acid Precursors in AFFF-Impacted Groundwater and Soil. *Environ. Sci. Technol.* **2013**, *47*, 8187–8195.

(145) Pottage, M. J.; Greaves, T. L.; Garvey, C. J.; Tabor, R. F. The effects of alkylammonium counterions on the aggregation of fluorinated surfactants and surfactant ionic liquids. *J. Colloid Interface Sci.* **2016**, *475*, 72–81.

(146) Lin, S. Y. A study of the equilibrium surface tension and the critical micelle concentration of mixed surfactant solutions. *Langmuir* **1999**, *15*, 4370–4376.

(147) Berry, J. D.; Neeson, M. J.; Dagastine, R. R.; Chan, D. Y. C.; Tabor, R. F. Measurement of surface and interfacial tension using pendant drop tensiometry. *J. Colloid Interface Sci.* **2015**, *454*, 226–237.

(148) Moody, C. A.; Field, J. A. Perfluorinated surfactants and the environmental implications of their use in fire-fighting foams. *Environmental Science and Technology* **2000**, *34*, 3864–3870.

(149) Barzen-Hanson, K. A.; Davis, S. E.; Kleber, M.; Field, J. A. Sorption of Fluorotelomer Sulfonates, Fluorotelomer Sulfonamido Betaines, and a Fluorotelomer Sulfonamido Amine in National Foam Aqueous Film-Forming Foam to Soil. *Environmental Science and Technology* **2017**, *51*, 12394–12404.

(150) Park, S.; Lee, L. S.; Medina, V. F.; Zull, A.; Waisner, S. Heat-activated persulfate oxidation of PFOA, 6:2 fluorotelomer sulfonate, and PFOS under conditions suitable for in-situ groundwater remediation. *Chemosphere* **2016**, *145*, 376–383.

(151) A. Bruton, T.; L. Sedlak, D. Treatment of Aqueous Film-Forming Foam by Heat-Activated Persulfate Under Conditions Representative of In Situ Chemical Oxidation. *Environ. Sci. Technol.* **2017**, *51*, 13878–13885.

(152) Burns, D. C.; Ellis, D. A.; Li, H.; McMurdo, C. J.; Webster, E. Experimental pKa determination for perfluorooctanoic acid (PFOA) and the potential impact of pKa concentration dependence on laboratory-measured partitioning phenomena and environmental modeling. *Environ. Sci. Technol.* **2008**, *42*, 9283–9288.

(153) Cheng, J.; Psillakis, E.; Hoffmann, M. R.; Colussi, A. J. Acid dissociation versus molecular association of perfluoroalkyl oxoacids: environmental implications. *J. Phys. Chem. A* **2009**, *113*, 8152–8156.

(154) Alonso-de-Linaje, V.; Mangayayam, M. C.; Tobler, D. J.; Rives, V.; Espinosa, R.; Dalby, K. N. Enhanced sorption of perfluorooctane sulfonate and perfluorooctanoate by hydrotalcites. *Environmental Technology and Innovation* **2021**, *21*, 1–13.

(155) Deng, S.; Yu, Q.; Huang, J.; Yu, G. Removal of perfluorooctane sulfonate from wastewater by anion exchange resins: Effects of resin properties and solution chemistry. *Water Res.* **2010**, *44*, 5188–5195.

(156) Johnson, R. L.; Anschutz, A. J.; Smolen, J. M.; Simcik, M. F.; Lee Penn, R. The adsorption of perfluorooctane sulfonate onto sand, clay, and iron oxide surfaces. *J. Chem. Eng. Data* **2007**, *52*, 1165–1170.

(157) Anderson, R. H.; Long, G. C.; Porter, R. C.; Anderson, J. K. Occurrence of select perfluoroalkyl substances at U.S. Air Force aqueous film-forming foam release sites other than fire-training areas: Field-validation of critical fate and transport properties. *Chemosphere* **2016**, *150*, 678–685.

(158) Krembs, F. Critical Analysis of the Field-Scale Application of In Situ Chemical Oxidation for the Remediation of Contaminated Groundwater, Ph.D. Thesis, Colorado School of Mines, 2008.

(159) Jiménez-Ángeles, F.; Firoozabadi, A. Hydrophobic Hydration and the Effect of NaCl Salt in the Adsorption of Hydrocarbons and Surfactants on Clathrate Hydrates. *ACS Central Science* **2018**, *4*, 820–831.

(160) Downes, N.; Ottewill, G. A.; Ottewill, R. H. An investigation of the behaviour of ammonium perfluoro-octanoate at the air/water interface in the absence and presence of salts. *Colloids and Surfaces* **1995**, *98*, 25–33.

(161) Kunieda, H.; Shinoda, K. Krafft points, critical micelle concentrations, surface tension, and solubilizing power of aqueous solutions of fluorinated surfactants. *J. Phys. Chem.* **1976**, *80*, 2468–2470.

(162) Abezgauz, L.; Kuperkar, K.; Hassan, P. A.; Ramon, O.; Bahadur, P.; Danino, D. Effect of Hofmeister anions on micellization and micellar growth of the surfactant cetylpyridinium chloride. *J. Colloid Interface Sci.* **2010**, *342*, 83–92.

(163) Qin, X.; Liu, M.; Zhang, X.; Yang, D. Proton NMR based investigation of the effects of temperature and NaCl on micellar properties of CHAPS. *J. Phys. Chem. B* **2011**, *115*, 1991–1998.

(164) Van de Pas, J. C.; Buytenhek, C. J.; Brouwn, L. F. The effects of salts and surfactants on the physical stability of lamellar liquid-crystalline systems. *Recl. Trav. Chim. Pays-Bas* **1994**, *113*, 231–236.

(165) Sammalkorpi, M.; Karttunen, M.; Haataja, M. Ionic surfactant aggregates in saline solutions: Sodium dodecyl sulfate (SDS) in the presence of excess sodium chloride (NaCl) or calcium chloride (CaCl2). *J. Phys. Chem. B* **2009**, *113*, 5863–5870.

(166) Yu, D.; Huang, X.; Deng, M.; Lin, Y.; Jiang, L.; Huang, J.; Wang, Y. Effects of inorganic and organic salts on aggregation behavior of cationic gemini surfactants. *J. Phys. Chem. B* **2010**, *114*, 14955–14964.

(167) Dutkiewicz, E.; Jakubowska, A. Effect of electrolytes on the physicochemical behaviour of sodium dodecyl sulphate micelles. *Colloid Polym. Sci.* **2002**, *280*, 1009–1014.

(168) Park, S.; Zenobio, J. E.; Lee, L. S. Perfluorooctane sulfonate (PFOS) removal with Pd0/nFe0 nanoparticles: Adsorption or aqueous Fe-complexation, not transformation? *J. Hazard. Mater.* **2018**, *342*, 20–28.

(169) Viberg, H.; Eriksson, P., *Perfluorooctane sulfonate and perfluorooctanoic acid*; Elsevier Inc.: 2017, pp 811–827.

(170) Pereiro, A. B.; Araújo, J. M. M.; Teixeira, F. S.; Marrucho, I. M.; Piñeiro, M. M.; Rebelo, L. P. N. Aggregation behavior and total miscibility of fluorinated ionic liquids in water. *Langmuir* **2015**, *31*, 1283–1295.

(171) Lunkenheimer, K.; Geggel, K.; Prescher, D. Role of Counterion in the Adsorption Behavior of 1:1 Ionic Surfactants at Fluid Interfaces - Adsorption Properties of Alkali Perfluoro-n-octanoates at the Air/Water Interface. *Langmuir* **2017**, *33*, 10216–10224.

(172) Void, M. J. Micellization Process with Emphasis on Premicelles. *Langmuir* **1992**, *8*, 1082–1085.

(173) López-Fontán, J. L.; Sarmiento, F.; Schulz, P. C. The aggregation of sodium perfluorooctanoate in water. *Colloid Polym. Sci.* **2005**, *283*, 862–871.

(174) Szutkowski, K.; Kołodziejska, Z.; Pietralik, Z.; Zhukov, I.; Skrzypczak, A.; Materna, K.; Kozak, M. Clear distinction between CAC and CMC revealed by high-resolution NMR diffusometry for a series of bis-imidazolium gemini surfactants in aqueous solutions. *RSC Adv.* **2018**, *8*, 38470–38482.

(175) Jakubowska, A. Interactions of divalent metal cations with headgroups of monomers, dimers, and trimers of anionic surfactant. *J. Mol. Liq.* **2021**, *336*.

(176) Fliermans, C. B.; Phelps, T. J.; Ringelberg, D.; Mikell, A. T.; White, D. C. Mineralization of trichloroethylene by heterotrophic enrichment cultures. *Appl. Environ. Microbiol.* **1988**, *54*, 1709–1714.

(177) Malachowsky, K. J.; Phelps, T. J.; Teboli, A. B.; Minnikin, D. E.; White, D. C. Aerobic mineralization of trichloroethylene, vinyl chloride, and aromatic compounds by rhodococcus species. *Appl. Environ. Microbiol.* **1994**, *60*, 542–548.

(178) Hinnant, K.; Snow, A.; Farley, J.; Giles, S.; Ananth, R. Comparison of Firefighting Performance between Commercial AFFF and Analytically Defined Reference AFFF Formulations.

(179) Kovalchuk, N. M.; Trybala, A.; Starov, V.; Matar, O.; Ivanova, N. Fluoro- Vs hydrocarbon surfactants: Why do they differ in wetting performance? *Adv. Colloid Interface Sci.* **2014**, *210*, 65–71.

(180) D'Agostino, L. A.; Mabury, S. A. Identification of novel fluorinated surfactants in aqueous film forming foams and commercial surfactant concentrates. *Environmental Science and Technology* **2014**, *48*, 121–129.

(181) Annunziato, K. M.; Doherty, J.; Lee, J.; Clark, J. M.; Liang, W.; Clark, C. W.; Nguyen, M.; Roy, M. A.; Timme-Laragy, A. R. Chemical Characterization of a Legacy Aqueous Film-Forming Foam Sample and Developmental Toxicity in Zebrafish (Danio rerio). *Environ. Health Perspect.* **2020**, *128*, 97006.

(182) Hamid, H.; Li, L. Y.; Grace, J. R. Review of the fate and transformation of per- and polyfluoroalkyl substances (PFASs) in landfills. *Environ. Pollut.* **2018**, *235*, 74–84.

(183) Liu, J.; Zhong, G.; Li, W.; Mejia Avendaño, S. Isomer-specific biotransformation of perfluoroalkyl sulfonamide compounds in aerobic soil. *Sci. Total Environ.* **2019**, *651*, 766–774.

(184) Nickerson, A.; E. Rodowa, A.; T. Adamson, D.; A. Field, J.; R. Kulkarni, P.; J. Kornuc, J.; P. Higgins, C. Spatial Trends of Anionic, Zwitterionic, and Cationic PFASs at an AFFF-Impacted Site. *Environ. Sci. Technol.* **2020**, *55*, 313–323.

(185) Mejia-Avendaño, S.; Zhi, Y.; Yan, B.; Liu, J. Sorption of Polyfluoroalkyl Surfactants on Surface Soils: Effect of Molecular Structures, Soil Properties, and Solution Chemistry. *Environmental Science and Technology* **2020**, *54*, 1513–1521.

(186) Ding, G.; Peijnenburg, W. J. G. M. Physicochemical properties and aquatic toxicity of poly- and perfluorinated compounds. *Crit. Rev. Environ. Sci. Technol.* **2013**, *43*, 598–678.

(187) Steffens, S. D.; Cook, E. K.; Sedlak, D. L.; Alvarez-Cohen, L. Under-reporting Potential of Per fl uorooctanesulfonic Acid (PFOS) under High-Ionic Strength Conditions. *Environmental Science & Technology Letters* **2021**, *18*, 1032–1037.

(188) McKenzie, E. R.; Siegrist, R. L.; McCray, J. E.; Higgins, C. P. The influence of a non-aqueous phase liquid (NAPL) and chemical oxidant application on perfluoroalkyl acid (PFAA) fate and transport, 2016.

(189) Ishiguro, M.; Koopal, L. K. Surfactant adsorption to soil components and soils. *Adv. Colloid Interface Sci.* **2016**, *231*, 59–102.

(190) Artificial Seawater. *Cold Spring Harb. Protoc.* **2012**.

(191) Arshadi, M.; Costanza, J.; Abriola, L. M.; Pennell, K. D. Comment on "Uptake of Poly- And Perfluoroalkyl Substances at the Air-Water Interface". *Environmental Science and Technology* **2020**, *54*, 7019–7020.

(192) Schaefer, C. E.; Nguyen, D.; Field, J. Response to the Comment on "Uptake of Poly- And Perfluoroalkyl Substances at the Air-Water Interface". *Environmental Science and Technology* **2020**, *54*, 7021–7022.

(193) Staszak, K.; Wieczorek, D.; Michocka, K. Effect of Sodium Chloride on the Surface and Wetting Properties of Aqueous Solutions of Cocamidopropyl Betaine. *J. Surfactants Deterg.* **2015**, *18*, 321–328.

(194) Dlugogorski, B. Z.; Schaefer, T. H. Compatibility of aqueous film-forming foams (AFFF) with sea water. *Fire Saf. J.* **2021**, *120*, 103288.

(195) Jakubowska, A. Interactions of different counterions with cationic and anionic surfactants. *J. Colloid Interface Sci.* **2010**, *346*, 398–404.

(196) Para, G.; Jarek, E.; Warszynski, P. The Hofmeister series effect in adsorption of cationic surfactants-theoretical description and experimental results. *Adv. Colloid Interface Sci.* **2006**, *122*, 39–55.

(197) Hill, C.; Czajka, A.; Hazell, G.; Grillo, I.; Rogers, S. E.; Skoda, M. W. A.; Joslin, N.; Payne, J.; Eastoe, J. Surface and bulk properties of surfactants used in fire-fighting. *J. Colloid Interface Sci.* **2018**, *530*, 686–694.

(198) Gaur, N.; Narasimhulu, K.; PydiSetty, Y. Recent advances in the bio-remediation of persistent organic pollutants and its effect on environment. *J. Clean. Prod.* **2018**, *198*, 1602–1631.

(199) Wackett, L. P.; Robinson, S. L. The ever-expanding limits of enzyme catalysis and biodegradation: polyaromatic, polychlorinated, polyfluorinated, and polymeric compounds. *Biochem. J* **2020**, *477*, 2875–2891.

(200) Wanninayake, D. M. Comparison of currently available PFAS remediation technologies in water: A review. *J. Environ. Manage.* **2021**, *283*, 111977.

(201) Wackett, L. P. Nothing lasts forever: understanding microbial biodegradation of polyfluorinated compounds and perfluorinated alkyl substances. *Microb. Biotechnol.* **2022**, *15*, 773–792.

(202) Wackett, L. P. Why Is the Biodegradation of Polyfluorinated Compounds So Rare? *mSphere* **2021**, *6*.

(203) Gribble, G. W. Occurrence of halogenated alkaloids. *Alkaloids Chem. Biol.* **2012**, *71*, 1–165.

(204) Yu, Y.; Zhang, K.; Li, Z.; Ren, C.; Chen, J.; Lin, Y. H.; Liu, J.; Men, Y. Microbial Cleavage of C-F Bonds in Two C6Per- And Polyfluorinated Compounds via Reductive Defluorination. *Environmental Science and Technology* **2020**, *54*, 14393–14402.

(205) Liou, J. S. C.; Szostek, B.; DeRito, C. M.; Madsen, E. L. Investigating the biodegradability of perfluorooctanoic acid. *Chemosphere* **2010**, *80*, 176–183.

(206) Chen, H.; Liu, M.; Munoz, G.; Vo Duy, S.; Sauvé, S.; Yao, Y.; Sun, H.; Liu, J. Fast Generation of Perfluoroalkyl Acids from Polyfluoroalkyl Amine Oxides in Aerobic Soils. *Environmental Science & Technology Letters* **2020**, *7*, 714–720.

(207) Olivares, C. I.; Yi, S.; Cook, E. K.; Choi, Y. J.; Montagnolli, R.; Byrne, A.; Higgins, C. P.; Sedlak, D. L.; Alvarez-Cohen, L. Aerobic BTEX biodegradation increases yield of perfluoroalkyl carboxylic acids from biotransformation of a polyfluoroalkyl surfactant, 6:2 FtTAoS. *Environ. Sci. Process. Impacts* **2022**, *24*, 439–446.

(208) Ellis, D. A.; Martin, J. W.; De Silva, A. O.; Mabury, S. A.; Hurley, M. D.; Sulbaek Andersen, M. P.; Wallington, T. J. Degradation of fluorotelomer alcohols: A likely atmospheric source of perfluorinated carboxylic acids. *Environmental Science and Technology* **2004**, *38*, 3316–3321.

(209) Wang, N.; Szostek, B.; Buck, R. C.; Folsom, P. W.; Sulecki, L. M.; Gannon, J. T. 8-2 Fluorotelomer alcohol aerobic soil biodegradation: Pathways, metabolites, and metabolite yields. *Chemosphere* **2009**, *75*, 1089–1096.

(210) Tseng, N.; Wang, N.; Szostek, B.; Mahendra, S. Biotransformation of 6:2 Fluorotelomer alcohol (6:2 FTOH) by a wood-rotting fungus. *Environmental Science and Technology* **2014**, *48*, 4012–4020.

(211) Colosi, L. M.; Pinto, R. A.; Huang, Q.; Weber, W. J. Peroxidase-mediated degradation of perfluorooctanoic acid. *Environ. Toxicol. Chem.* **2009**, *28*, 264–271.

(212) Luo, Q.; Wang, Z.; Feng, M.; Chiang, D.; Woodward, D.; Liang, S.; Lu, J.; Huang, Q. Factors controlling the rate of perfluorooctanoic acid degradation in laccase-mediator systems: The impact of metal ions. *Environ. Pollut.* **2017**, *224*, 649–657.

(213) Baldrian, P. Fungal laccases – occurrence and properties. *FEMS Microbiol. Rev.* **2006**, *30*, 215–242.

(214) Christopher, L. P.; Yao, B.; Ji, Y. Lignin biodegradation with laccase-mediator systems. *Frontiers in Energy Research* **2014**, *2*, 12.

(215) Mayer, A. M. Polyphenol oxidases in plants-recent progress. *Phytochemistry* **1986**, *26*, 11–20.

(216) Thomas, B. R.; Yonekura, M.; Morgan, T. D.; Czapla, T. H.; Hopkins, T. L.; Kramer, K. J. A trypsin-solubilized laccase from pharate pupal integument of the tobacco hornworm, Manduca sexta. *Insect Biochem.* **1989**, *19*, 611–622.

(217) Chauhan, P. S.; Goradia, B.; Saxena, A. Bacterial laccase: recent update on production, properties and industrial applications. *3 Biotech* **2017**, *7*.

(218) Ashe, B.; Nguyen, L. N.; Hai, F. I.; Lee, D.-J.; van de Merwe, J. P.; Leusch, F. D. L.; Price, W. E.; Nghiem, L. D. Impacts of redox-mediator type on trace organic contaminants degradation by laccase: Degradation efficiency, laccase stability and effluent toxicity. *Int. Biodeterior. Biodegradation* **2016**, *113*, 169–176.

(219) Li, K.; Xu, F.; Eriksson, K. E. Comparison of fungal laccases and redox mediators in oxidation of a nonphenolic lignin model compound. *Appl. Environ. Microbiol.* **1999**, *65*, 2654–2660.

(220) Hata, T.; Shintate, H.; Kawai, S.; Okamura, H.; Nishida, T. Elimination of carbamazepine by repeated treatment with laccase in the presence of 1-hydroxybenzotriazole. *J. Hazard. Mater.* **2010**, *181*, 1175–1178.

(221) Othman, A. M.; Elshafei, A. M.; Elsayed, M. A.; Hassan, M. M. Decolorization of Cibacron Blue 3G-A Dye by Agaricus bisporus CU13 Laccase - Mediator System: A Statistical Study for Optimization via Response Surface Methodology. *Annual Research & Review in Biology* **2018**, *25*, 1–13.

(222) Mizuno, H.; Hirai, H.; Kawai, S.; Nishida, T. Removal of estrogenic activity of isobutylparaben and n-butylparaben by laccase in the presence of 1-hydroxybenzotriazole. *Biodegradation* **2009**, *20*, 533–539.

(223) Stoll, S.; Schweiger, A. EasySpin, a comprehensive software package for spectral simulation and analysis in EPR. *J. Magn. Reson.* **2006**, *178*, 42–55.

(224) Galli, C.; Gentili, P.; Lanzalunga, O.; Lucarini, M.; Pedulli, G. F. Spectrophotometric, EPR and kinetic characterisation of the [nitroxyl] radical from 1-hydroxybenzotriazole, a key reactive species in mediated enzymatic oxidations. *Chem. Commun.* **2004**, 2356–2357.

(225) Garzillo, A. M.; Colao, M. C.; Buonocore, V.; Oliva, R.; Falcigno, L.; Saviano, M.; Santoro, A. M.; Zappala, R.; Bonomo, R. P.; Bianco, C.; Giardina, P.; Palmieri, G.; Sannia, G. Structural and kinetic characterization of native laccases from Pleurotus ostreatus, Rigidoporus lignosus, and Trametes trogii. *J. Protein Chem.* **2001**, *20*, 191–201.

(226) Huang, Q. Remediation of Perfluoroalkyl Contaminated Aquifers SERDP Project. **2013**, 1–32.

(227) Luo, Q.; Liang, S.; Huang, Q. Laccase induced degradation of perfluorooctanoic acid in a soil slurry. *J. Hazard. Mater.* **2018**, *359*, 241–247.

(228) Erkoç, Ş.; Erkoç, F. Structural and electronic properties of PFOS and LiPFOS. *Journal of Molecular Structure: THEOCHEM* **2001**, *549*, 289–293.

(229) Naghdi, M.; Taheran, M.; Brar, S. K.; Kermanshahi-pour, A.; Verma, M.; Surampalli, R. Y. Biotransformation of carbamazepine by laccase-mediator system: Kinetics, byproducts and toxicity assessment. *Process Biochem.* **2018**, *67*, 147–154.

(230) Hai, F. I.; Yang, S.; Asif, M. B.; Sencadas, V.; Shawkat, S.; Sanderson-Smith, M.; Gorman, J.; Xu, Z.-Q.; Yamamoto, K. Carbamazepine as a Possible Anthropogenic Marker in Water: Occurrences, Toxicological Effects, Regulations and Removal by Wastewater Treatment Technologies. *Water* **2018**, *10*, 107.

(231) Liu, K.; Yu, J. C. C.; Dong, H.; Wu, J. C. S.; Hoffmann, M. R. Degradation and Mineralization of Carbamazepine Using an Electro-Fenton Reaction Catalyzed by Magnetite Nanoparticles Fixed on an Electrocatalytic Carbon Fiber Textile Cathode. *Environmental Science and Technology* **2018**, *52*, 12667–12674.

(232) Piontek, K.; Antorini, M.; Choinowski, T. Crystal Structure of a Laccase from the FungusTrametes versicolor at 1.90-Å Resolution Containing a Full Complement of Coppers *. *J. Biol. Chem.* **2002**, *277*, 37663–37669.

(233) Kumar, R.; Kaur, J.; Jain, S.; Kumar, A. Optimization of laccase production from Aspergillus flavus by design of experiment technique: Partial purification and characterization. *Journal of Genetic Engineering and Biotechnology* **2016**, *14*, 125–131.

(234) Munk, L.; Andersen, M. L.; Meyer, A. S. Influence of mediators on laccase catalyzed radical formation in lignin. *Enzyme Microb. Technol.* **2018**, *116*, 48–56.

(235) Eriksen, K. T.; Raaschou-Nielsen, O.; McLaughlin, J. K.; Lipworth, L.; Tjønneland, A.; Overvad, K.; Sørensen, M. Association between plasma PFOA and PFOS levels and total cholesterol in a middle-aged Danish population. *PLoS One* **2013**, *8*.

(236) Maso, L.; Trande, M.; Liberi, S.; Moro, G.; Daems, E.; Linciano, S.; Sobott, F.; Covaceuszach, S.; Cassetta, A.; Fasolato, S.; Moretto, L. M.; De Wael, K.; Cendron, L.; Angelini, A. Unveiling the binding mode of perfluorooctanoic acid to human serum albumin. *Protein Sci.* **2021**, *30*, 830–841.

(237) Forsthuber, M.; Kaiser, A. M.; Granitzer, S.; Hassl, I.; Hengstschläger, M.; Stangl, H.; Gundacker, C. Albumin is the major carrier protein for PFOS, PFOA, PFHxS, PFNA and PFDA in human plasma. *Environ. Int.* **2020**, *137*, 105324.

(238) Xu, D.; Liu, C.; Yan, X.; Shen, T. Study on the interactions of PFOS and PFOA with bovine serum albumin. *2011 International Conference on Remote Sensing, Environment and Transportation Engineering, RSETE 2011 - Proceedings* **2011**, 7168–7171.

(239) Hernandez, E. T.; Koo, B.; Sofen, L. E.; Amin, R.; Togashi, R. K.; Lall, A. I.; Gisch, D. J.; Kern, B. J.; Rickard, M. A.; Francis, M. B. Proteins as adsorbents for PFAS removal from water. *Environmental Science: Water Research and Technology* **2022**, *8*, 1188–1194.

(240) Salvalaglio, M.; Muscionico, I.; Cavallotti, C. Determination of energies and sites of binding of PFOA and PFOS to human serum albumin. *J. Phys. Chem. B* **2010**, *114*, 14860–14874.

(241) Mehra, R.; Muschiol, J.; Meyer, A. S.; Kepp, K. P. A structural-chemical explanation of fungal laccase activity. *Sci. Rep.* **2018**, *8*, 1–16.

(242) Cranwill, A. Potential of a Laccase from Trametes versicolor to Degrad Per- and Polyfluoroalkyl Substances in Water, Ph.D. Thesis, 2022.

(243) Kalra, S. S. Ultrasound and Fungi Mediated Degradation of Model Emerging Contaminants: Per- and Polyfluoroalkyl Substances & Nitrotriazolone, Ph.D. Thesis, UCLA, 2021.

(244) Banks, R. E.; Tatlow, J. C. In *Organofluorine Chemistry: Principles and Commercial Applications*, Banks, R. E., Smart, B. E., Tatlow, J. C., Eds.; Springer US: Boston, MA, 1994, pp 1–24.

(245) Cousins, I. T.; Ng, C. A.; Wang, Z.; Scheringer, M. Why is high persistence alone a major cause of concern? *Environ. Sci. Process. Impacts* **2019**, *21*, 781–792.

(246) Brandsma, S. H.; Koekkoek, J. C.; van Velzen, M. J. M.; de Boer, J. The PFOA substitute GenX detected in the environment near a fluoropolymer manufacturing plant in the Netherlands. *Chemosphere* **2019**, *220*, 493–500.

(247) Ahearn, A. A regrettable substitute: The story of GenX. *Environ. Health Perspect.* **2019**.

(248) Briddell, C. Water repellency: The choices, trade-offs and challenges behind a greener dry, en, https://communities.acs.org/t5/GCI-Nexus-Blog/Water-repellency-The-choices-trade-offs-and-challenges-behind-a/ba-p/15945, Accessed: 2022-11-21, 2015.

(249) Delimi, A.; Galopin, E.; Coffinier, Y.; Pisarek, M.; Boukherroub, R.; Talhi, B.; Szunerits, S. Investigation of the corrosion behavior of carbon steel coated with fluoropolymer thin films. *Surf. Coat. Technol.* **2011**, *205*, 4011–4017.

(250) Paley, M. 5 things to know about DOD's research on 'fluorine-free' firefighting foam, en, https://www.defense.gov/News/News-Stories/Article/Article/1953510/5-things-to-know-about-dods-research-on-fluorine-free-firefighting-foam/, Accessed: 2022-11-21.

(251) Muensterman, D. J.; Titaley, I. A.; Peaslee, G. F.; Minc, L. D.; Cahuas, L.; Rodowa, A. E.; Horiuchi, Y.; Yamane, S.; Fouquet, T. N. J.; Kissel, J. C.; Carignan, C. C.; Field, J. A. Disposition of Fluorine on New Firefighter Turnout Gear. *Environ. Sci. Technol.* **2022**, *56*, 974–983.